Supporting Information

for

Active-Template Synthesis of "Click" [2]Rotaxane Ligands: Self-Assembly of Mechanically Interlocked Metallo-Supramolecular Dimers, Macrocycles and Oligomers.

Asif Noor, Stephen C. Moratti and James D. Crowley*

Department of Chemistry, University of Otago, PO Box 56, Dunedin, New Zealand

E-mail: jcrowley@chemistry.otago.ac.nz;

Tel: +64 3 479 7731

Fax: +64 3 479 7906

Table of Contents

1 General 3

2 Synthesis of Macrocycle **1** 6

2.1 Diol **S2** 6

2.2 Ditosylate **S3** 8

2.3 Macrocycle **1** 10

2.4 Ag(I) complex of macrocycle **1**-Ag 13

2.5 Cu(I) complex of macrocycle **1**-Cu 14

2.6 Stopper **S10** 16

2.7 Stopper **S11** 18

2.8 Stopper **3b** 20

3 Active Template Synthesis of [2]Rotaxanes 23

3.1 [2]Rotaxane **4a** 23

3.2 [2]Rotaxane **4b** 27

4 Synthesis of Terpyridine Functionalized [2]Rotaxane Ligands 32

4.1 Ligand **S13**[4] 32

4.2 Ligand **S14** 35

4.3 Macrocycle Ligand **S15** 37

4.4 [2]Rotaxane Ligand **5a** 41

4.5 [2]Rotaxane Ligand **5b** 44

5 Fe(II) Complexes of [2]Rotaxane Ligands 48

5.1 [Fe(**S14**)$_2$](BF$_4$)$_2$ 48

5.2 [Fe(**S15**)$_2$](BF$_4$)$_2$ 50

5.3 [Fe(**5a**)$_2$](BF$_4$)$_2$ 52

5.4 [Fe(**5b**)](BF$_4$)$_2$ 57

5.5 [Fe(**5b**)]$_n$(PF$_6$)$_{2n}$ 62

6 Molecular Modelling of the Interlocked Assemblies 63

7 GPC and UV/Vis Analyses 69

8 ^{1}H DOSY NMR Experiments 71

9 X-Ray Data Collection and Structure Refinement 79

9.1 Macrocycle **1** 79

9.2 Ag(I) complex of macrocycle **1**-Ag 80

9.3 [Fe(**S14**)$_2$](BF$_4$)$_2$ 82

10 Selected Stacked ^{1}H NMR Spectra 86

11 References: 87

1 General

Unless otherwise stated, all reagents were purchased from commercial sources and used without further purification. Dry dichloromethane (CH_2Cl_2), tetrahydrofuran (THF) and acetonitrile (CH_3CN) were obtained by passing the solvents through an activated alumina column on a PureSolvTM solvent purification system (Innovative Technologies, Inc., MA). Petrol refers to the fraction of petroleum ether boiling in the range 40-60 °C. Flash column chromatography was carried out using Kiesegel C60 (Fisher) as the stationary phase. Analytical TLC was performed on pre-coated silica gel plates (0.25 mm thick, 60F254, Merck, Germany) and observed under UV light. All melting points were determined using a Sanyo Gallenkamp apparatus and are uncorrected. ^{1}H, ^{13}C, ^{1}H DOSY, NOESY, ROESY and COSY NMR spectra were recorded either on a 400 MHz Varian/Agilent 400-MR or Varian/Aglient 500 MHz AR spectrometer at 298 K. Chemical shifts are reported in parts per million (ppm) and referenced to residual solvent peaks ($CDCl_3$: ^{1}H δ 7.26 ppm, ^{13}C δ 77.16 ppm; CD_3CN: ^{1}H δ 1.94, ^{13}C δ 1.32, 118.26 ppm, DMSO-d_6: ^{1}H δ 2.50 ppm; ^{13}C δ 39.52 ppm, acetone-d_6: ^{1}H δ 2.05 ppm; ^{13}C δ 29.84 ppm). Coupling constants (*J*) are reported in Hertz (Hz). Standard abbreviations indicating multiplicity were used as follows: m = multiplet, q = quartet, t = triplet, dt = double triplet, d = doublet, dd = double doublet, s = singlet , ABq = AB quartet. Microanalyses were performed at the Campbell Microanalytical Laboratory at University of Otago. High resolution electrospray ionization mass spectra (HR-ESMS) were collected on a Bruker micrOTOF-Q spectrometer. UV-visible absorption spectra were acquired with a Shimadzu UV-2600 spectrophotometer. GPC analysis were performed on a Polymer Laboratories (Agilent tech.) PL-GPC 50-*Plus* with two PL-Gel 20 μm Mixed-A columns in series with a pre-column installed. Molecular weights were calculated using a polystyrene standard calibration curve using a UV detector.

Safety Note: Low molecular weight organic azides are potential explosives, care must be taken during their handling.[1] A standard PVC blast shield was used when necessary. Additionally, copper azides and acetylides are explosive when dry, and their traces should be removed before the CuAAC reaction products are dried. This was achieved by pouring the crude reaction mixture into 100 mL of 0.1 M ammonium hydroxide/ethylenediaminetetraacetic acid (NH_4OH/EDTA) solution was made up by mixing 30 g EDTA with 900 mL water and 100 mL NH_4OH.

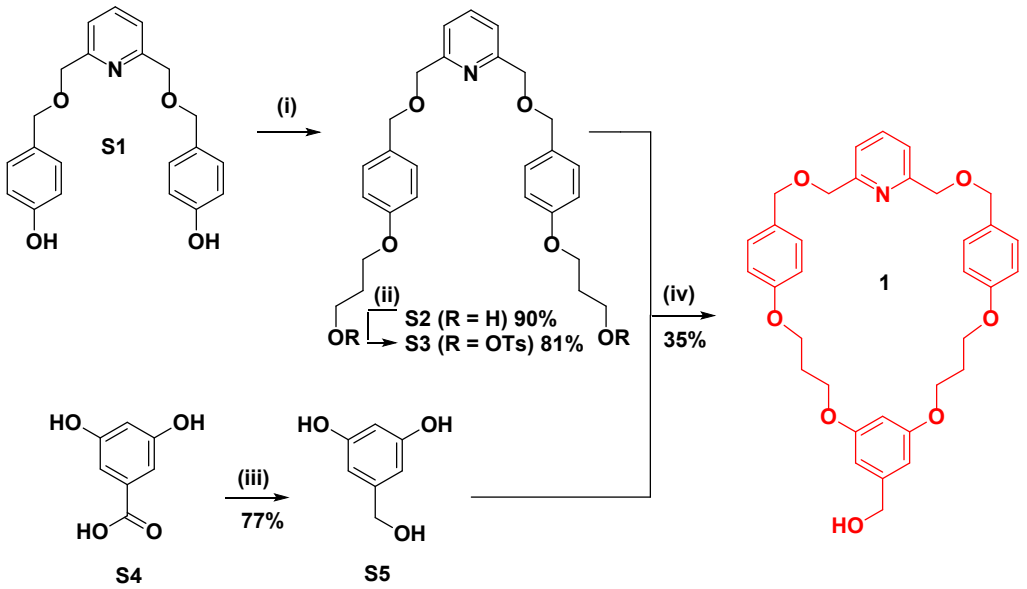

Scheme S 1 Synthesis of macrocycle **1**, (i) 1-bromopropanol, K_2CO_3, DMF, RT, 24 h, (ii) TsCl, triethylamine, DMAP, CH_2Cl_2, RT, 24 h, (iii) BH_3-DMS, THF, reflux, 24 h, (iv) Cs_2CO_3, DMF, 55 °C, 5 days.

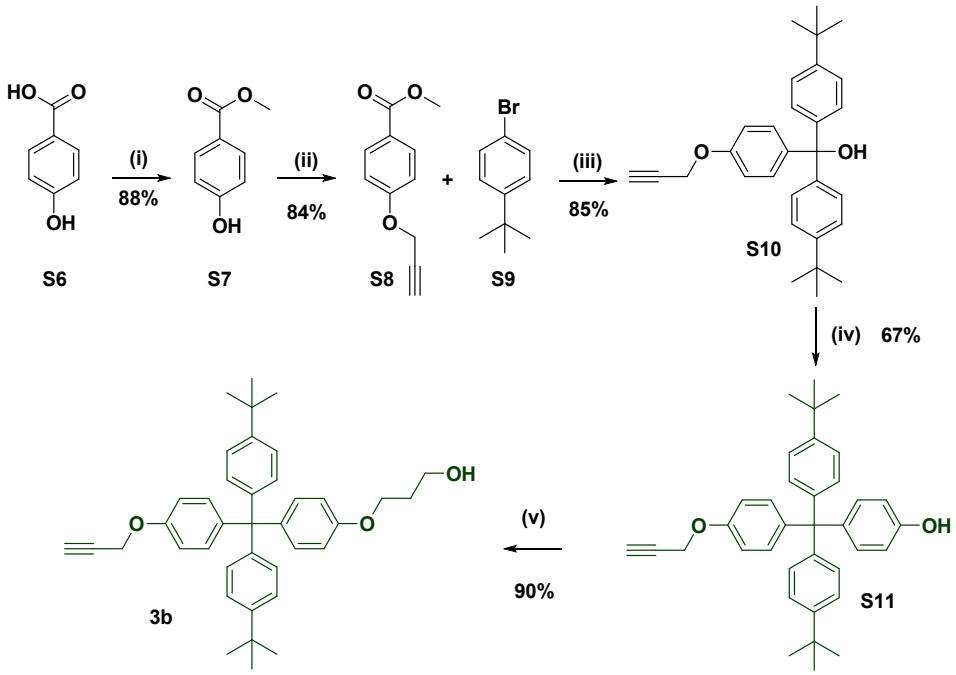

Scheme S 2 Synthesis of the bifunctionalised stopper **3b**, (i) MeOH/H_2SO_4, reflux, 24 h, (ii) propargyl bromide, K_2CO_3, acetone, reflux, 24 h, (iii) Mg, THF, reflux, 24 h, (iv) phenol, CH_3COCl, 100 °C, 48 h, (v) 1-bromopropanol, K_2CO_3, acetone, reflux, 24 h.

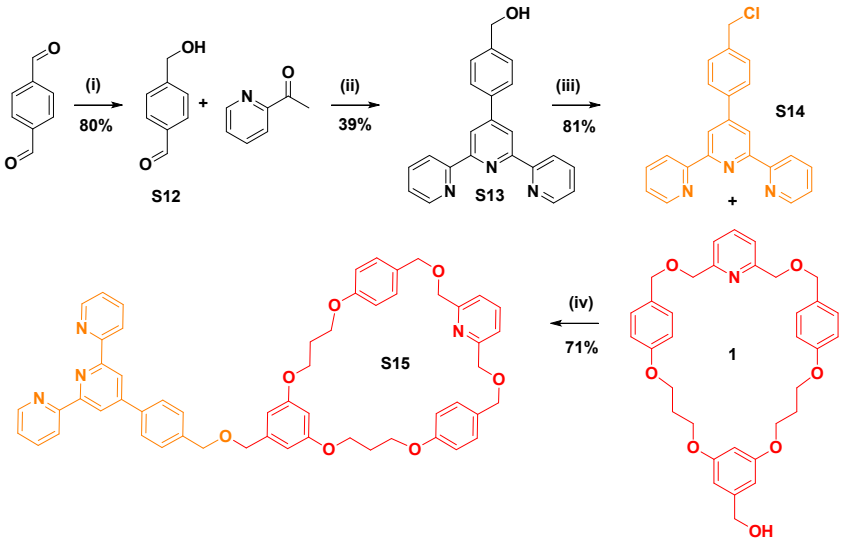

Scheme S 3 Synthetic route to the terpyridine functionalised macrocycle, **S15**: (i) $NaBH_4$, ethanol/THF, 0-5 °C, 8 h, (ii) NH_4OH, methanol, reflux, 48 h, (iii) $SOCl_2$, reflux, 2 h, (iv) NaH, DMF, RT, 24h.

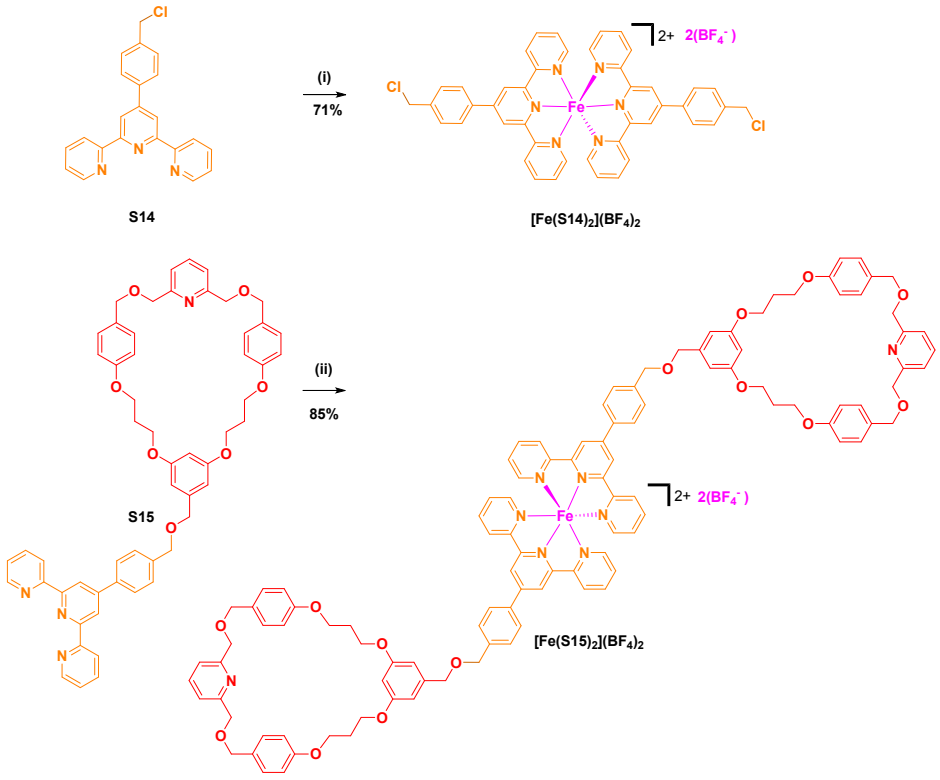

Scheme S 4 Preparation of Fe(II) model complexes of ligand **S14** and **S15**; (i) $[Fe(H_2O)_6](BF_4)_2$, acetonitrile, RT, 10 min, (ii) $[Fe(H_2O)_6](BF_4)_2$, acetonitrile, RT, 10 min.

2 Synthesis of Macrocycle 1

2.1 Diol S2

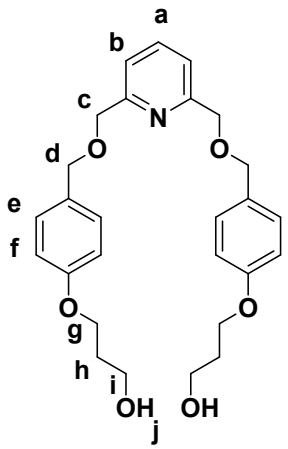

A mixture of diphenol **S1**[2] (4.00 g, 11.38 mmol) and K_2CO_3 (4.72 g, 34.1 mmol) in anhydrous DMF (25 mL) were stirred at RT for 1 h. 3-Bromo-1-propanol (2.5 mL, 28.5 mmol) was added via syringe and the mixture was stirred at RT for 24 h under a nitrogen atmosphere. The mixture was filtered and the solvent removed under reduced pressure. The residue was dissolved in CH_2Cl_2 (100 mL) and the resulting solution was washed with water (2 × 30 mL) and brine (2 × 30 mL). The solvent of the organic layer was removed under reduced pressure. The residue was purified by silica gel column chromatography with ethyl acetate as eluent to give **S2** (4.8 g, 90%) as yellow oil that solidified upon standing. ^{1}H NMR (400 MHz, DMSO-d_6) δ 7.82 (t, J = 7.7 Hz, 1H, H_a), 7.36 (d, J = 7.7 Hz, 2H, H_b), 7.28 (d, J = 8.7 Hz, 4H, H_e), 6.91 (d, J = 8.7 Hz, 4H, H_f), 4.54 (s, 4H, H_c), 4.53 (s, 2H, H_j) 4.51 (s, 4H, H_d), 4.02 (t, J = 6.4 Hz, 4H, H_g), 3.55 (q, J = 6.2 Hz, 4H, H_i), 1.85 (p, J = 6.3 Hz, 4H, H_h). ^{13}C NMR (100 MHz, DMSO-d_6) δ 158.21, 157.62, 137.39, 129.88, 129.33, 119.83, 114.17, 72.12, 71.60, 64.51, 57.28, 32.11; HR-ESMS: *m/z* = 468.2381 [**S2**+H]$^+$ (calc. for $C_{27}H_{34}NO_6$, 468.2342); Anal. calc. for $C_{27}H_{33}NO_6$); C, 69.36; H, 7.11; N, 3.00. Found: C, 69.42; H, 7.29; N, 2.83.

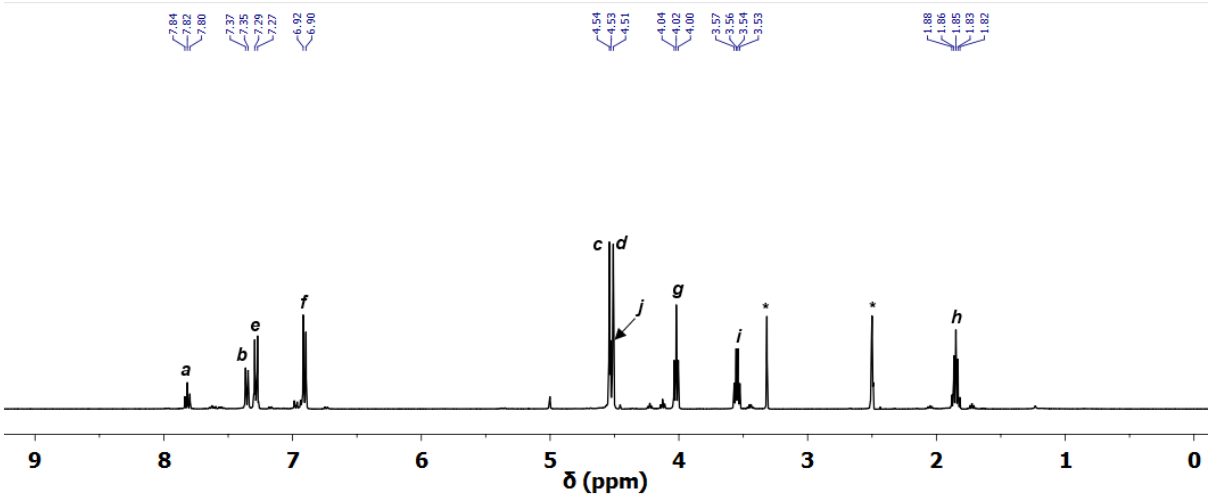

Figure S 1 ^{1}H NMR spectrum (400 MHz, DMSO-d_6, 298K) of **S2** (* peaks due to H_2O and DMSO).

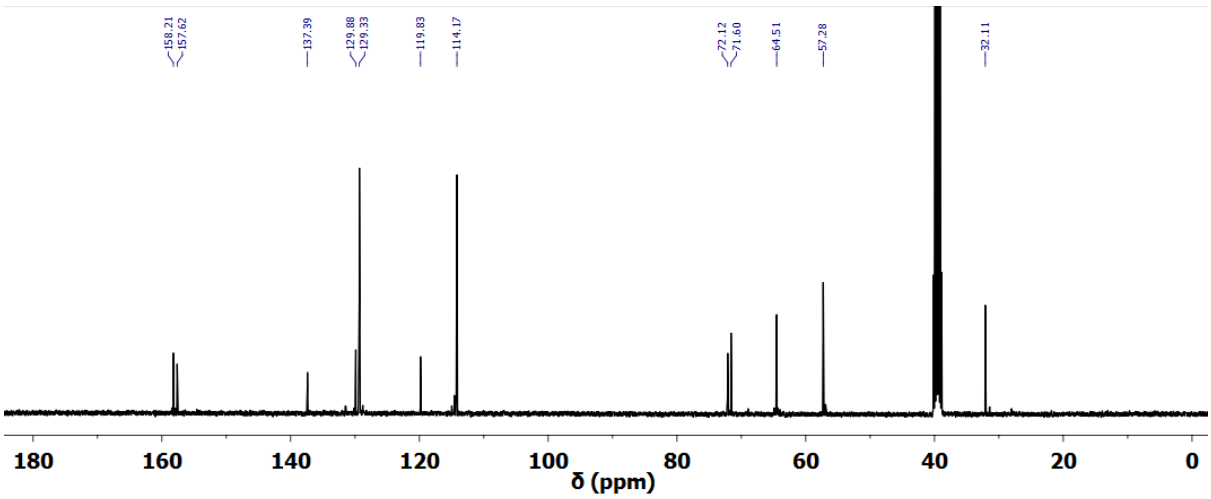

Figure S 2 ^{13}C NMR spectrum (400 MHz, DMSO-d_6, 298K) of **S2**.

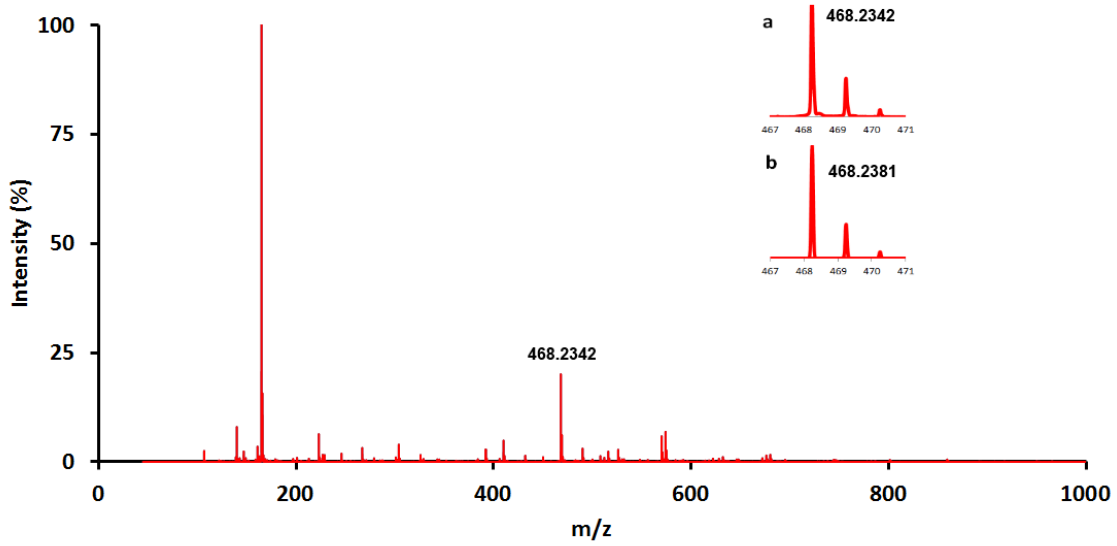

Figure S 3 HR-ESMS spectrum of **S1**, inset a) observed and b) calculated isotopic patterns for [**S1**+H]$^+$ at *m/z* = 468.2342.

2.2 Ditosylate S3

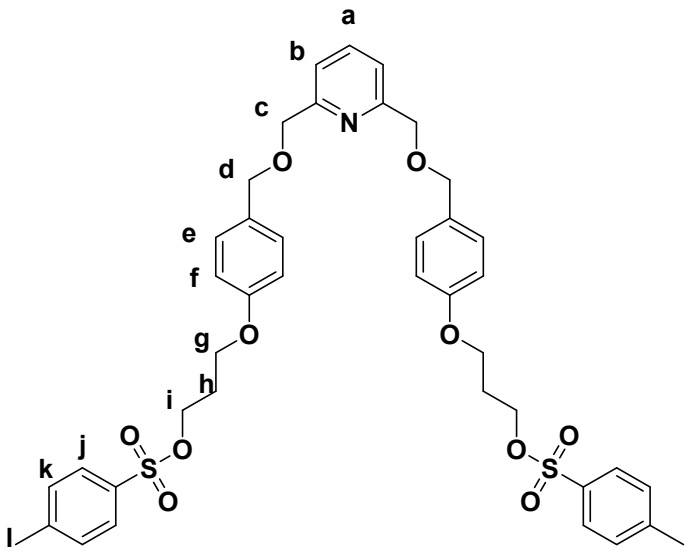

A solution of **S2** (3.00 g, 6.42 mmol) in CH_2Cl_2 (300 mL) was cooled to 0 °C, and then triethylamine (4.03 mL, 28.9 mmol) and DMAP (0.031 g, 0.257 mmol) were added. To this cooled solution, tosyl chloride (3.06 g, 16.04 mmol) in CH_2Cl_2 (30 mL) was added drop wise. The reaction mixture was then stirred at RT for 24 h. Water (100 mL) was then added and the layers separated. The aqueous layer was extracted with CH_2Cl_2 (100 mL) and the combined organic layers were washed with brine (100 mL) and dried over $MgSO_4$. The solvent was removed under reduced pressure, and the residue was purified by column

chromatography (silica gel, ethyl acetate) to give **S3** (4.029 g, 81%) as yellow oil that solidified upon standing. ^{1}H NMR (400 MHz, DMSO-d_6) δ 7.82 (t, J = 7.7 Hz, 1H, H_a), 7.75 (d, J = 8.3 Hz, 4H, H_j), 7.41 – 7.34 (m, 6H, H_b, H_k), 7.27 (d, J = 8.6 Hz, 4H, H_e), 6.79 (d, J = 8.6 Hz, 4H, H_f), 4.55 (s, 4H, H_c), 4.51 (s, 4H, H_d), 4.18 (t, J = 6.1 Hz, 4H, H_g), 3.89 (t, J = 6.0 Hz, 4H, H_i), 2.34 (s, 6H, H_l), 2.01 (p, J = 6.1 Hz, 4H, H_h). ^{13}C NMR (100 MHz, DMSO-d_6) δ 158.14, 158.06, 145.32, 137.88, 132.61, 130.63, 130.54, 129.71, 127.95, 120.30, 114.59, 72.59, 72.03, 68.09, 63.50, 28.59, 21.51. HR-ESMS: m/z = 798.2383 [**S3** + Na]$^+$ (calc. for $C_{41}H_{46}N_1O_{10}S_2$, 798.2342); Anal. calc. for $C_{41}H_{45}NO_{10}S_2$•0.5($CH_3COOC_2H_5$: C, 62.71; H, 6.07; N, 1.72. Found: C, 62.69 ; H, 6.11; N, 1.76.

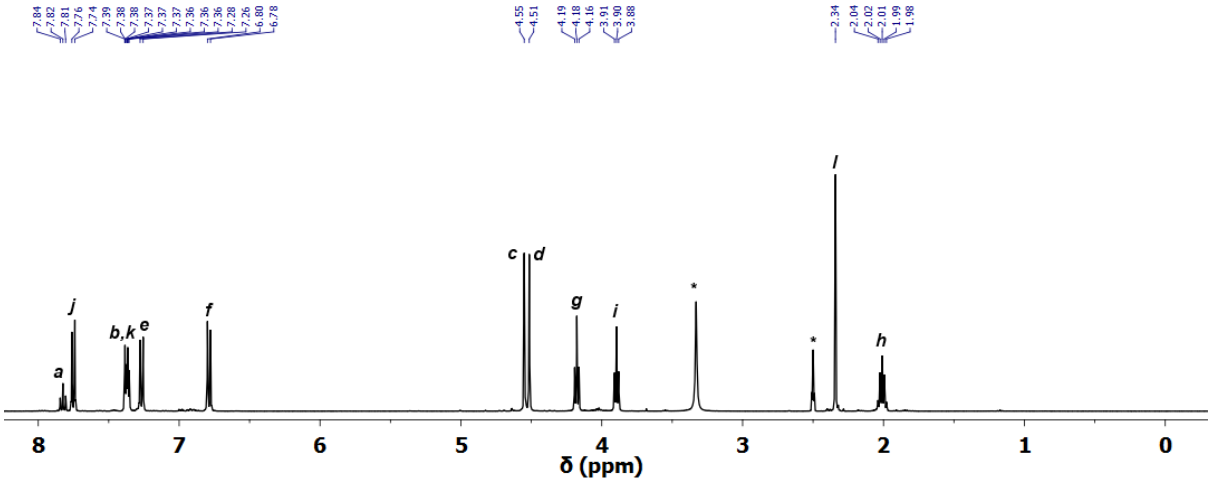

Figure S 4 ^{1}H NMR spectrum (400 MHz, DMSO-d_6, 298K) of **S3** (* peaks due to H_2O and DMSO).

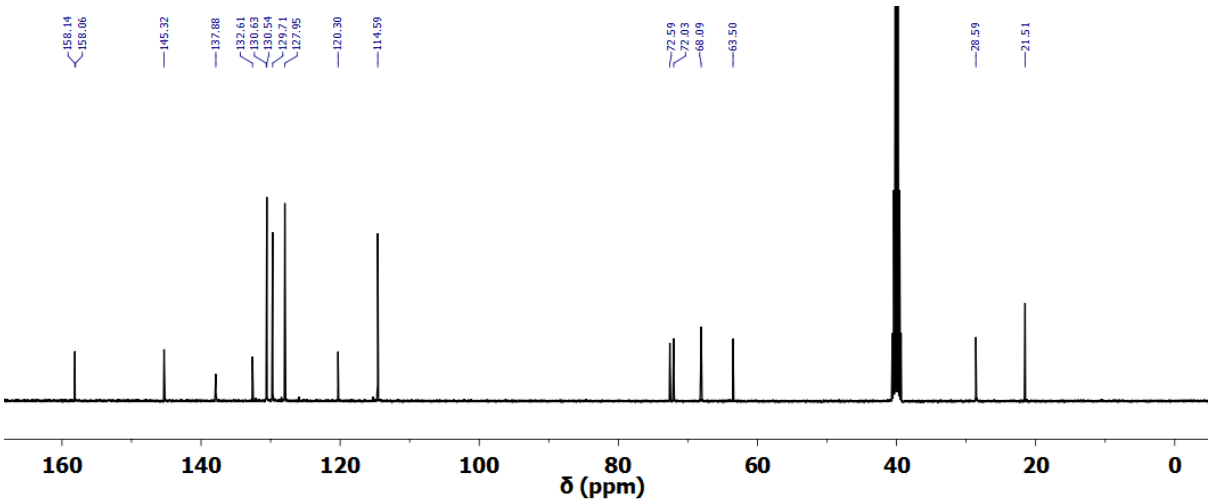

Figure S 5 ^{13}C NMR spectrum (100 MHz, DMSO-d_6, 298K) of **S3**.

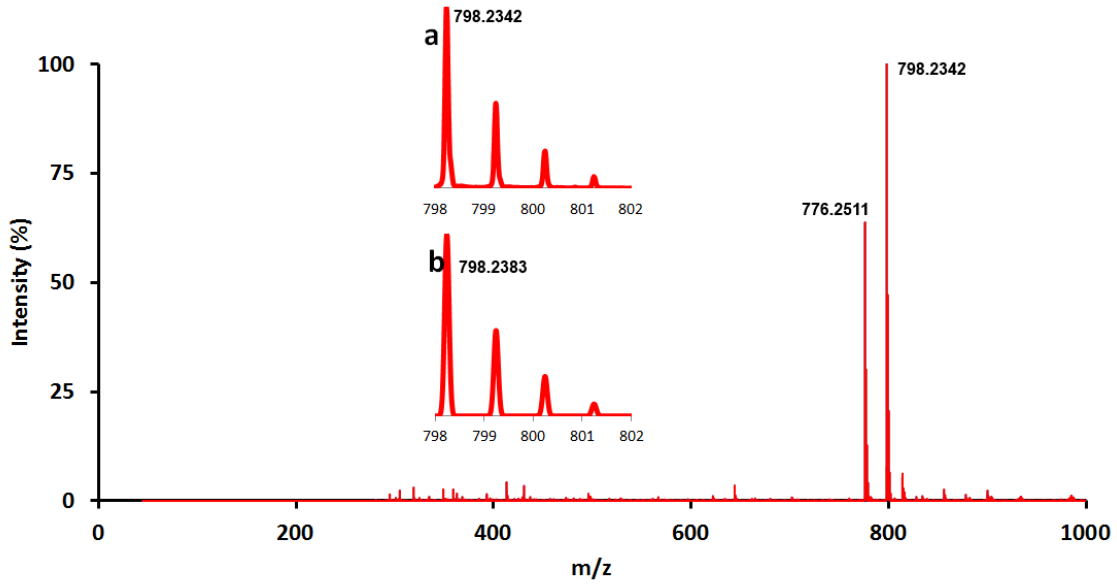

Figure S 6 HR-ESMS spectrum of **S3**, inset a) observed and b) calculated isotopic patterns for [**S3**+Na]$^+$ at *m/z* = 798.2342, also showing peaks due to [**S3**+H]$^+$ ions at *m/z* =776.2511.

2.3 Macrocycle 1

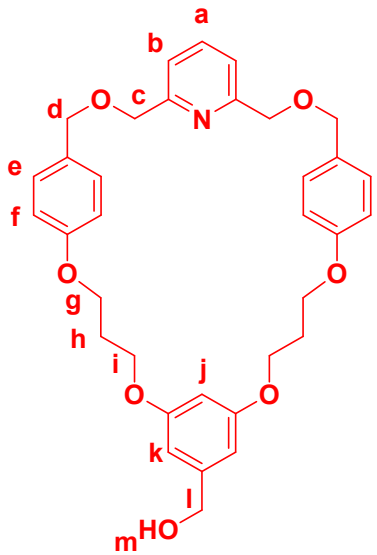

A solution of **S3** (3.50 g, 4.51 mmol) in DMF (50 mL) and 3,5-dihydroxybenzyl alcohol **S5**[3] (0.70 g, 4.96 mmol) in DMF (50 mL) were added slowly over 48 hours via syringe pump to a suspension of Cs_2CO_3 (5.88 g, 18.04 mmol) in DMF (350 mL) at 55 °C. The mixture was stirred at the same temperature for another 48 hours. The reaction mixture was cooled, filtered and solvent was removed under reduced pressure. The residue was taken

in CH_2Cl_2 (100 mL), washed with saturated aqueous NH_4Cl solution (2 × 30 mL) and dried over anhydrous Na_2SO_4. The solvent was removed under reduced pressure, and the residue was purified by silica gel column chromatography (silica gel, ethyl acetate/petrol, 4:1) to give macrocycle **1** (0.95 g, 35%) as colourless solid. Melting point 118-120 °C; ^{1}H NMR (400 MHz, $CDCl_3$) δ 7.68 (t, J = 7.9 Hz, 1H, H_a), 7.35 (d, J = 7.8 Hz, 2H, H_b), 7.23 (d, J = 8.3 Hz, 4H, H_e), 6.83 (d, J = 8.6 Hz, 4H, H_f), 6.48 (s, 2H, H_k), 6.36 (s, 1H, H_j), 4.60 (s, 4H, H_d), 4.55 (d, J = 4.3 Hz, 2H, H_l), 4.37 (s, 4H, H_c), 4.20 – 4.02 (m, 8H, H_g, H_i), 2.21 (p, J = 5.9 Hz, 4H, H_h), 1.91 (t, J = 5.7 Hz, 1H, H_m). ^{13}C NMR (100 MHz, $CDCl_3$) δ 160.42, 158.82, 157.90, 143.46, 137.25, 130.14, 129.80, 119.92, 114.60, 104.95, 101.34, 72.34, 71.19, 65.38, 64.31, 64.21, 29.39; HR-ESMS: *m/z* = 594.2462 [**1**+Na]$^+$ (calc. for $C_{34}H_{37}NO_7Na$, 594.2451); Anal. calc. for $C_{34}H_{37}NO_7$: C, 71.43; H, 6.52; N, 2.45. Found: C, 71.20; H, 6.58; N, 2.43.

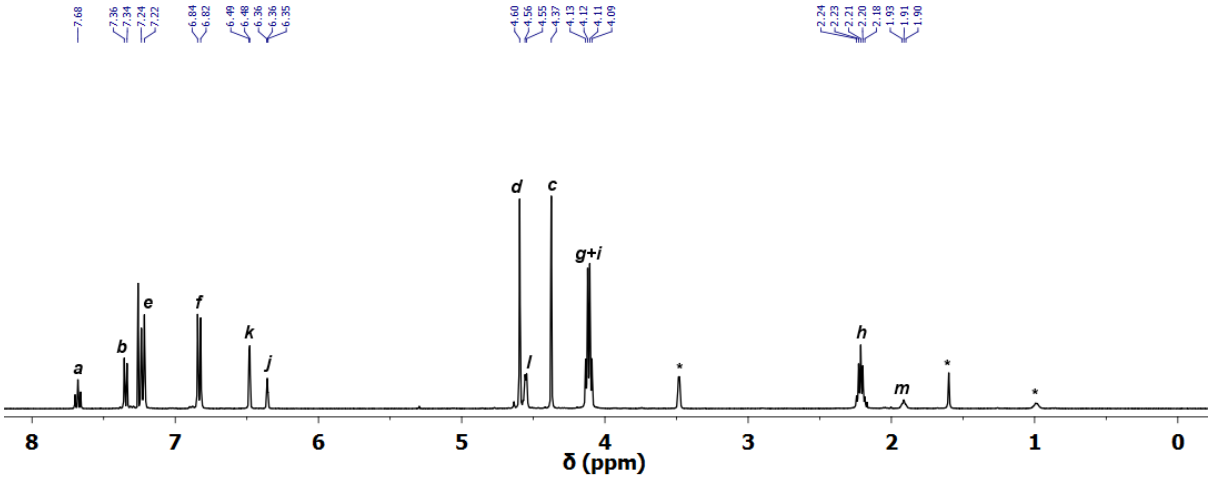

Figure S 7 ^{1}H NMR spectrum (400 MHz, $CDCl_3$, 298K) of **1** (* peaks due to H_2O and methanol).

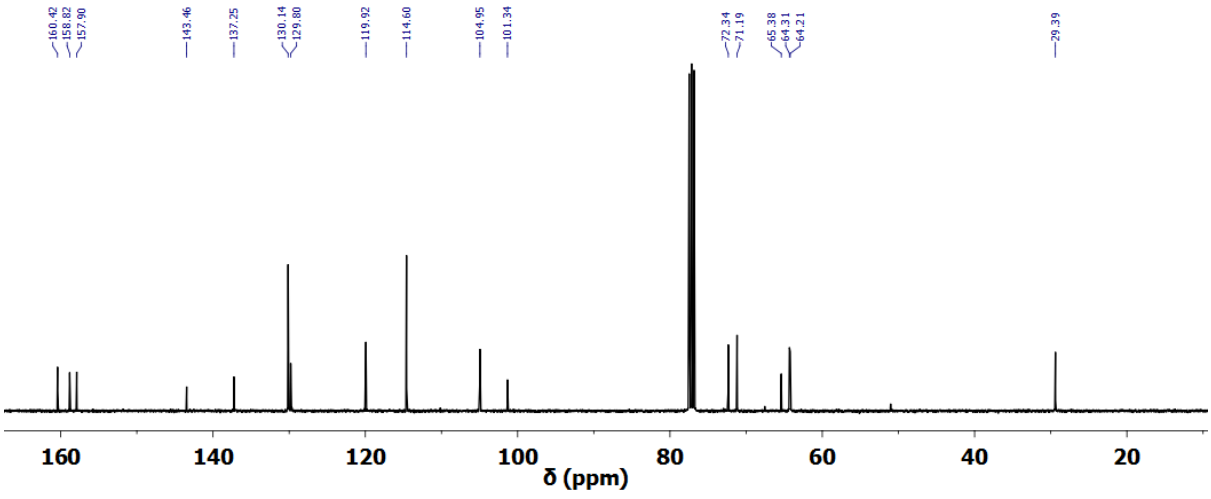

Figure S 8 ^{13}C NMR spectrum (100 MHz, $CDCl_3$, 298K) of **1**.

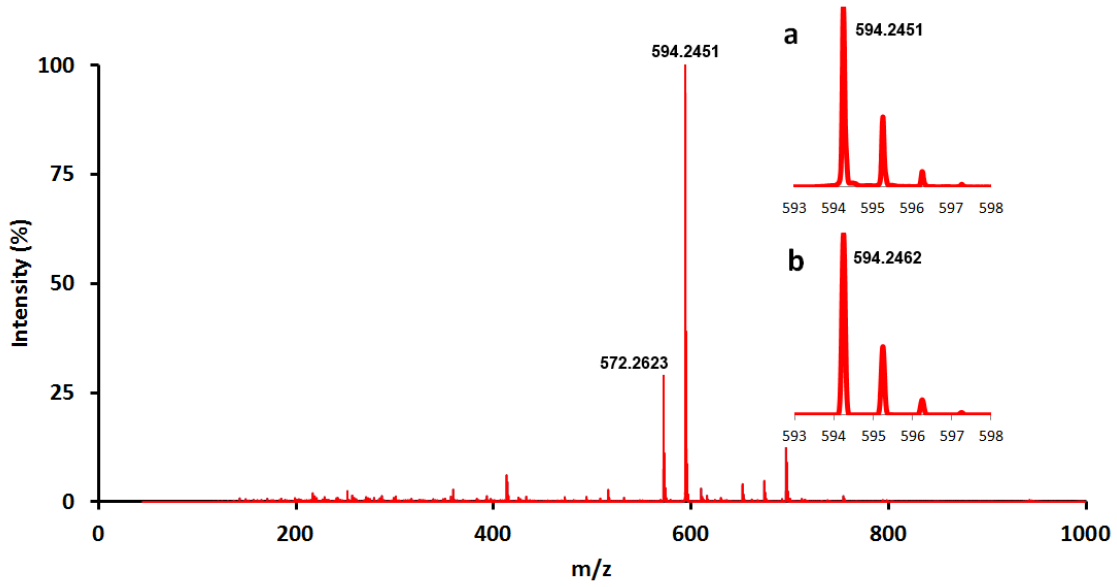

Figure S 9 HR-ESMS spectrum of **1**, inset a) observed and b) calculated isotopic patterns for $[\mathbf{1}+Na]^+$ at *m/z* = 594.2462, also showing peaks due to $[\mathbf{1}+H]^+$ ions at *m/z* = 572.2623.

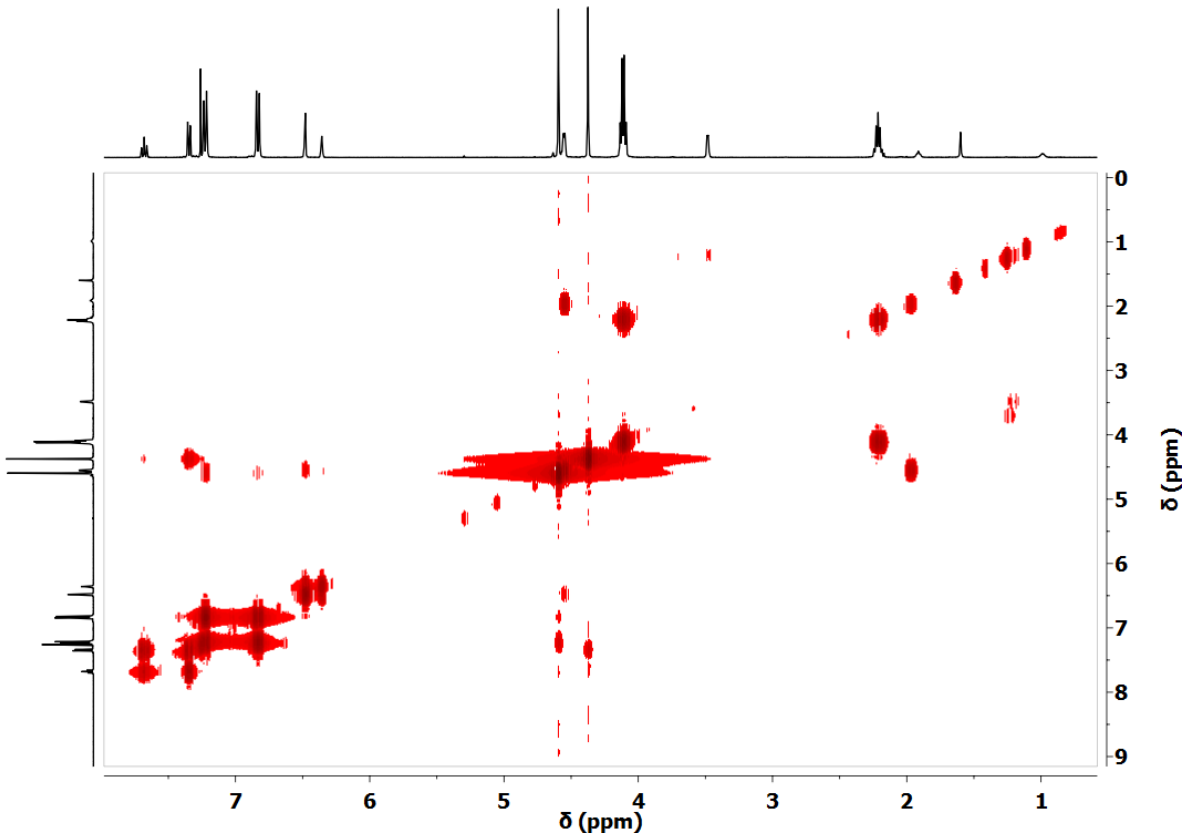

Figure S 10 ^1H COSY NMR spectrum (400 MHz, $CDCl_3$, 298K) of **1**.

2.4 Ag(I) complex of macrocycle 1-Ag

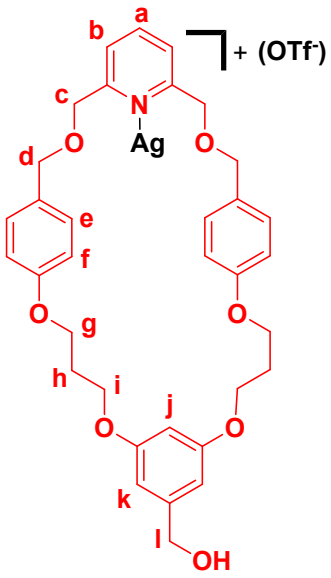

A solution of macrocycle **1** (25 mg, 0.044 mmol) and AgOTf (11 mg, 0.044 mmol) in methanol (10 ml) was stirred at RT for 1 h. The solution was concenrated to 2 mL, and then was vapour diffused with diethyl ether to obtain X-ray quality crystals of **1-Ag**. ^{1}H NMR (400 MHz, acetone-d_6) δ 8.06 (t, J = 7.7 Hz, 1H, H_a), 7.55 (d, J = 7.8 Hz, 2H, H_b), 7.21 (d, J = 8.5 Hz, 4H, H_e), 6.81 (d, J = 8.6 Hz, 4H, H_f), 6.59 (d, J = 2.3 Hz, 2H, H_k), 6.39 (t, J = 2.3 Hz, 1H, H_j), 4.68 (s, 4H, H_d), 4.57 (d, J = 5.3 Hz, 2H, H_l), 4.49 (s, 4H, H, H_c), 4.17 (t, J = 5.9 Hz, 4H, H_g), 4.12 (t, J = 5.7 Hz, 4H, H_i), 2.20 (p, J = 5.8 Hz, 4H, H_h); HR-ESMS: *m/z* = 678.1615 [**1**+**Ag**]$^+$ (calc. for $C_{34}H_{37}AgNO_7$, 678.1578).

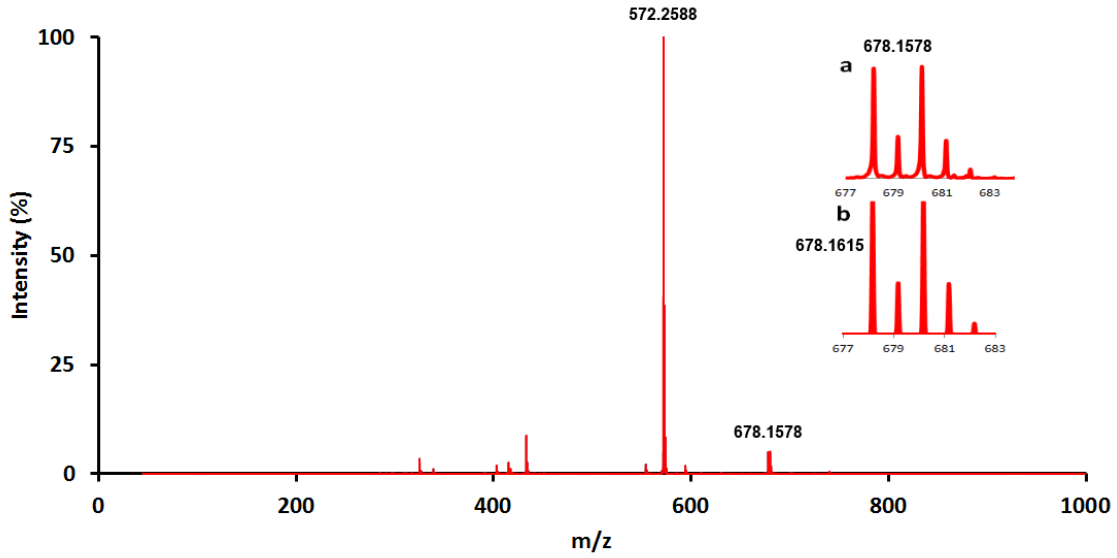

Figure S 11 HR-ESMS spectrum of **1-Ag**, inset a) observed and b) calculated isotopic patterns for [**1-Ag**]$^+$ at *m/z* = 678.1578, also showing peaks due to [**1**+H]$^+$ ions at *m/z* = 572.2588.

2.5 Cu(I) complex of macrocycle 1-Cu

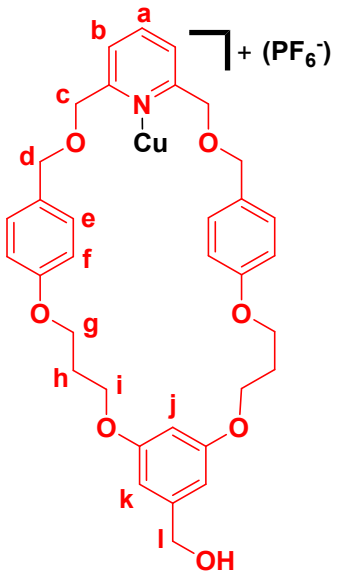

A solution of macrocycle **1** (25 mg, 0.044 mmol) and $[Cu(CH_3CN)_4](PF_6)$ (16 mg, 0.044 mmol) in acetonitrile (10 ml) was stirred at RT for 1 h. The solution was concentrated to 2 mL, and then vapour diffused with diethyl ether to generate small colourless crystals of **1-Cu**. ^{1}H NMR (400 MHz, acetone-d_6) δ 8.09 (t, J = 7.7 Hz, 1H, H_a), 7.60 (d, J = 7.9 Hz, 2H, H_b), 7.31 (d, J = 8.7 Hz, 4H, H_e), 6.93 (d, J = 8.1 Hz, 4H, H_f), 6.58 (s, 2H, H_k), 6.38 (s, 1H, H_j), 4.76 (s, 4H, H_d), 4.64 (s, 4H, H_c), 4.57 (s, 2H, H_l), 4.17 (d, J = 6.5 Hz, 8H, H_g, H_i),

2.35 – 2.13 (m, 4H, H_h); HR-ESMS: *m/z* = 634.1861 [**1**+**Cu**]$^+$ (calc. for $C_{34}H_{37}CuNO_7$, 634.1811).

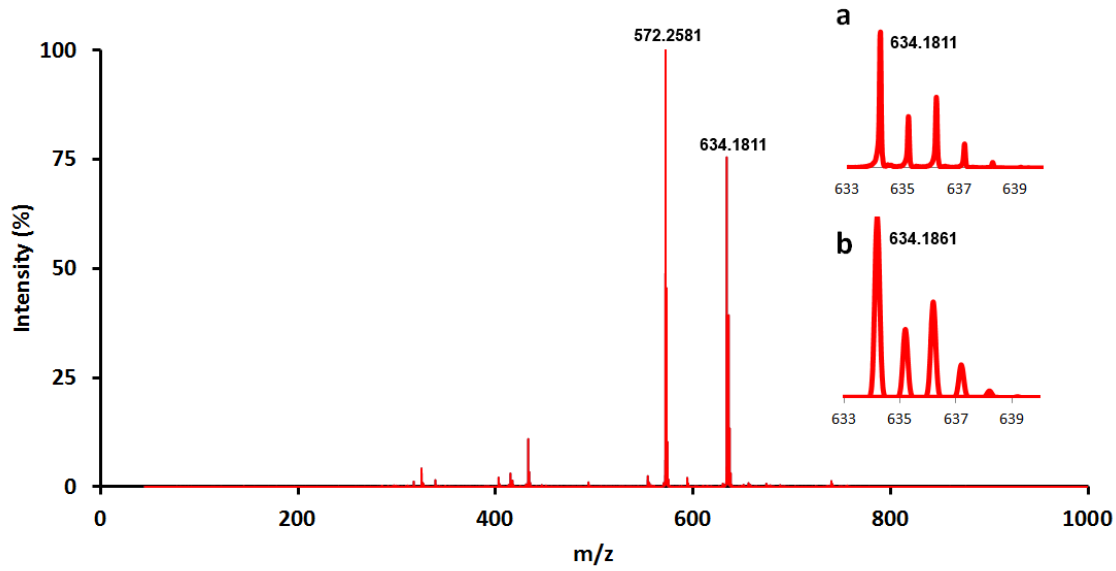

Figure S 12 HR-ESMS spectrum of **1-Cu**, inset a) observed and b) calculated isotopic patterns for [**1-Cu**]$^+$ at *m/z* = 634.1811, also showing peaks due to [**1**+H]$^+$ ions at *m/z* = 572.2581.

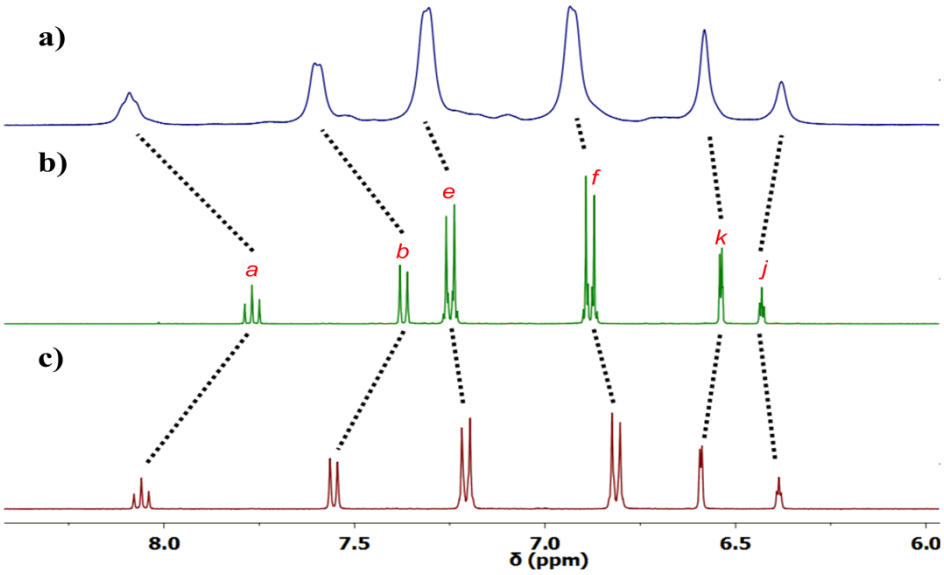

Figure S 13 Partial stacked ^{1}H NMR spectra (400 MHz, acetone-d_6, 298K) of a) **1-Cu**, b) **1** and c) **1-Ag**.

2.6 Stopper S10

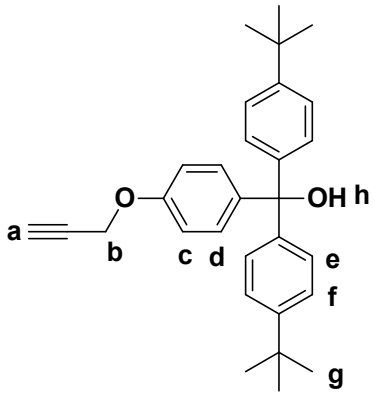

Mg turnings (3.37 g, 137 mmol) were cleaned by ultra-sonication for 30 min in ether, and then were vacuum dried and placed in a two neck flask fitted with a condenser, dropping funnel and a nitrogen inlet. The assembly was evacuated and flushed with nitrogen three times, and then THF (500 mL) was added followed by a dropwise addition of 4-tert-butylphenyl bromide **S9** (22.41 mL, 126 mmol) at RT. The mixture was then refluxed for a further 4 h until all solid Mg disappeared. The mixture was cooled to 0 °C and **S8** (8.0 g, 42.1 mmol) in THF (50 mL) was added dropwise. The reaction mixture was then refluxed for further a 24 h. Water (200 mL) was added and the resulting solution was acidified with dilute HCl (50 mL). The mixture was extracted with CH_2Cl_2 (3 × 200 ml) and combined organic layers were washed with saturated NH_4Cl (200 mL) and brine (200 mL) and then dried over $MgSO_4$. The solvent of the organic layer was removed under reduced pressure and the residue was purified by column chromatography (silica gel, ethyl acetate/petrol, 1:10) to give **S10** (15.32 g, 85%) as yellow oil that solidified upon standing. ^{1}H NMR (400 MHz, $CDCl_3$) δ 7.32 (d, *J* = 8.7 Hz, 4H, H_f), 7.22 (d, *J* = 8.8 Hz, 2H, H_d), 7.18 (d, *J* = 8.7 Hz, 4H, H_e), 6.91 (d, *J* = 8.8 Hz, 2H, H_c), 4.68 (d, *J* = 2.4 Hz, 2H, H_b), 2.70 (s, 1H, H_h), 2.51 (t, *J* = 2.4 Hz, 1H, H_a), 1.31 (s, 18H, H_g); ^{13}C NMR (100 MHz, $CDCl_3$) δ 156.71, 150.07, 144.27, 140.59, 129.30, 127.64, 124.89, 114.15, 81.52, 78.78, 75.63, 55.96, 34.60, 31.50; HR-ESMS: *m/z* = 449.2451 [**S10**+Na]$^+$ (calc. for $C_{30}H_{34}NaO_2$, 449.2483); Anal. calc. for $C_{30}H_{34}O_2$: C, 84.47; H, 8.03; found: C, 84.48; H, 8.09.

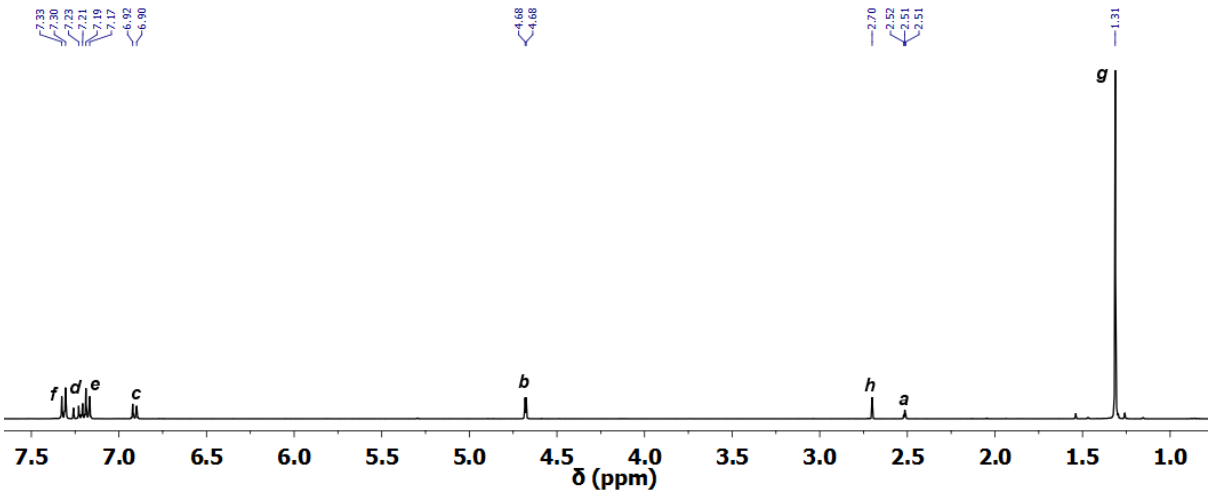

Figure S 14 ^{1}H NMR spectrum (400 MHz, $CDCl_3$, 298K) of **S10**.

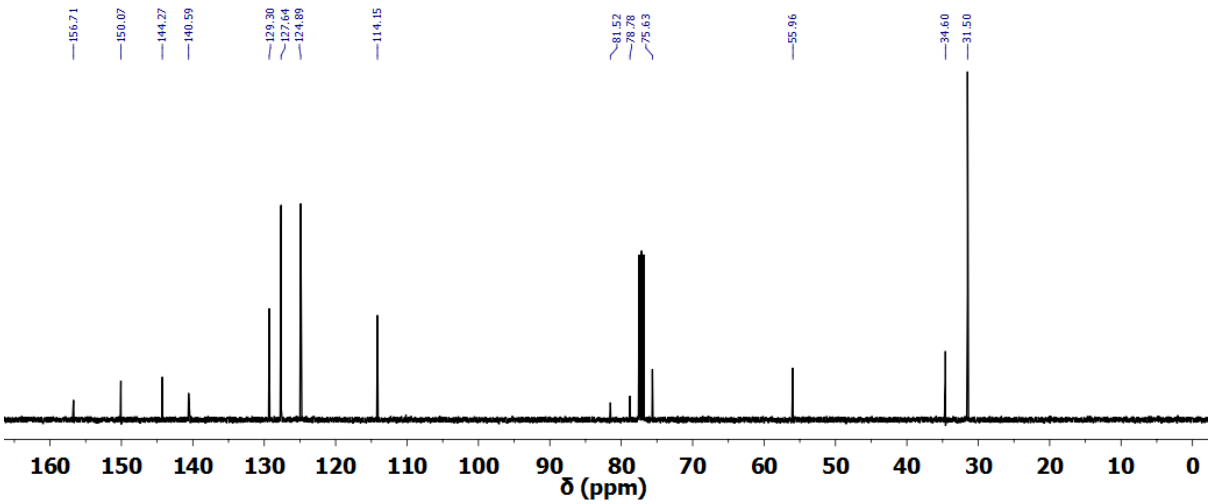

Figure S 15 ^{13}C NMR spectrum (100 MHz, $CDCl_3$, 298K) of **S10**.

2.7 Stopper S11

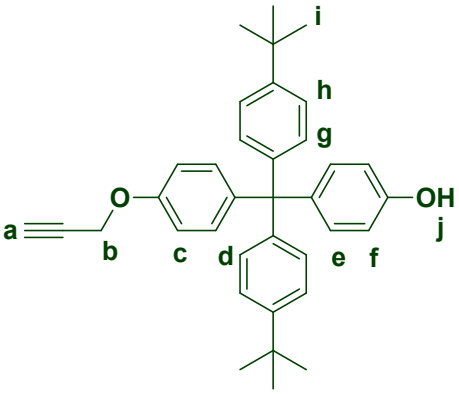

A solution of **S10** (14 g, 32.8 mmol) in acetyl chloride (75 mL) was refluxed for 24 h, and then was cooled to RT. Unreacted acetyl chloride was removed under reduced pressure and phenol (34.0 g, 361 mmol) was added to the residue. The mixture was heated at 100 °C for a further 24 h. After cooling to RT, the solid was washed with hot water (3 × 100 mL) and cold water (3 × 100 mL), followed by 1% sodium hydroxide solution (2 × 100 mL) and finally with water (2 × 100 mL) again. The solid was dissolved in CH_2Cl_2 (200 mL) and the resulting solution was dried over $MgSO_4$, and the solvent was removed under reduced pressure. The residue was purified by column chromatography (silica gel, ethyl acetate/petrol, 1:4) to give **S11** (11.11 g, 67%) as yellow solid. Melting point 60-62 °C; ^{1}H NMR (500 MHz, $CDCl_3$) δ 7.23 (d, J = 8.6 Hz, 4H, H_h), 7.10 (d, J = 8.9 Hz, 2H, H_d), 7.07 (d, J = 8.8 Hz, 4H, H_e), 7.04 (d, J = 8.9 Hz, 2H, H_g), 6.84 (d, J = 8.9 Hz, 2H, H_c), 6.70 (d, J = 8.8 Hz, 2H, H_f), 4.66 (d, J = 2.4 Hz, 2H, H_b), 2.51 (t, J = 2.4 Hz, 1H, H_a), 1.30 (s, 18H, H_i); ^{13}C NMR (125 MHz, $CDCl_3$) δ 155.65, 153.46, 148.57, 144.21, 140.68, 139.92, 132.52, 132.31, 130.77, 124.28, 114.17, 113.55, 78.92, 75.53, 62.96, 55.94, 34.45, 31.52; HR-ESMS: *m/z* = 525.2764 [**S11**+Na]$^+$ (calc. for $C_{36}H_{38}NaO_2$, 525.2788); Anal. calc. for $C_{36}H_{38}O_2$•0.25($CH_3COOC_2H_5$):: C, 84.69; H, 7.68; found: C, 84.78; H, 7.64.

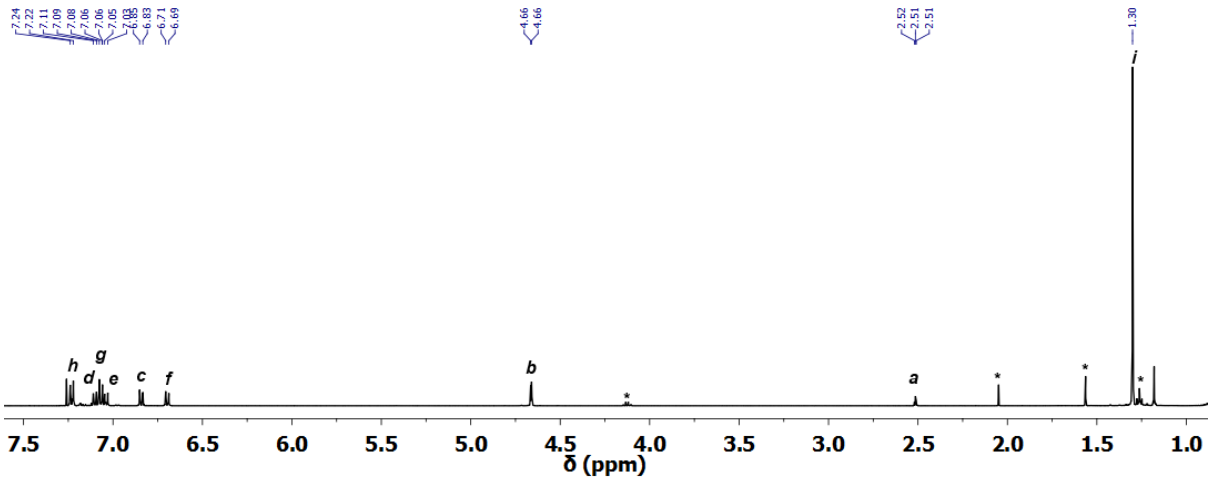

Figure S 16 ^{1}H NMR spectrum (500 MHz, $CDCl_3$, 298K) of **S11** (* peaks due to H_2O and ethyl acetate).

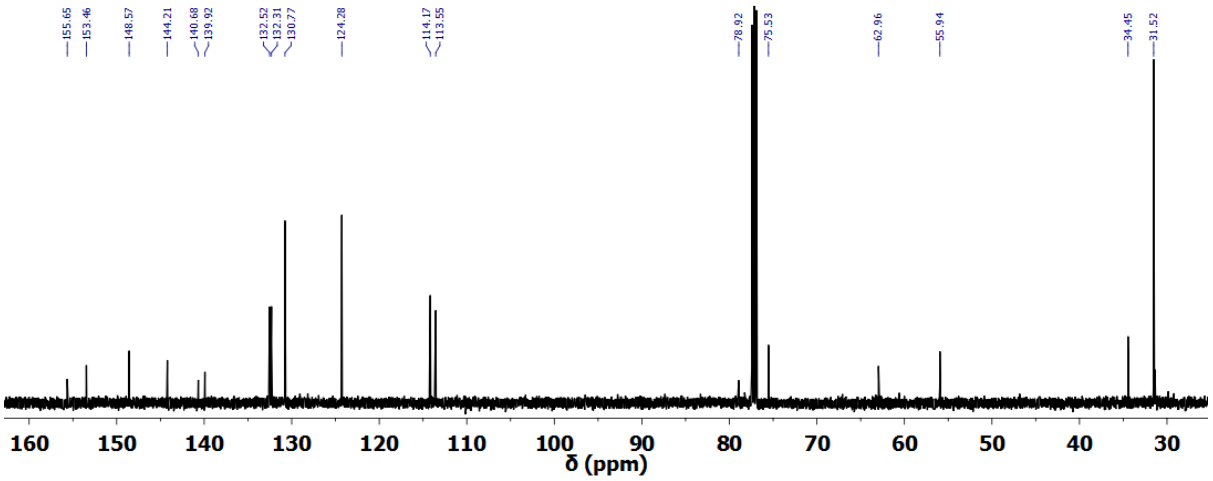

Figure S 17 ^{13}C NMR spectrum (125 MHz, $CDCl_3$, 298K) of **S11**.

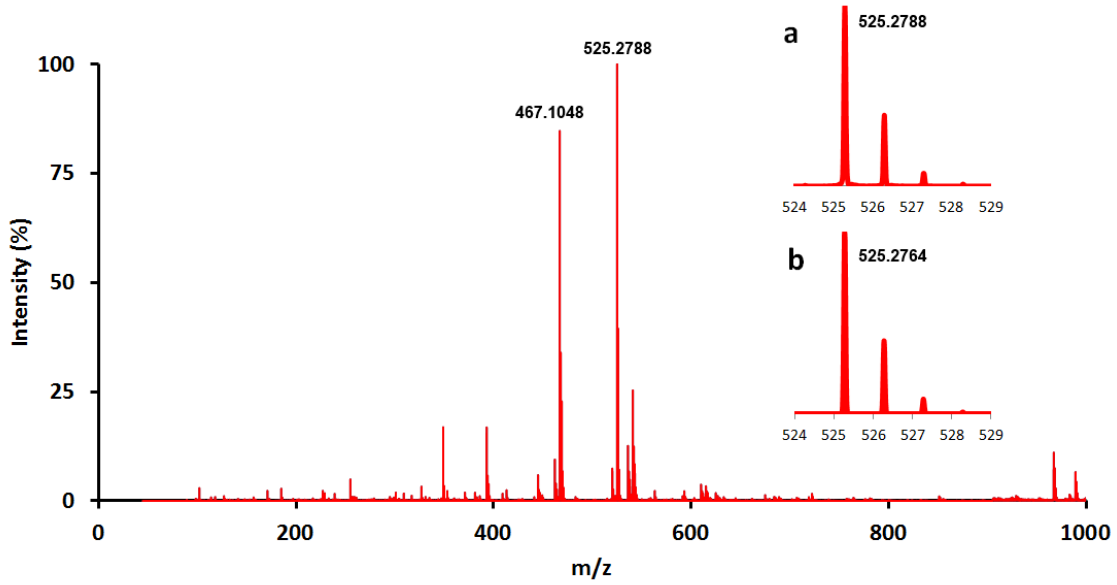

Figure S 18 HR-ESMS spectrum of **S11**, inset a) observed and b) calculated isotopic patterns for [**S11**+Na]$^+$ at *m/z* = 525.2788.

2.8 Stopper 3b

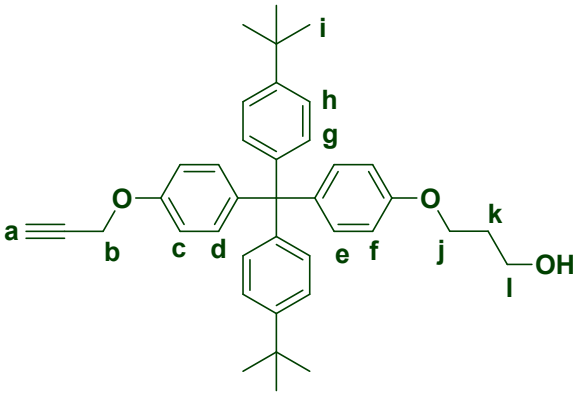

A mixture of **S11** (5.0 g, 10.23 mmol) and K_2CO_3 (4.24 g, 30.7 mmol) in acetone (250 mL) was stirred for 1 h at RT. 3-Bromo-1-propanol (1.11 mL, 12.28 mmol) was added via syringe and the mixture was stirred at reflux for 24 h under a nitrogen atmosphere. The mixture was cooled, filtered and the solvent removed under reduced pressure. The residue was dissolved in CH_2Cl_2 (100 mL) and was washed with water (2 × 50 mL) and brine (2 × 50 mL). The solvent was removed under reduced pressure and the residue was subjected to column chromatography (silica gel, ethyl acetate/petrol, 1:4) to give **3b** (5.12 g, 90%) as colourless solid. Melting point 145-147 °C; ^{1}H NMR (400 MHz, $CDCl_3$) δ 7.23 (d, *J* = 8.6 Hz, 4H, H_h), 7.14 – 7.04 (m, 8H, H_d, H_e, H_g), 6.84 (d, *J* = 8.9 Hz, 2H, H_c), 6.77 (d, *J* = 8.9 Hz, 2H, H_f), 4.66 (d, *J* = 2.4 Hz, 2H, H_b), 4.11 (t, *J* = 5.9 Hz, 2H, H_l), 3.86 (t, *J* = 5.9 Hz,

2H, H_j), 2.51 (t, J = 2.4 Hz, 1H, H_a), 2.03 (p, J = 5.9 Hz, 2H, H_k), 1.30 (s, 18H, H_i); ^{13}C NMR (100 MHz, $CDCl_3$) δ 156.53, 155.47, 148.38, 144.05, 140.51, 139.76, 132.16, 132.14, 130.60, 124.11, 113.37, 113.01, 78.76, 75.36, 65.71, 62.79, 60.70, 55.77, 34.28, 31.99, 31.36; HR-ESMS: *m/z* = 583.3183 [**3b**+Na]$^+$ (calc. for $C_{39}H_{44}NaO_3$, 583.3175); Anal. calc. for $C_{39}H_{44}O_3$: C, 83.53; H, 7.91; Found: C, 83.15; H, 8.14

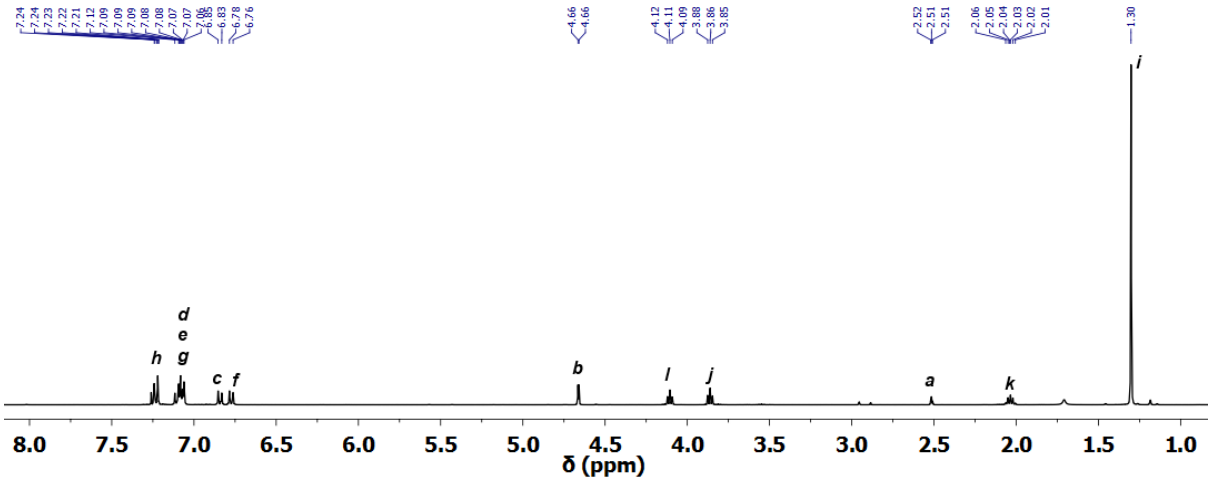

Figure S 19 ^1H NMR spectrum (400 MHz, $CDCl_3$, 298K) of **3b**

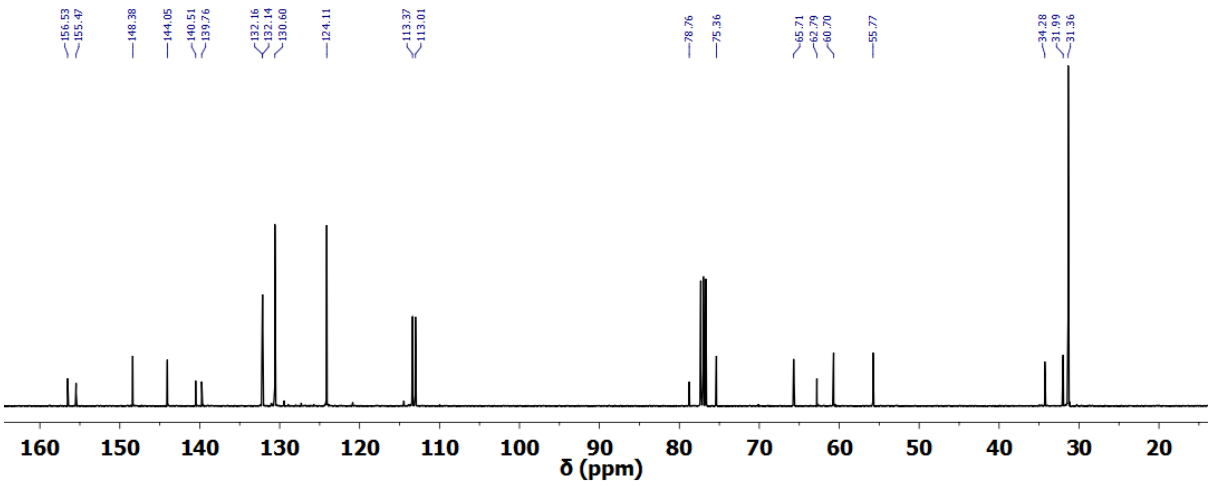

Figure S 20 ^{13}C NMR spectrum (100 MHz, $CDCl_3$, 298K) of **3b**

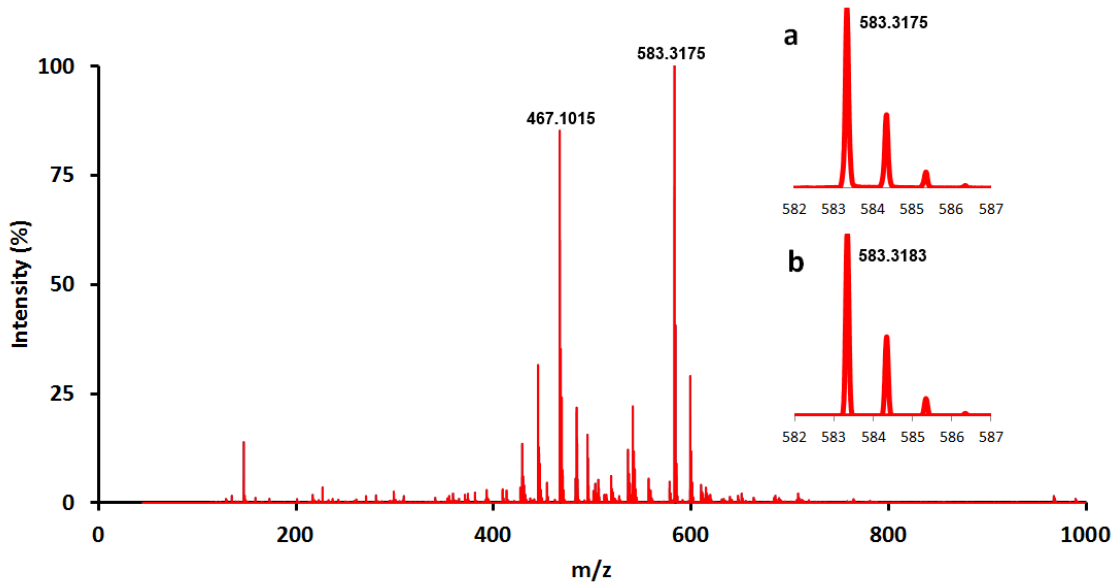

Figure S 21 HR-ESMS spectrum of **3b**, inset a) observed and b) calculated isotopic patterns for [**3b**+Na]$^+$ at *m/z* = 583.3176.

3 Active Template Synthesis of [2]Rotaxanes

3.1 [2]Rotaxane 4a

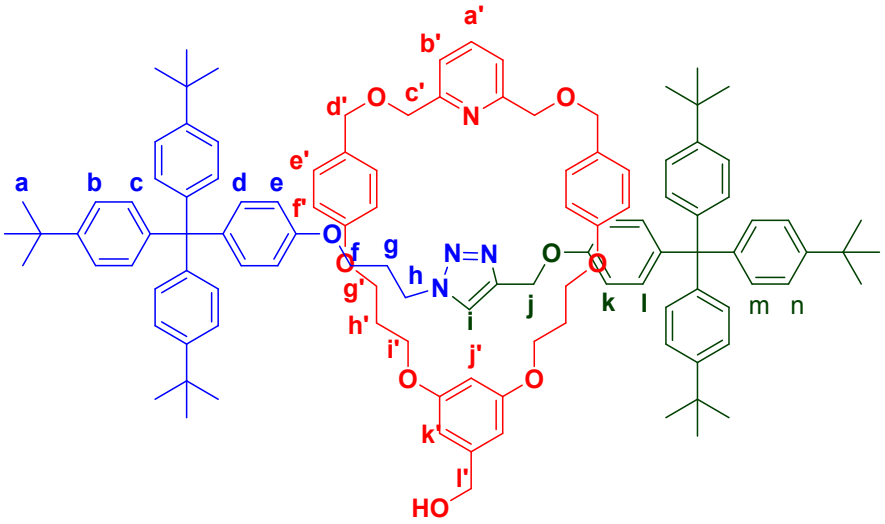

A solution of macrocycle **1** (75 mg, 0.131 mmol) and $[Cu(CH_3CN)_4](PF_6)$ (49 mg, 0.131 mmol) in dry CH_2Cl_2 (10 mL) under nitrogen was stirred for 1 h. The azide **2**[2] (0.386 mg, 0.656 mmol) and the alkyne **3a**[2] (0.356 mg, 0.656 mmol) were then added. The mixture was refluxed for 48 h, and then diluted with CH_2Cl_2 (10 mL), followed by a methanol (10 mL) solution of KCN (85 mg, 1.3 mmol). The resulting suspension was stirred for 2 h then the solvents were evaporated by heating the mixture at 80 ^{0}C in an oil bath. The residue was partitioned between water (50 mL) and CH_2Cl_2 (75 mL) and the layers were separated. The aqueous layer was extracted with CH_2Cl_2 (2 × 75 mL) and the combined organic layers were washed with water (50 mL) and brine (50 mL). After drying over $MgSO_4$, the solvent was removed under reduced pressure and the residue was purified by column chromatography (silica gel, chloroform/methanol, 99:1) to give pure rotaxane **4a** (175 mg, 78%) as colourless solid. Melting point 108-110 °C; ^{1}H NMR (500 MHz, acetone-d_6) δ 7.60 (t, J = 7.7 Hz, 1H, $H_{a'}$), 7.45 (s, 1H, H_i), 7.34 – 7.26 (m, 14H, $H_{b'}$, H_b, H_n), 7.16 – 7.09 (m, 12H, H_c, H_m), 7.04 – 6.94 (m, 8H, H_l. $H_{e'}$, H_d), 6.74 (d, J = 8.9 Hz, 2H, H_k), 6.55 (d, J = 8.6 Hz, 4H, $H_{f'}$), 6.50 (d, J = 2.0, 1.1 Hz, 2H, $H_{k'}$), 6.47 (d, J = 8.9 Hz, 2H, H_e), 6.41 (t, J = 2.3 Hz, 1H, H_j), 4.84 (s, 2H, H_j), 4.49 (s, 2H, $H_{l'}$), 4.47 (s, 4H, $H_{d'}$), 4.25 (s, 4H, $H_{c'}$), 4.08 – 4.00 (m, 4H, $H_{i'}$), 3.96 (t, J = 5.9 Hz, 4H, $H_{g'}$), 3.85 (t, J = 7.1 Hz, 2H, H_h), 3.36 (t, J = 6.0 Hz, 2H, H_f), 2.15 – 2.07 (m, 4H, $H_{h'}$), 1.72 – 1.60 (m, 2H, H_g), 1.30 (s, 27H, H_a or H_o), 1.30 (s, 27H, H_a or H_o).; ^{13}C NMR (125 MHz, acetone-d_6) δ 161.04, 159.47, 158.79, 157.32, 149.11, 149.09, 145.83, 145.81, 145.37, 145.30, 143.97, 140.33, 140.18, 137.81, 132.71, 132.57, 131.47, 131.45,

130.62, 130.48, 125.07, 125.05, 124.54, 120.54, 115.02, 114.26, 114.12, 105.26, 100.93, 72.64, 71.77, 64.98, 64.94, 64.78, 64.71, 64.58, 63.92, 62.09, 47.23, (34.88 x 2), 31.69, 31.69, 30.24, 29.92; HR-ESMS: *m/z* = 1724.9920 [**4a**+Na]$^+$ (calc. for $C_{114}H_{132}N_4NaO_9$, 1724.9792); Anal. calc. for $C_{114}H_{132}N_4O_9$: C, 80.43; H, 7.82; N, 3.29. Found: C, 80.19; H, 7.95; N, 3.27.

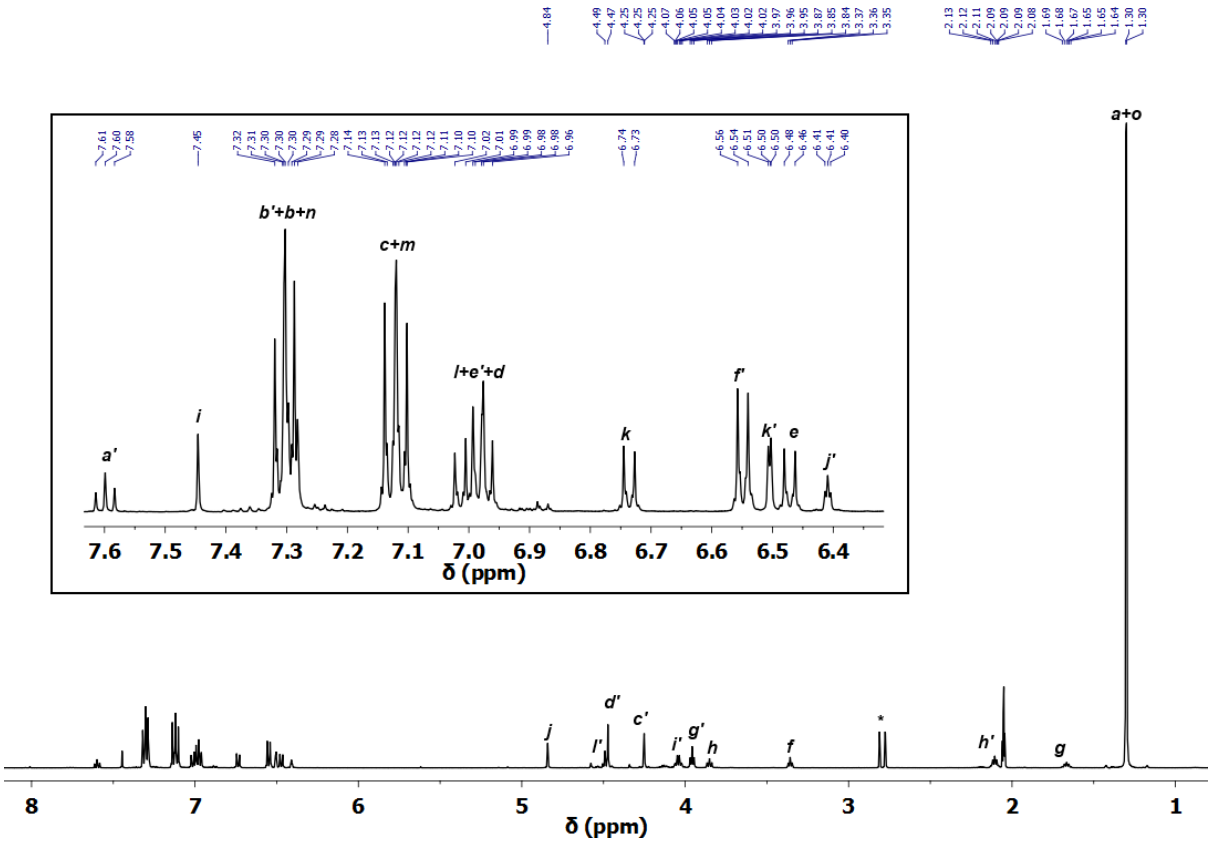

Figure S 22 ^{1}H NMR spectrum (500 MHz, acetone-d_6, 298K) of **4a** (* peaks due to H_2O and methanol).

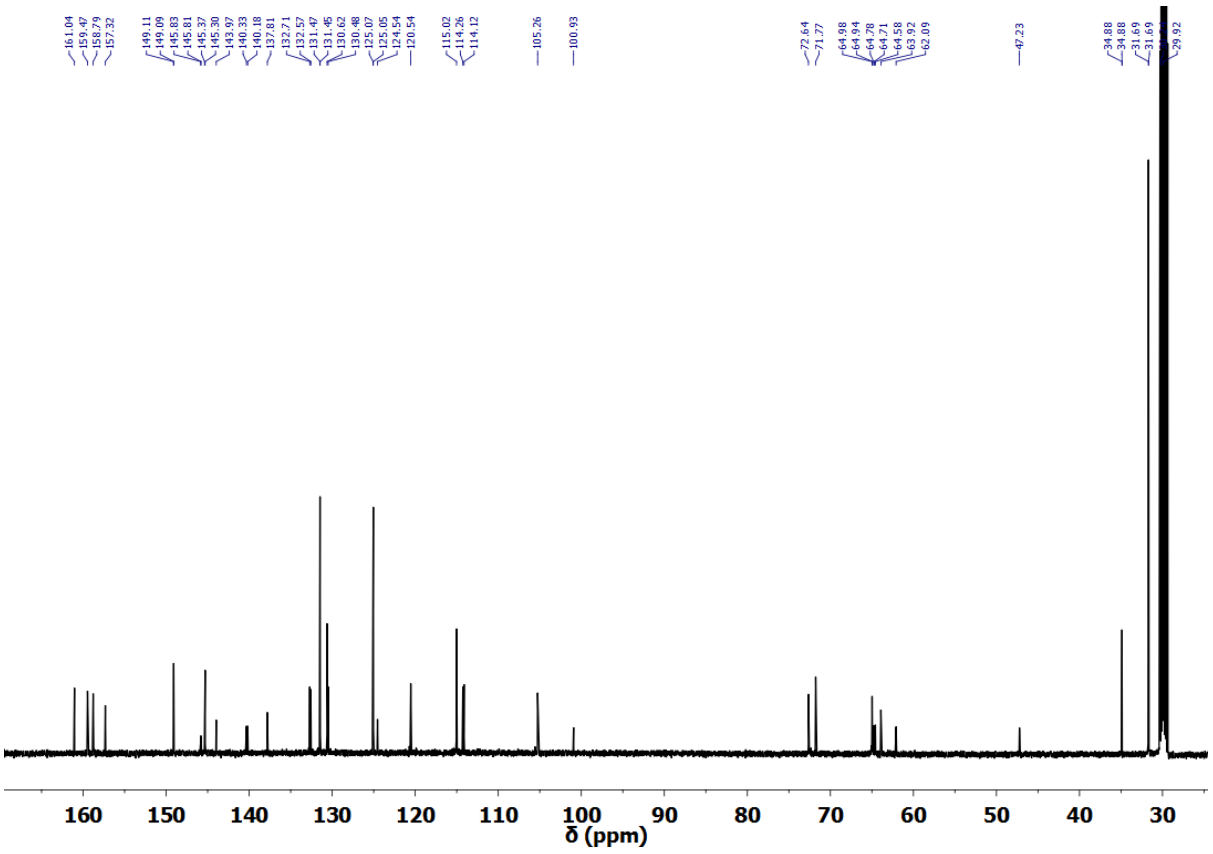

Figure S 23 ^{13}C NMR spectrum (125 MHz, acetone-d_6, 298K) of **4a**

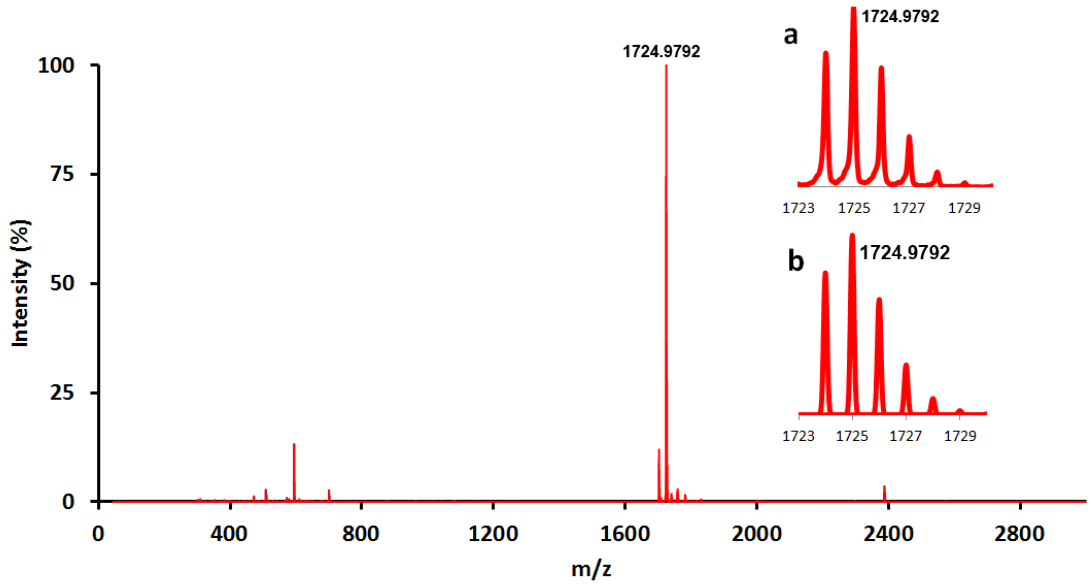

Figure S 24 HR-ESMS spectrum of **4a**, inset a) observed and b) calculated isotopic patterns for [**4a**+Na]$^+$ at *m/z* = 1724.9792.

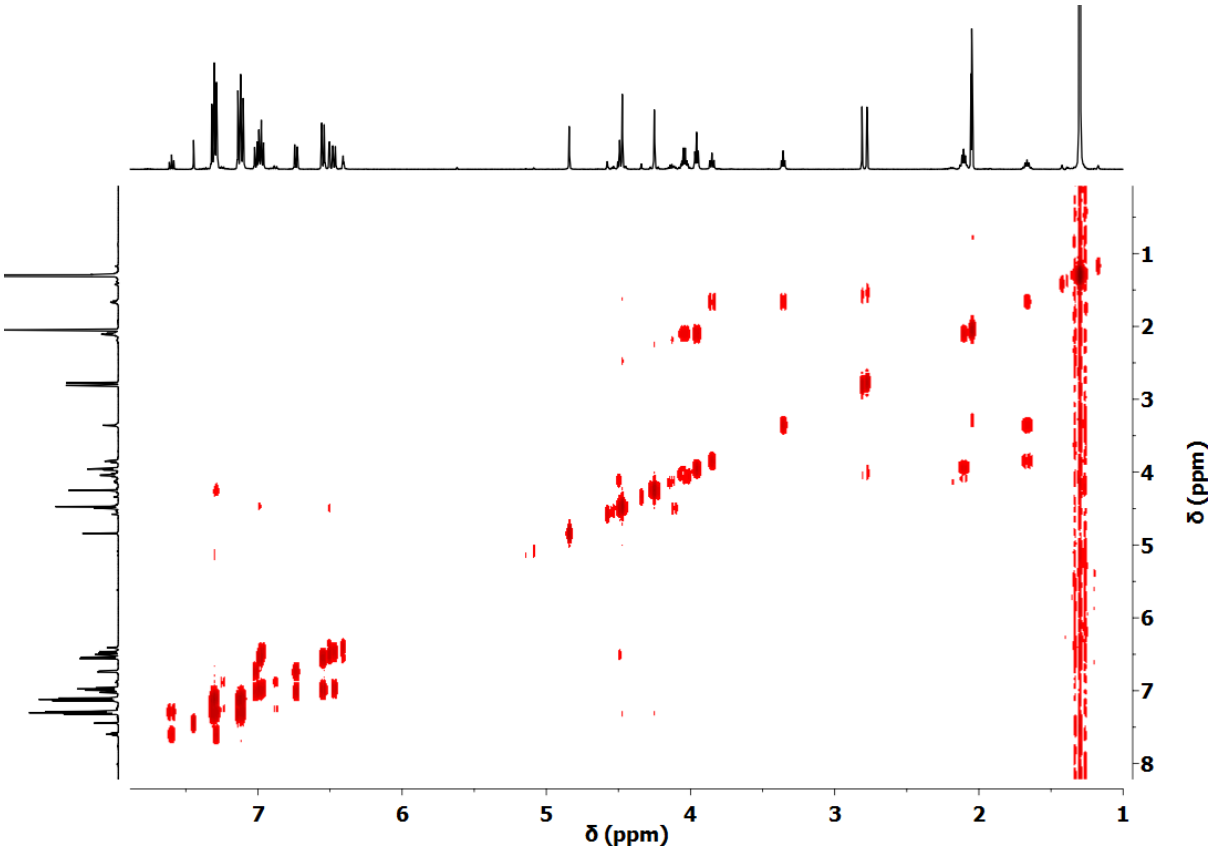

Figure S 25 ^{1}H COSY NMR spectrum (500 MHz, acetone-d_6, 298K) of **4a**

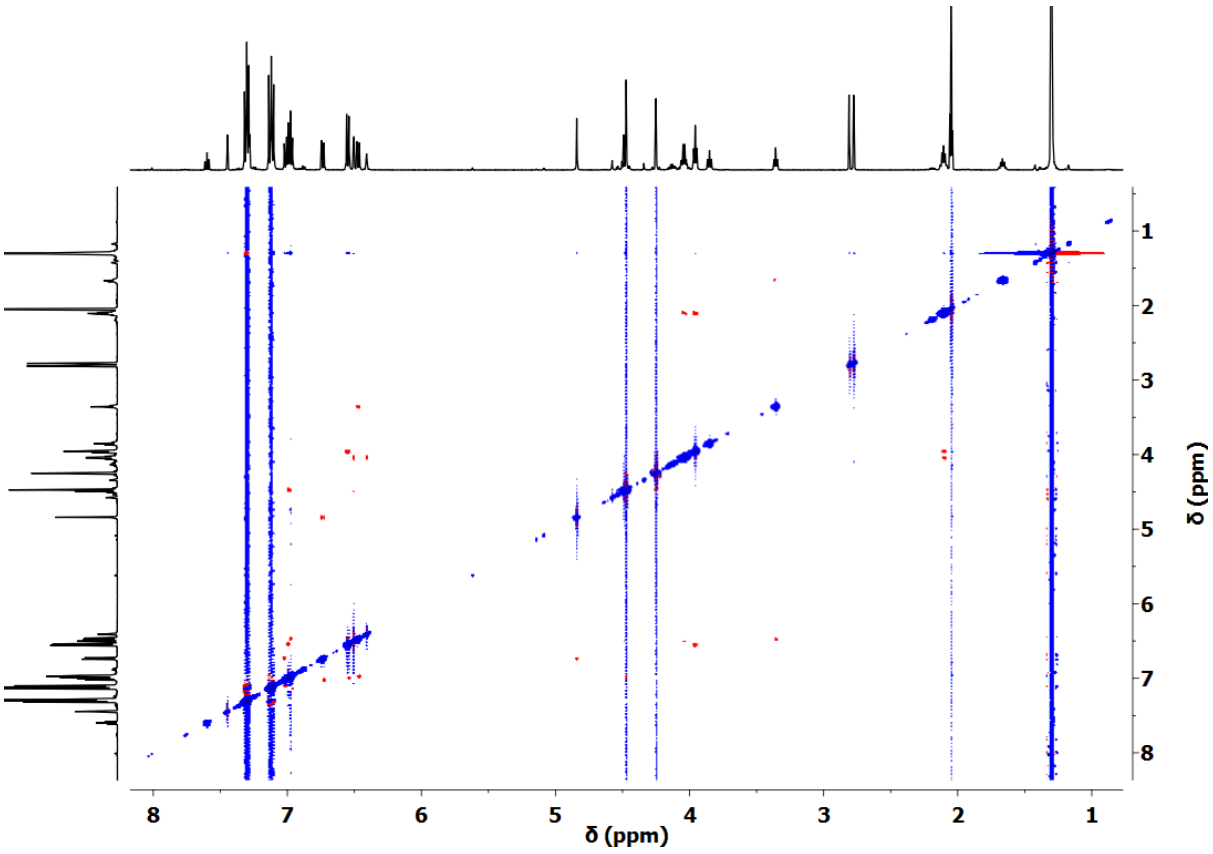

Figure S 26 ^{1}H ROESY NMR spectrum (500 MHz, acetone-d_6, 298K) of **4a**

3.2 [2]Rotaxane 4b

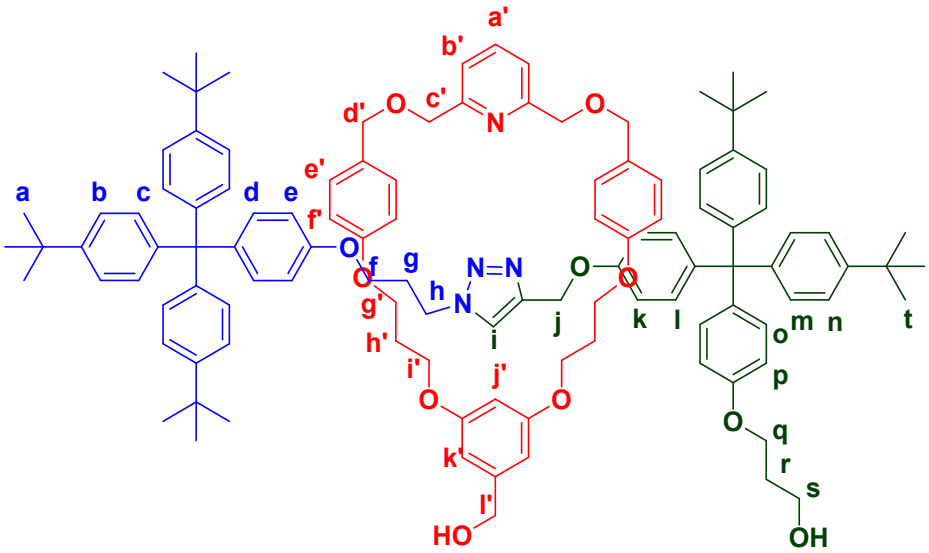

A solution of macrocycle **1** (200 mg, 0.35 mmol) and $[Cu(CH_3CN)_4](PF_6)$ (143 mg, 0.350 mmol) in dry CH_2Cl_2 (20 mL) under a nitrogen atmosphere was stirred for 1 h. The

azide **2**[2] (1028 mg, 1.749 mmol) and the alkyne **3b** (981 mg, 1.749 mmol) were then added. The mixture was refluxed for 48 h then diluted with CH_2Cl_2 (20 mL), followed by a methanol (20 mL) solution of KCN (228 mg, 3.50 mmol). The resulting suspension was stirred for 2 h at room temperature then the solvents evaporated by heating the mixture at 80 ^{0}C in an oil bath. The residue was partitioned between water (50 mL) and CH_2Cl_2 (75 mL) and the layers were separated. The aqueous layer was extracted with CH_2Cl_2 (2 × 75 mL) and the combined organic layers were washed with water (50 mL) and brine (50 mL). After drying over $MgSO_4$, the solvent was removed under reduced pressure and the residue was subjected to column chromatography (silica gel, chloroform/methanol, 99:1) to give pure rotaxane **4b** (432 mg, 72%) as colourless solid. Melting point 110-112 °C; ^{1}H NMR (500 MHz, acetone-d_6) δ 7.61 (t, J = 7.7 Hz, 1H, $H_{a'}$), 7.45 (s, 1H, H_i), 7.34 – 7.26 (m, 12H, $H_{b'}$, H_b, H_n), 7.16 – 7.07 (m, 10H, H_c, H_m), 7.06 (d, J = 9.1, 2.9 Hz, 2H, H_o), 7.04 – 6.93 (m, 8H, H_l, $H_{e'}$, H_d), 6.81 (d, 2H, H_p), 6.75 (d, 2H, H_k), 6.55 (d, 4H, $H_{f'}$), 6.51 (d, J = 2.3 Hz, 2H, $H_{k'}$), 6.47 (d, J = 9.0 Hz, 2H, H_e), 6.41 (t, J = 2.3 Hz, 1H, $H_{j'}$), 4.85 (s, 2H, H_j), 4.49 (s, 2H, $H_{l'}$), 4.48 (s, 4H, $H_{d'}$), 4.25 (unresolved ABq, 4H, $H_{c'}$), 4.10 – 4.00 (m, 6H, H_q, $H_{i'}$), 3.96 (t, J = 5.9 Hz, 4H, $H_{g'}$), 3.85 (t, J = 7.1 Hz, 2H, H_h), 3.72 (td, J = 5.9, 1.9 Hz, 2H, H_s), 3.35 (t, J = 6.0 Hz, 2H, H_f), 2.11 (p, 4H, $H_{h'}$), 1.95 (p, J = 6.2 Hz, 2H, H_r), 1.66 (p, 2H, H_g), 1.30 (s, 27H, H_a), 1.30 (s, 18H, H_t).; ^{13}C NMR (125 MHz, acetone-d_6) δ 161.04, 159.47, 158.79, 158.03, 157.32, 149.08, 145.82, 145.45, 145.37, 143.96, 140.48, 140.18, 140.17, 137.82, 132.80, 132.76, 132.67, 132.57, 132.55, 131.45, 131.43, 130.62, 130.49, 125.07, 125.04, 124.55, 120.55, 115.02, 114.26, 114.12, 114.00, 105.26, 100.93, 72.64, 71.77, 65.43, 64.98, 64.95, 64.78, 64.71, 64.58, 63.92, 63.63, 62.09, 59.09, 58.95, 47.23, 34.88, 34.87, 33.41, 31.69, 31.69 ; HR-ESMS: *m/z* = 1720.9842 [**4b**+**H**]$^+$ (calc. for $C_{113}H_{131}N_4O_{11}$, 1720.9830); Anal. calc. for $C_{113}H_{130}N_4O_{11}$•0.25($CHCl_3$): C, 77.72; H, 7.50; N, 3.20, Found: C, 77.74; H, 7.75; N, 3.19.

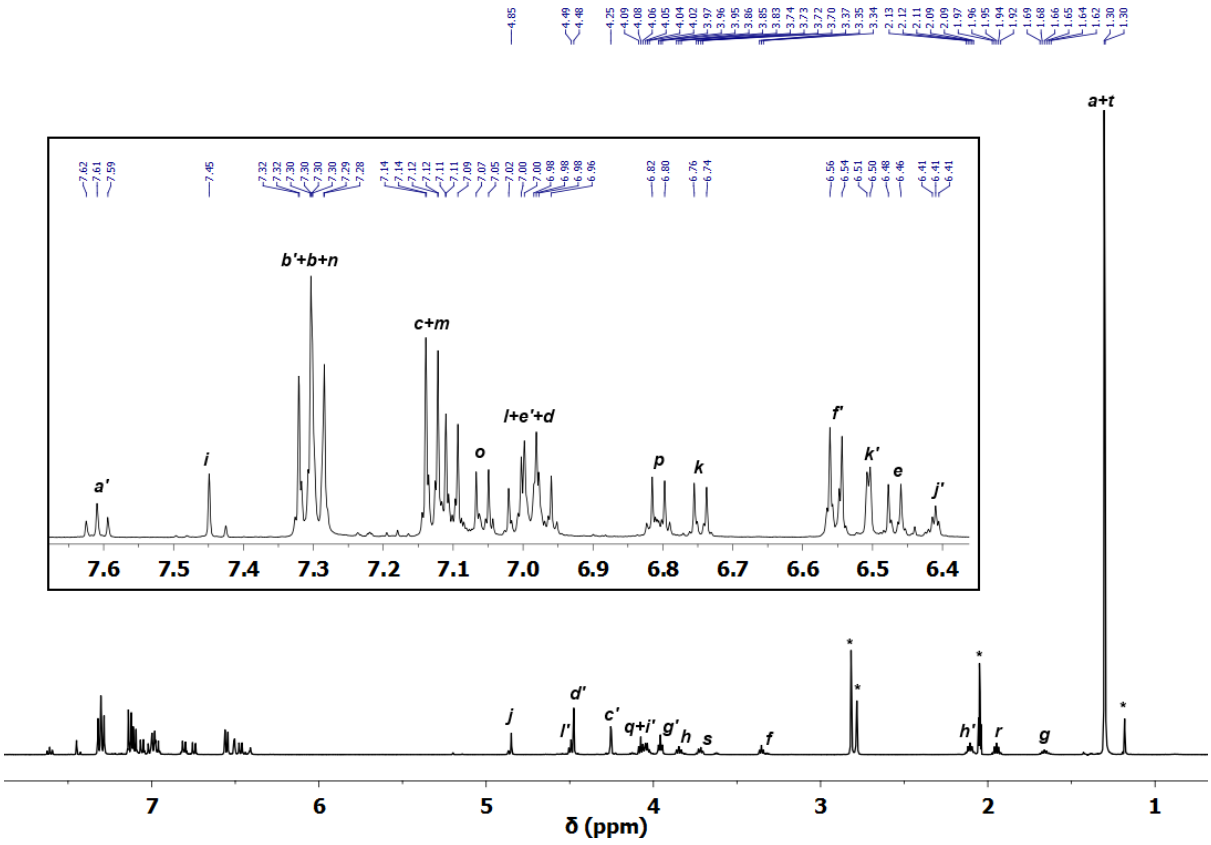

Figure S 27 ^{1}H NMR spectrum (500 MHz, acetone-d_6, 298K) of **4b** (* peaks due to H_2O, acetone and methanol)

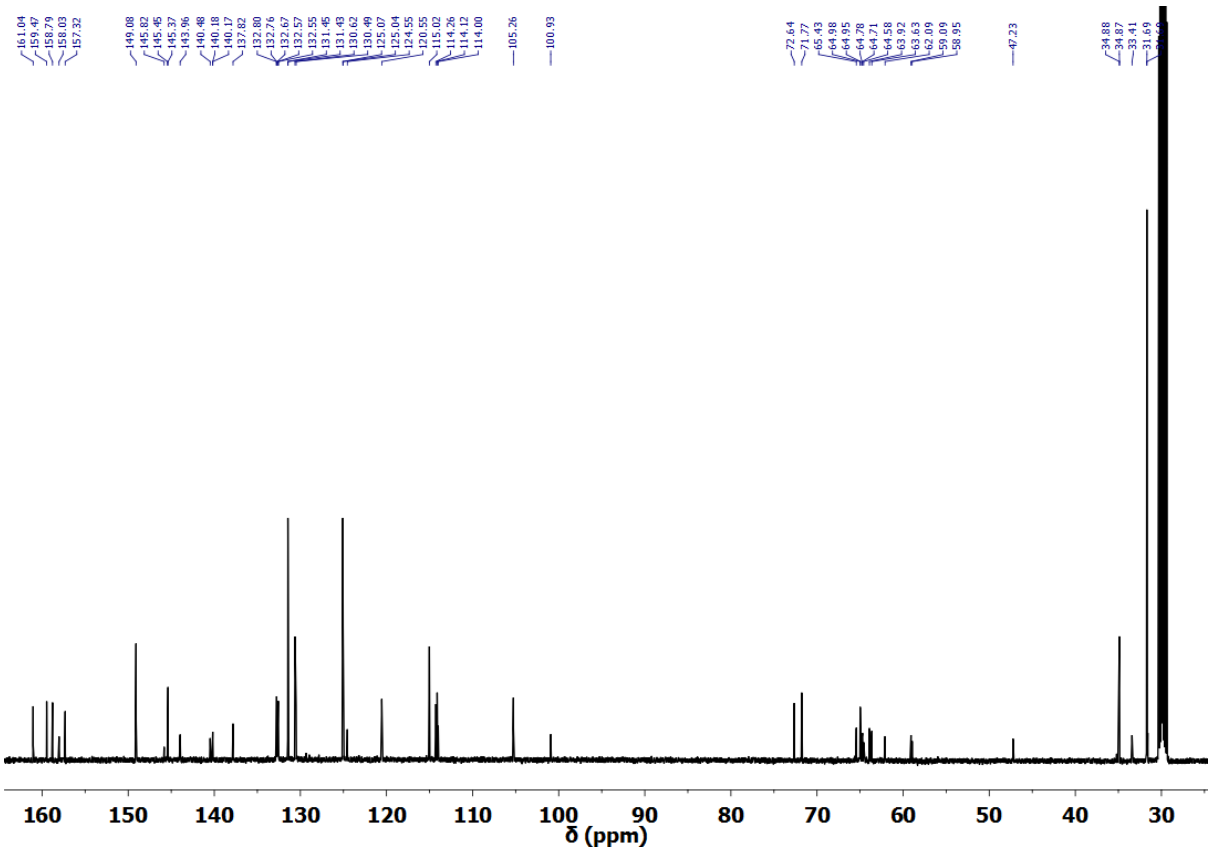

Figure S 28 ^{1}H NMR spectrum (500 MHz, acetone-d_6, 298K) of **4b**

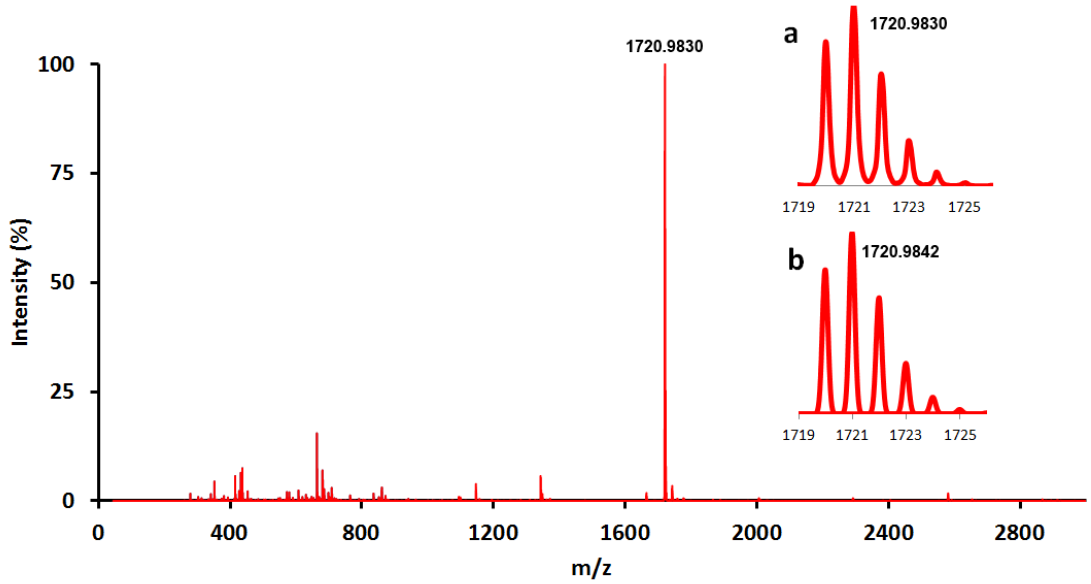

Figure S 29 HR-ESMS spectrum of **4b**, inset a) observed and b) calculated isotopic patterns for [**4b**+H]$^{+}$ at *m/z* = 1720.9830.

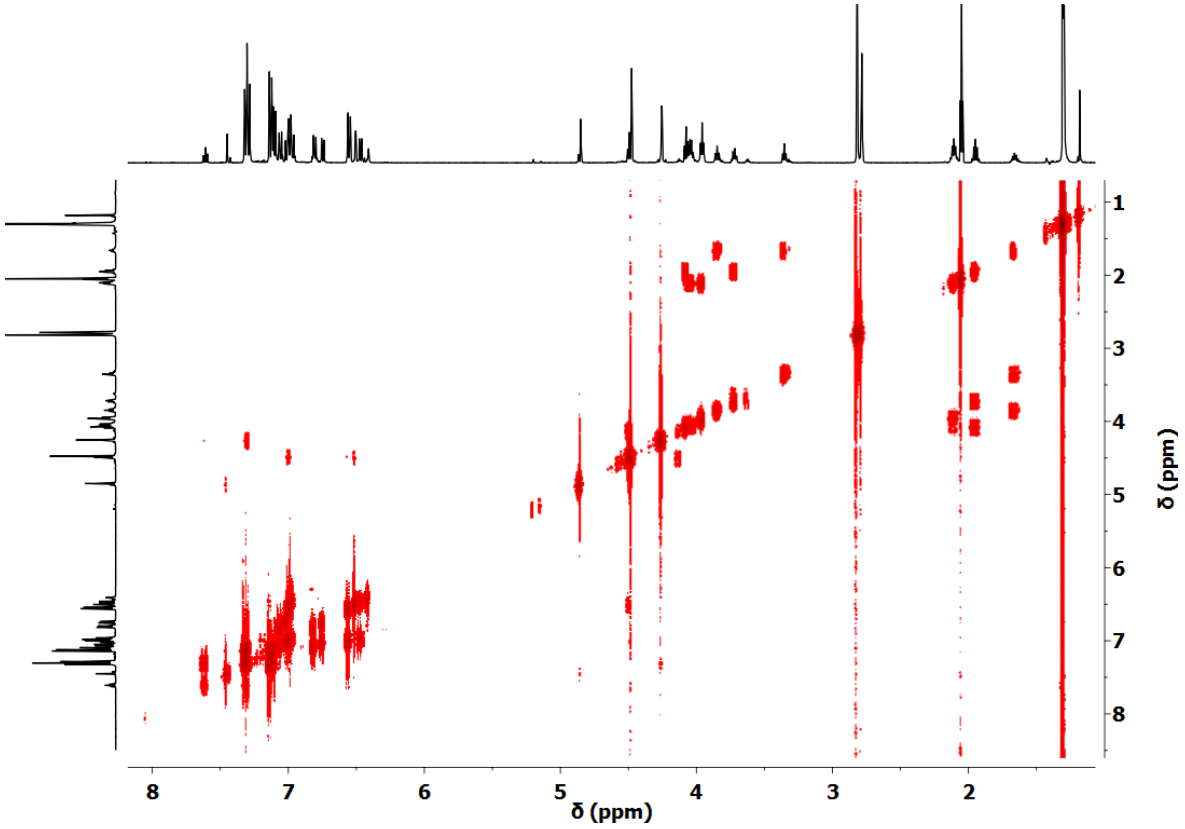

Figure S 30 ^{1}H COSY NMR spectrum (500 MHz, acetone-d_6, 298K) of **4b**

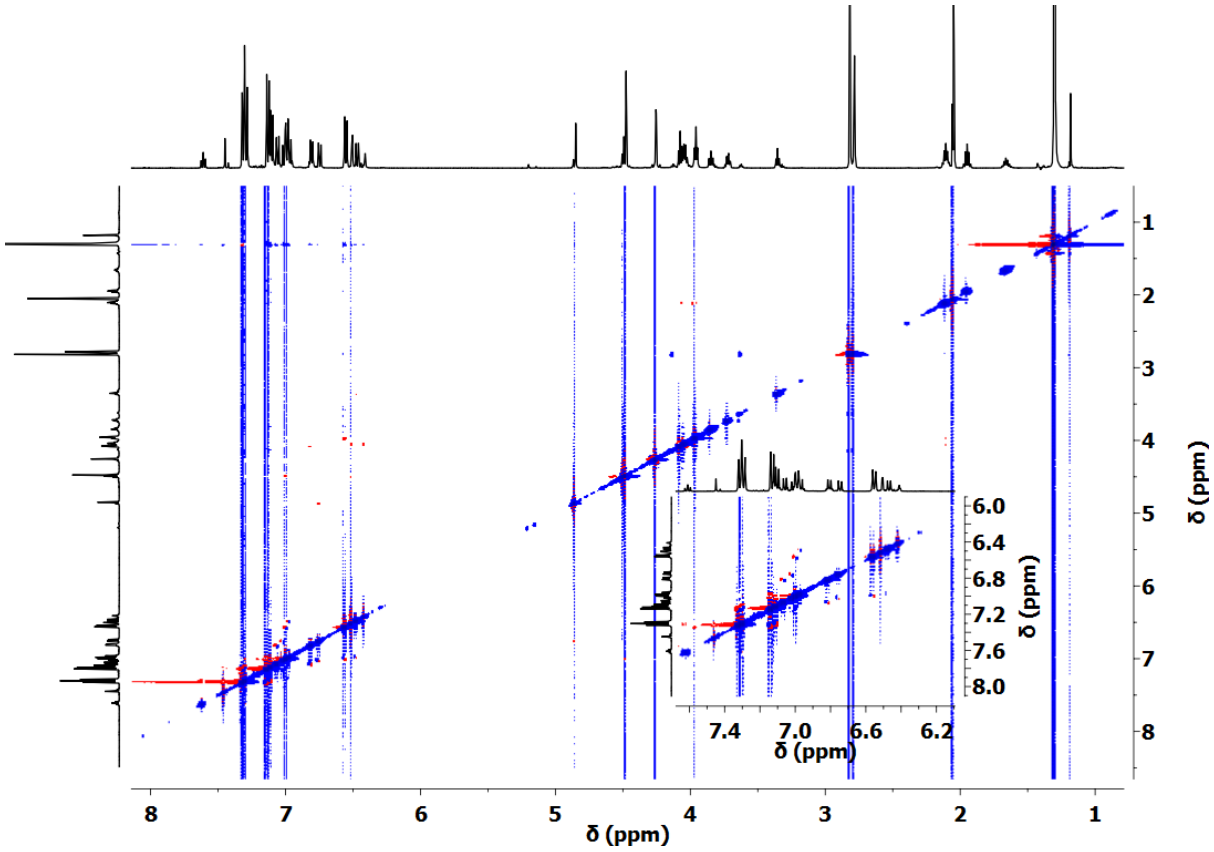

Figure S 31 ^{1}H NOESY NMR spectrum (500 MHz, acetone-d_6, 298K) of **4b**

4 Synthesis of Terpyridine Functionalized [2]Rotaxane Ligands

4.1 Ligand S13[4]

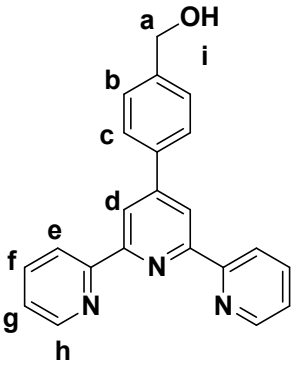

4-(Hydroxymethyl)benzaldehyde **S12** (3.00 g, 22.03 mmol) was dissolved in methanol (400 mL). 2-Acetylpyridine (5.19 mL, 46.3 mmol), NaOH (0.88 g, 22.03 mmol) and aqueous NH_4OH (123 mL. 35%) solution were added. The reaction mixture was refluxed

for 48 h then cooled to RT and neutralized with 2 M HCl. The mixture was concentrated under reduced pressure and the residue was partitioned between ethyl acetate (200 mL) and water (200 mL). The aqueous layer was extracted with ethyl acetate (2 × 200 mL) and the combined organic layers were washed with brine (200 mL) and dried over $MgSO_4$. After removal of solvent under reduced pressure, the crude product was recrystallized with methanol to give **S13** as colourless solid (2.9 g, 39%). ^{1}H NMR (400 MHz, DMSO-d_6) δ 8.80 – 8.75 (m, 2H, H_h), 8.73 (s, 2H, H_d), 8.71 – 8.65 (m, 2H, H_e), 8.09 – 8.00 (m, 2H, H_f), 7.91 (d, J = 8.2 Hz, 2H, H_c), 7.58 – 7.49 (m, 4H, H_b, H_g), 5.33 (t, J = 5.7 Hz, 1H, H_i), 4.61 (d, J = 5.7 Hz, 2H, H_a).; ^{13}C NMR (100 MHz, DMSO-d_6) δ 155.67, 154.97, 149.37, 149.35, 144.18, 137.47, 135.70, 127.29, 126.61, 124.53, 120.93, 117.74, 62.49.; HR-ESMS: *m/z* =362.1264 [**S13**+Na]$^+$ (calc. for $C_{22}H_{17}N_3NaO$, 362.1253).

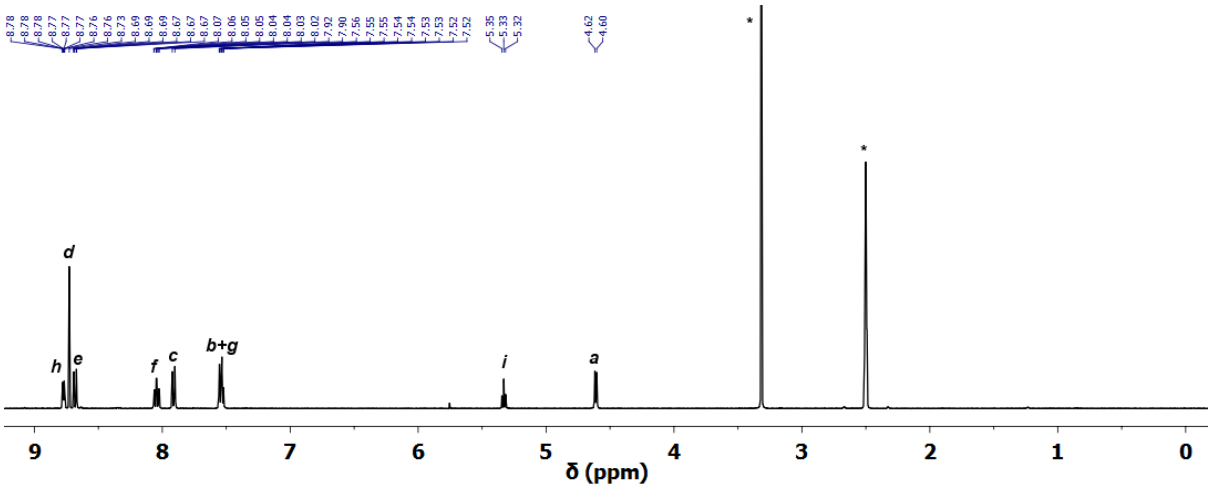

Figure S 32 ^{1}H NMR spectrum (400 MHz, DMSO-d_6, 298K) of **S13** (* peaks due to H_2O and DMSO)

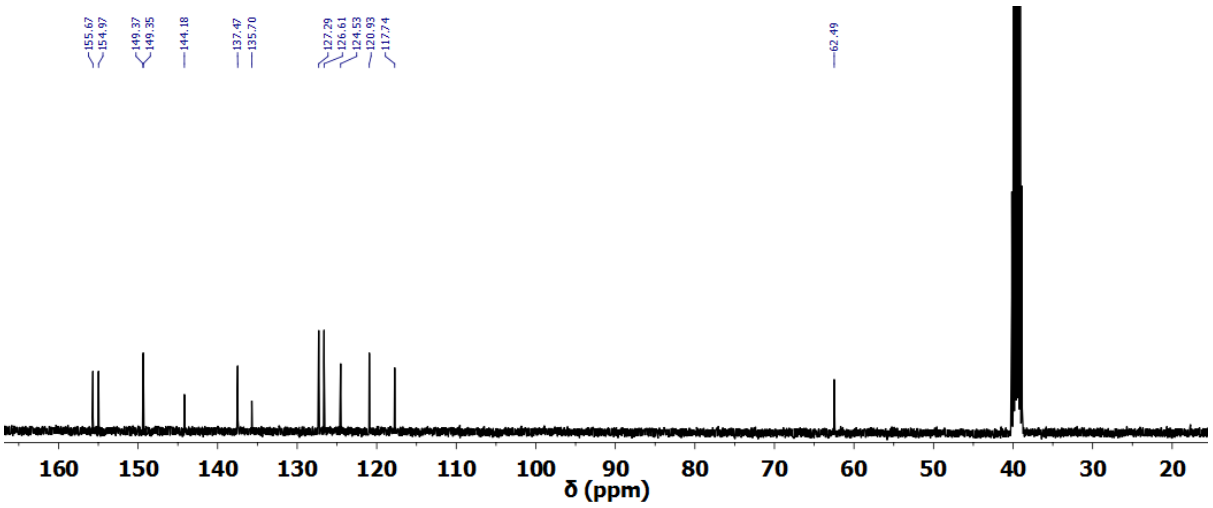

Figure S 33 ^{13}C NMR spectrum (400 MHz, DMSO-d_6, 298K) of **S13**

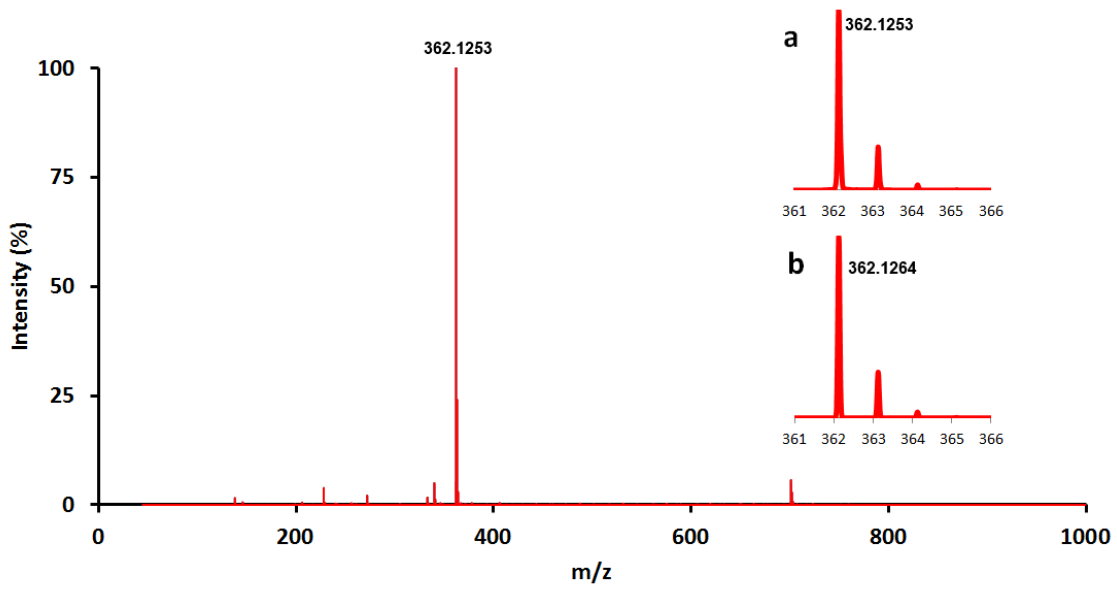

Figure S 34 HR-ESMS spectrum of **S13**, inset a) observed and b) calculated isotopic patterns for [**S13**+Na]$^+$ at *m/z* = 362.1263.

4.2 Ligand S14

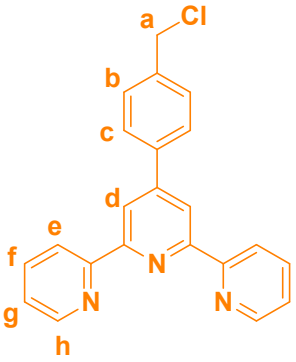

S13 (2.00 g, 5.89 mmol) was dissolved in $SOCl_2$ (10 mL) and the solution was refluxed for 2 h. The mixture was cooled and excess $SOCl_2$ was removed under reduced pressure. The residue was dissolved in chloroform (100 mL) and washed with a 10% aqueous sodium carbonate solution (50 mL) and brine (50 mL). The solvent was removed and the residue was recrystallized from methanol to give **S14** (1.70 g, 81%) as pink crystals. Melting point 140-142 °C; ^{1}H NMR (400 MHz, DMSO-d_6) δ 8.77 – 8.71 (m, 2H, H_h), 8.68 (s, 2H, H_d), 8.66 – 8.61 (m, 2H, H_e), 8.01 (td, J = 7.8, 1.8 Hz, 2H, H_f), 7.92 (d, J = 8.2 Hz, 2H, H_c), 7.63 (d, J = 8.2 Hz, 2H, H_b), 7.50 (ddd, J = 7.5, 4.7, 1.2 Hz, 2H, H_g), 4.85 (s, 2H, H_a).; ^{13}C NMR (100 MHz, DMSO-d_6) δ 155.73, 154.89, 149.35, 148.86, 138.96, 137.47, 137.34, 129.83, 127.22, 124.56, 120.95, 117.89, 45.64; HR-ESMS: m/z = 358.1106 [**S14**+H]$^+$ (calc. for $C_{22}H_{17}N_3Cl$, 358.1109); Anal. calc. for $C_{22}H_{16}ClN_3$: C, 73.84; H, 4.51; N, 11.74; Found: C, 73.77; H, 4.53; N, 11.68.

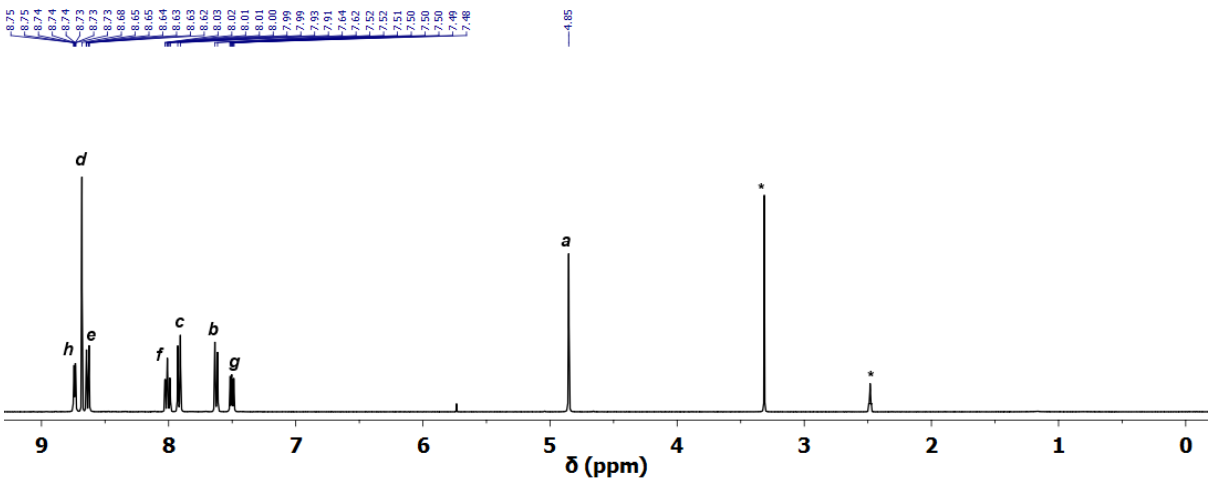

Figure S 35 ^{1}H NMR spectrum (400 MHz, DMSO-d_6, 298K) of **S14** (* peaks due to H_2O and DMSO)

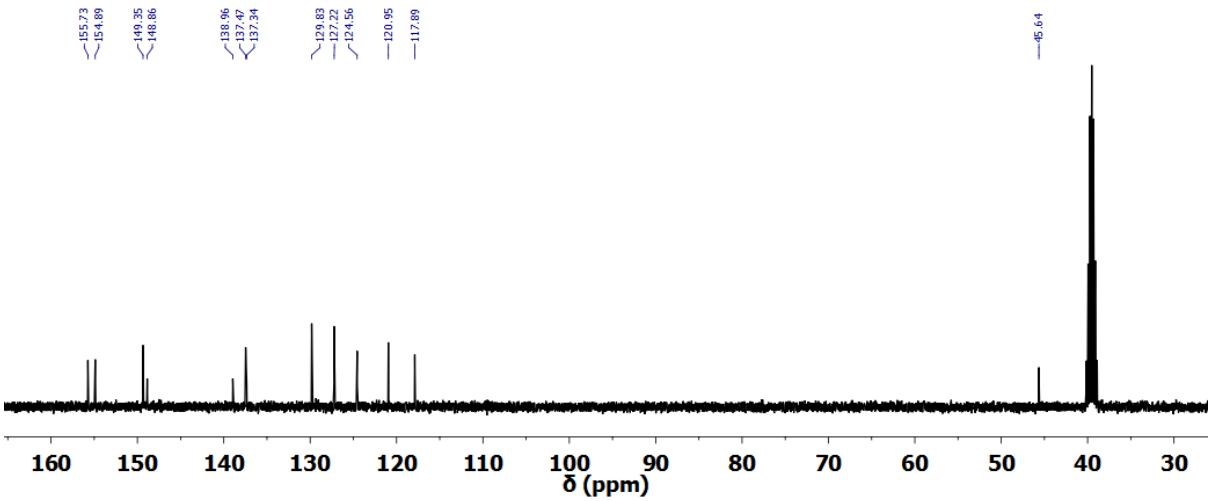

Figure S 36 ^{13}C NMR spectrum (100 MHz, DMSO-d_6, 298K) of **S14**

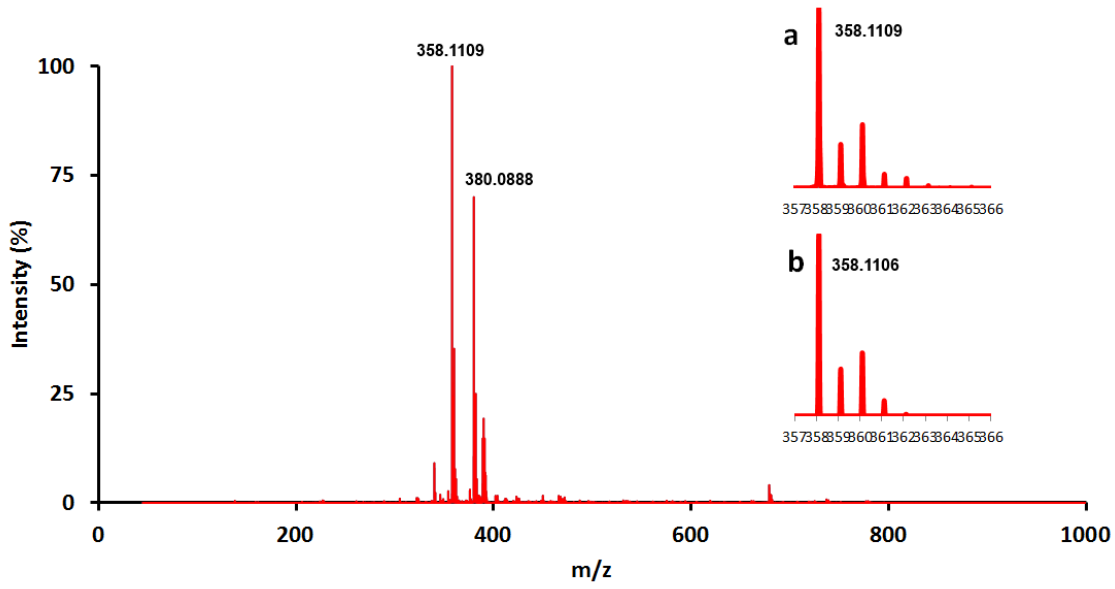

Figure S 37 HR-ESMS spectrum of **S14**, inset a) observed and b) calculated isotopic patterns for [**S14**+H]$^+$ ions at *m/z* = 258.1109, also showing peaks due to [**S14**+Na]$^+$ ions at *m/z* = 380.0888.

4.3 Macrocycle Ligand S15

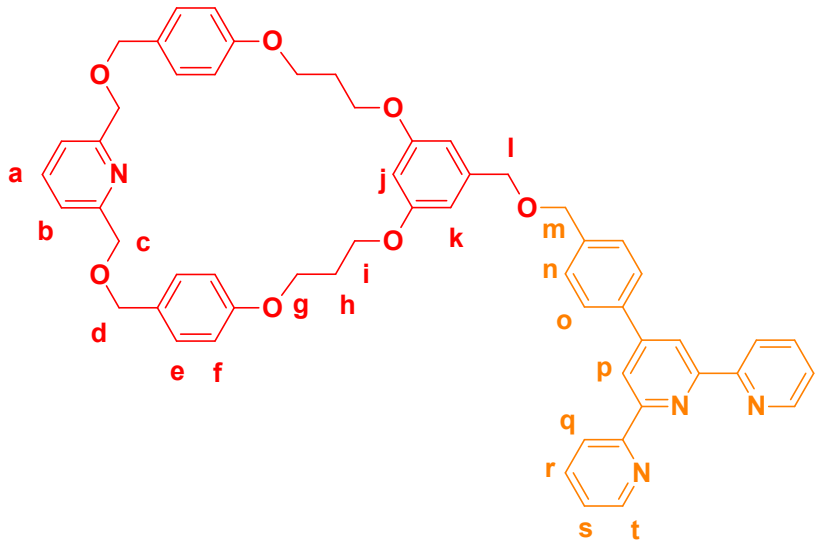

A solution of macrocycle **1** (100 mg, 0.175 mmol), terpy **S14** (94 mg, 0.262 mmol) and NaH (20.99 mg, 0.875 mmol, 95%) in anhydrous DMF (10 mL) was stirred for 48 h at RT under a nitrogen atmosphere. The reaction mixture was quenched with methanol (2 mL) and solvents evaporated. The residue was partitioned between water (30 mL) and $CHCl_3$/IPA (50 mL, 3:1). The aqueous phase was extracted with $CHCl_3$/IPA (3:1, 2 × 50 mL) and the combined organic layers were washed with brine (50 mL) and dried over $MgSO_4$. The solvent was removed under reduced pressure and the residue was purified by column chromatography (silica gel, ethyl acetate) to give **S15** (110 mg, 71%) as colourless solid. Melting point 70-72 °C; ^{1}H NMR (400 MHz, acetone-d_6) δ 8.85 (s, 2H, H_p), 8.78 – 8.72 (m, 4H, H_t, H_q), 8.04 – 7.98 (m, 2H, H_r), 7.96 (d, J = 8.3 Hz, 2H, H_o), 7.75 (t, J = 7.7 Hz, 1H, H_a), 7.63 (d, J = 8.5 Hz, 2H, H_n), 7.48 (ddd, J = 7.5, 4.6, 1.3 Hz, 2H, H_s), 7.36 (d, J = 7.7 Hz, 2H, H_b), 7.24 (d, J = 8.9 Hz, 4H, H_e), 6.88 (d, J = 8.7 Hz, 4H, H_f), 6.60 (d, 2H, H_k), 6.51 (t, J = 2.2 Hz, 1H, H_j), 4.68 (s, 2H, H_m), 4.57 (s, 6H, H_d. H_l), 4.34 (s, 4H, H_c), 4.21 – 4.10 (m, 8H, H_i, H_g), 2.26 – 2.13 (m, 4H, H_h).; ^{13}C NMR (100 MHz, acetone-d_6) δ 161.23, 159.68, 158.80, 157.09, 156.69, 150.74, 150.20, 141.93, 141.20, 138.38, 137.91, 137.74, 130.96, 130.62, 129.27, 127.85, 125.06, 121.83, 120.69, 119.15, 115.10, 106.72, 101.22, 72.82, 72.32, 72.13, 71.80, 65.18, 65.03, 29.92.; HR-ESMS: *m/z* = 893.3909 [**S15**+H]$^+$ (calc. for $C_{56}H_{53}N_4O_7$, 893.3912); Anal. calc. for $C_{56}H_{52}N_4O_7$•($CH_3COOC_2H_5$): C, 73.45; H, 6.16; N, 5.71. Found: C, 73.43; H, 6.30; N, 5.87.

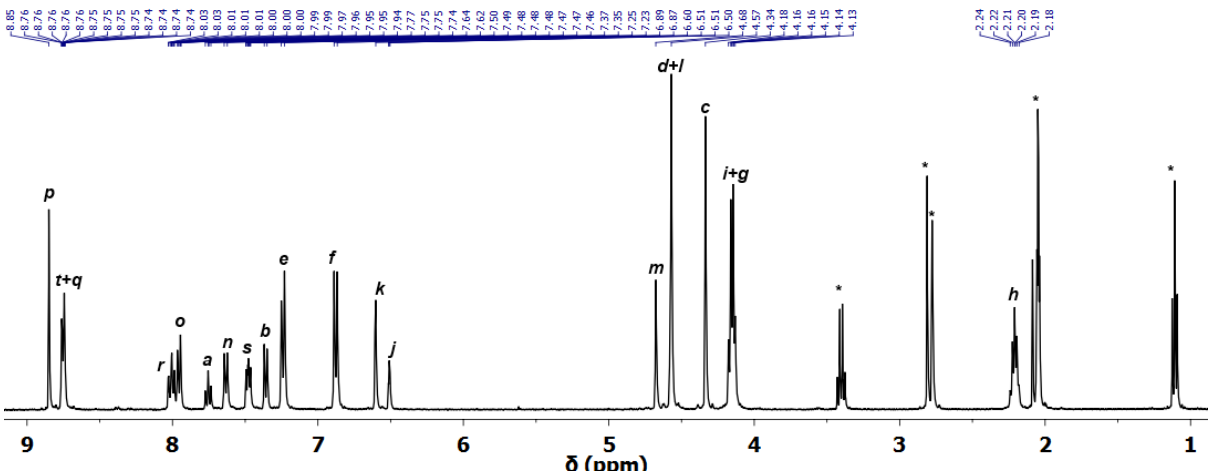

Figure S 38 ^{1}H NMR spectrum (400 MHz, acetone-d_6, 298K) of **S15** (* peaks due to H_2O, diethyl ether and methanol)

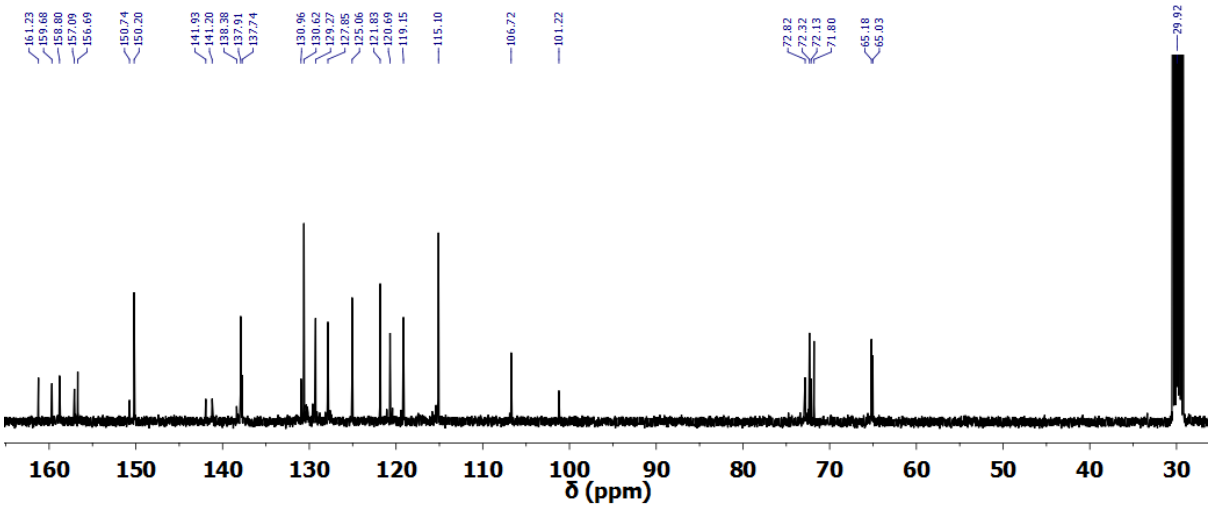

Figure S 39 ^{13}C NMR spectrum (100 MHz, acetone-d_6, 298K) of **S15**

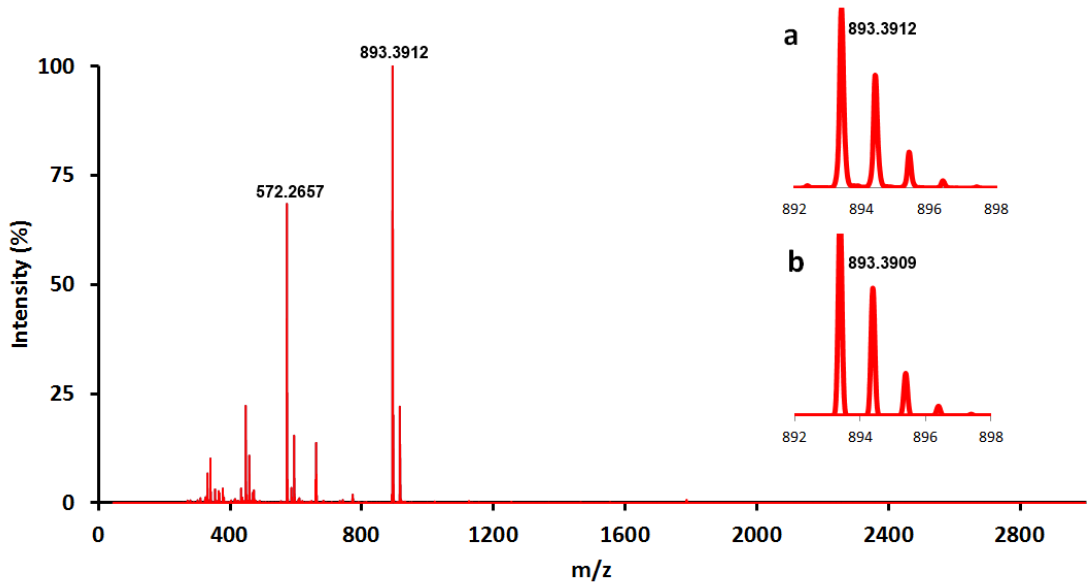

Figure S 40 HR-ESMS spectrum of **S15**, inset a) observed and b) calculated isotopic patterns for [**S15**+H]$^+$ at *m/z* = 893.3912, also showing peaks due to [**1**+H]$^+$ ions at *m/z* = 572.2657.

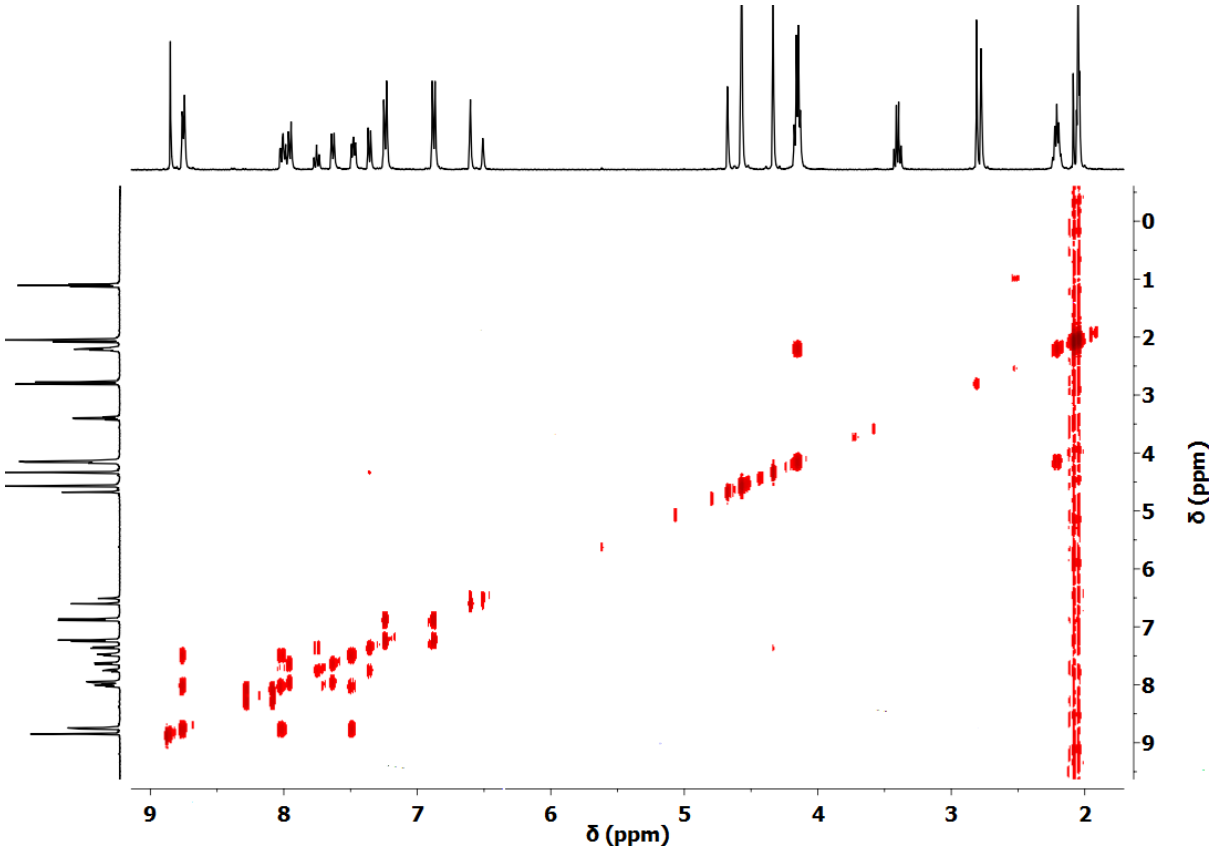

Figure S 41 ^{1}H COSY NMR spectrum (500 MHz, acetone-d_6, 298K) of **S15**

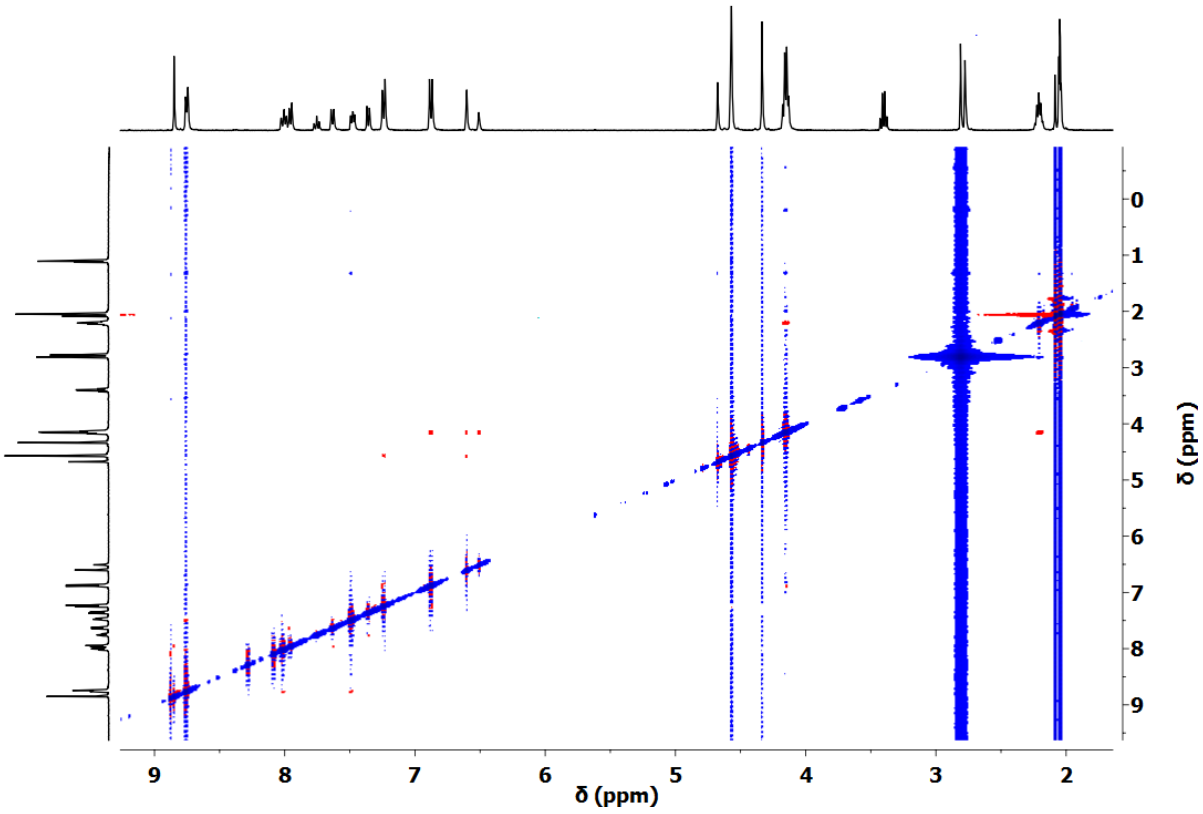

Figure S 42 ^{1}H NOESY NMR spectrum (500 MHz, acetone-d_6, 298K) of **S15**

4.4 [2]Rotaxane Ligand 5a

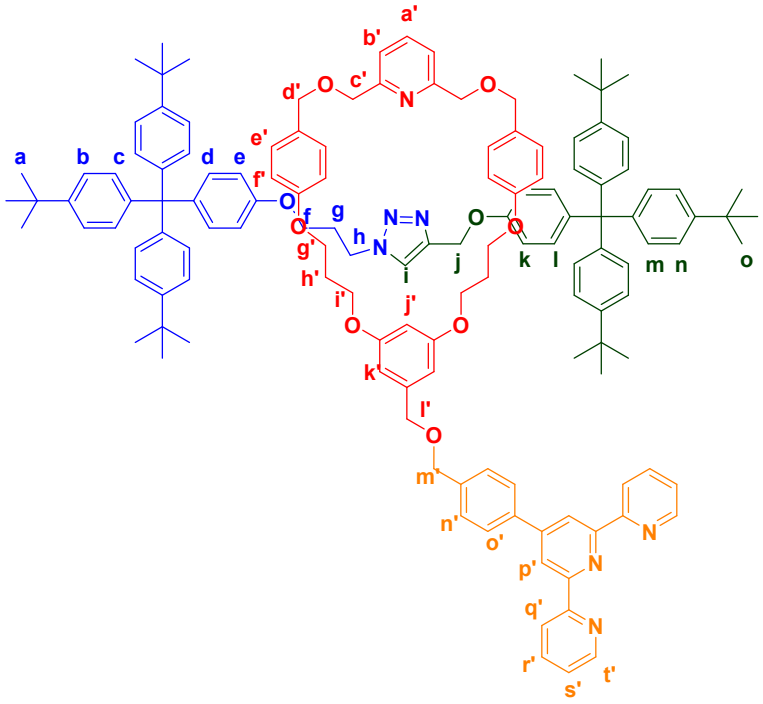

A solution of **4a** (80 mg, 0.047 mmol), terpy **S14** (25 mg, 0.07 mmol) and NaH (6 mg, 0.235, 95%) in anhydrous DMF (5 mL) was stirred for 48 hours at RT under a nitrogen atmosphere. The reaction mixture was quenched with methanol (2 mL) and the solvents evaporated under reduced pressure. The residue was partitioned between water (30 mL) and $CHCl_3$/IPA (3:1, 50 mL). The aqueous phase was extracted with $CHCl_3$/IPA (2 × 50 mL) and the combined organic layers were washed with brine (50 mL) and dried over $MgSO_4$. The solvent was removed under reduced pressure and the residue was purified by column chromatography (silica gel, ethyl acetate/petrol, 1:1) to give **5a** (59 mg, 62%) as colourless solid. Melting point 120-122 °C; ^{1}H NMR (500 MHz, acetone-d_6) δ 8.83 (s, 2H, $H_{P'}$), 8.75 (dt, J = 7.9, 1.1 Hz, 2H, $H_{q'}$), 8.71 (ddd, J = 4.7, 1.8, 0.9 Hz, 2H, $H_{t'}$), 7.99 (ddd, J = 8.0, 7.5, 1.8 Hz, 2H, $H_{r'}$), 7.83 (d, J = 8.2 Hz, 2H, $H_{o'}$), 7.59 (t, J = 7.7 Hz, 1H, $H_{a'}$), 7.52 (d, J = 8.6 Hz, 2H, $H_{n'}$), 7.46 (ddd, J = 7.5, 4.7, 1.2 Hz, 2H, $H_{s'}$), 7.43 (s, 1H, H_i), 7.31 – 7.24 (m, 14H, $H_{b'}$, H_b, H_n), 7.15 – 7.08 (m, 12H, H_c, H_m), 7.03 – 6.95 (m, 8H, H_l, $H_{e'}$, H_d), 6.75 (d, J = 8.9 Hz, 2H, H_k), 6.57 – 6.53 (m, 6H, $H_{f'}$, $H_{k'}$), 6.47 (t, J = 2.3 Hz, 1H, $H_{j'}$), 6.44 (d, J = 8.9 Hz, 2H, H_e), 4.87 (s, 2H, H_j), 4.60 (s, 2H, $H_{m'}$), 4.49 (s, 2H, $H_{l'}$), 4.46 (s, 4H, $H_{d'}$), 4.25 (s, 4H, $H_{c'}$), 4.10 – 4.02 (m, 4H, $H_{g'}$), 3.96 (t, J = 5.8 Hz, 4H, $H_{i'}$), 3.81 (t, J = 7.1 Hz, 2H, H_h), 3.31 (t, J = 6.0 Hz, 2H, H_f), 2.14 – 2.08 (m, 4H, $H_{h'}$), 1.65 – 1.57 (m, 2H, H_g), 1.28 (s, 27H, H_a or H_o), 1.27 (s, 27H, H_a or H_o); ^{13}C NMR (125 MHz, acetone-d_6) δ 161.15, 159.46, 158.78,

157.32, 157.28, 157.07, 156.71, 150.64, 150.17, 149.06, 149.02, 145.40, 145.30, 143.97, 141.83, 141.06, 140.34, 140.17, 138.25, 137.88, 137.80, 132.71, 132.55, 131.45, 131.44, 130.60, 130.47, 129.19, 127.84, 125.07, 125.04, 125.03, 124.48, 121.82, 120.56, 119.17, 115.02, 114.28, 114.11, 106.29, 101.62, 72.80, 72.62, 72.18, 71.77, 65.03, 64.91, 64.73, 63.92, 63.91, 62.13, 47.18, 34.86, 34.86, 31.70, 31.69, 30.09, 29.93; HR-ESMS: *m/z* = 1012.5728 [**5a**+2H]$^{2+}$ (calc. for $C_{136}H_{149}N_7O_9$, 1012.6032); Anal. calc. for $C_{136}H_{148}N_7O_9$•($CHCl_3$): C, 76.71; H, 7.05; N, 4.57. Found: C, 76.40; H, 7.02; N, 4.61.

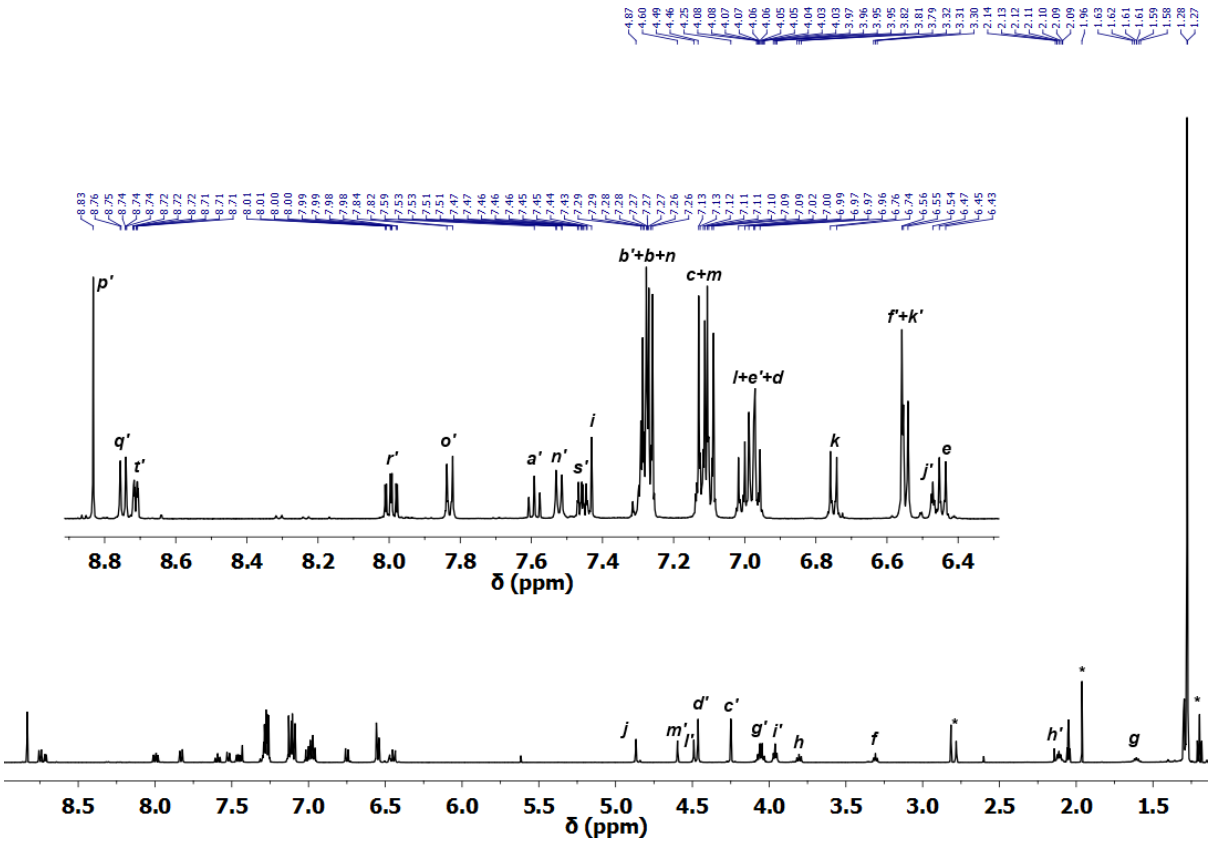

Figure S 43 ^{1}H NMR spectrum (500 MHz, acetone-d_6, 298K) of **5a** (* peaks due to H_2O, ethyl acetate and methanol)

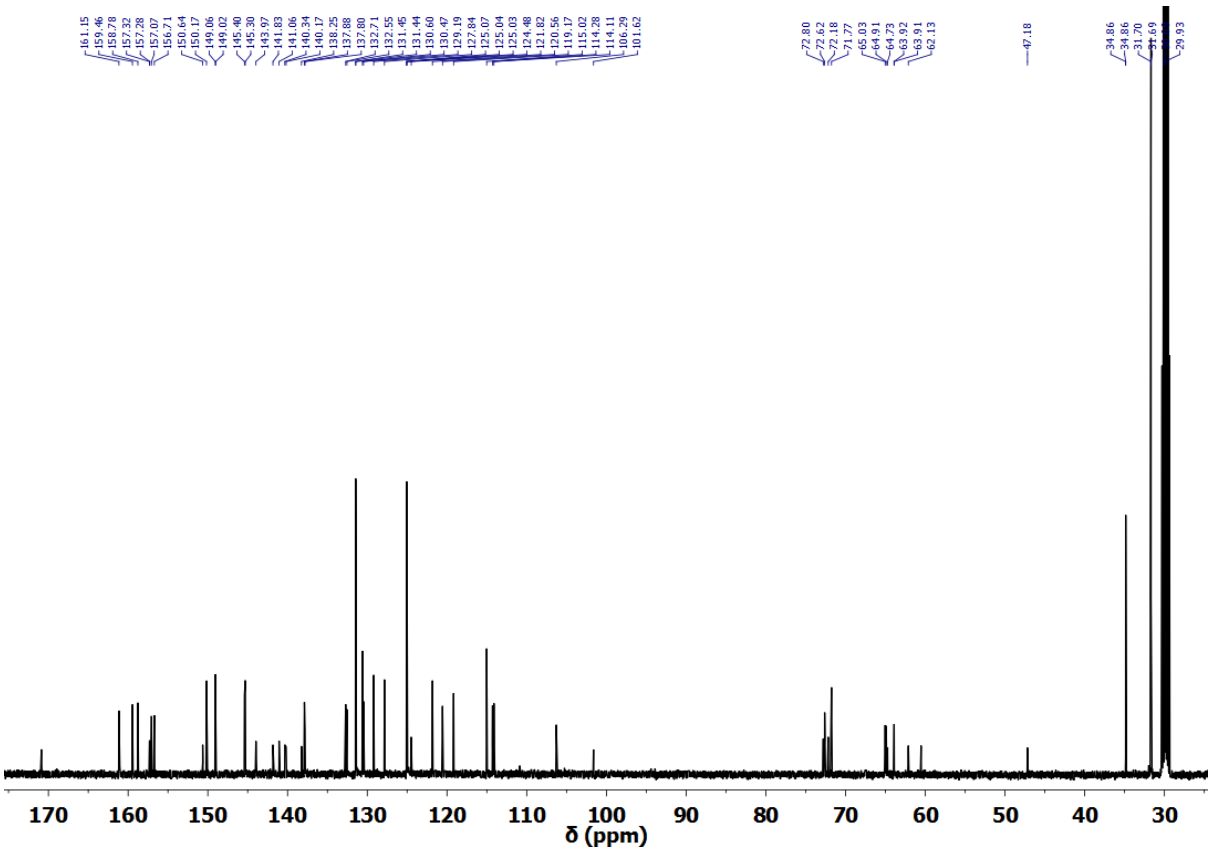

Figure S 44 ^{13}C NMR spectrum (125 MHz, acetone-d_6, 298K) of **5a**

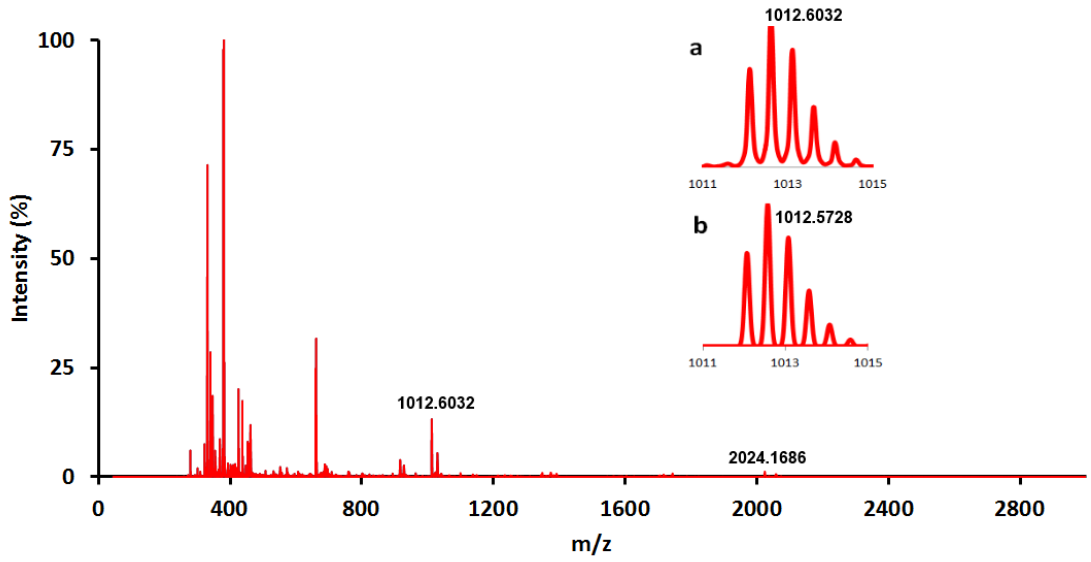

Figure S 45 HR-ESMS spectrum of **5a**, inset a) observed and b) calculated isotopic patterns for [**5a**+2H]$^{2+}$ at *m/z* = 1012.6032, also showing peaks due to [**5a**+H]$^{+}$ ions at *m/z* = 2024.1686 (other peaks due to some unknown fragments).

4.5 [2]Rotaxane Ligand 5b

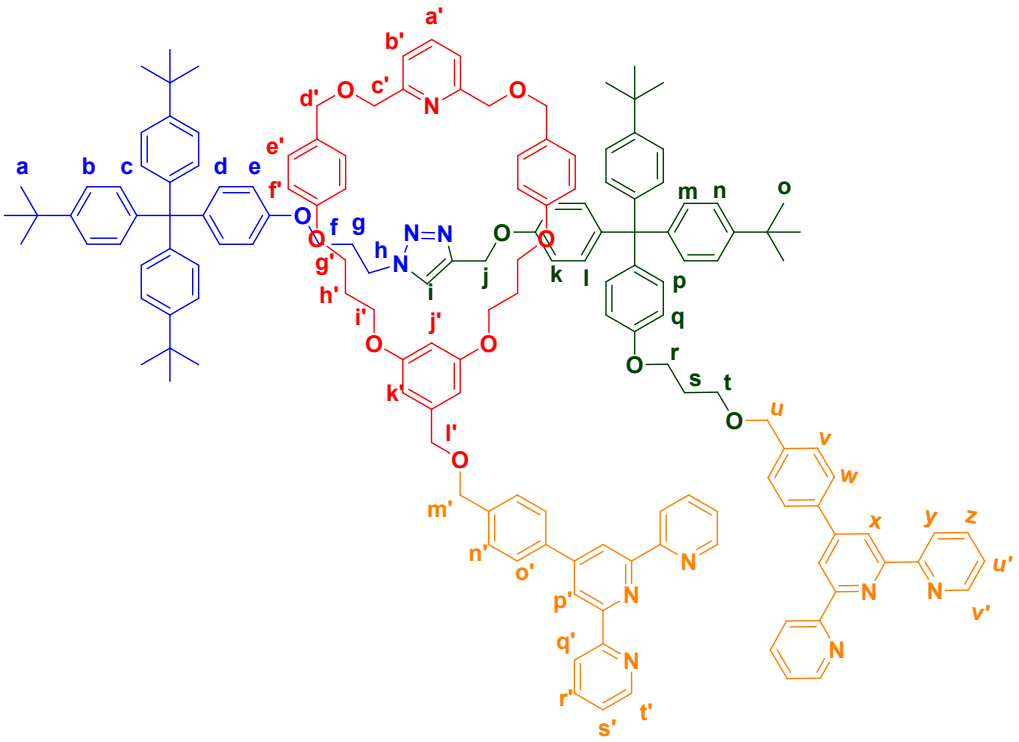

A solution of **4b** (350 mg, 0.203 mmol), terpy **S14** (218 mg, 0.610 mmol) and NaH (24 mg, 0.290 mmol, 95%) in anhydrous DMF (20 mL) was stirred for 48 hours at RT under a nitrogen atmosphere. The reaction mixture was quenched with methanol (2 mL) and the solvents were removed under reduced pressure. The residue was partitioned between water (30 mL) and $CHCl_3$/IPA (3:1, 50 mL). The aqueous phase was extracted with $CHCl_3$/IPA (3:1, 2 × 50 mL) and the combined organic layers were washed with brine (50 mL) and dried over $MgSO_4$. The solvent was removed under reduced pressure and the residue was purified by column chromatography (silica gel, ethyl acetate/petrol, 1:1) to give **5b** (201 mg, 42%) as colourless solid. Melting point 122-124 °C; ^{1}H NMR (500 MHz, acetone-d_6) δ 8.81 (s, 2H, $H_{p'}$ or H_x), 8.78 (s, 2H, $H_{p'}$ or H_x), 8.75 – 8.67 (m, 8H, $H_{t'}$, $H_{q'}$, H_y, $H_{v'}$), 8.00 – 7.94 (m, 4H, $H_{r'}$, H_z), 7.84 – 7.80 (m, 4H, $H_{o'}$, H_w), 7.58 (t, J = 7.7 Hz, 1H, $H_{a'}$), 7.53 – 7.49 (m, 4H, H_v, $H_{n'}$), 7.47 – 7.41 (m, 4H, $H_{s'}$, H_u), 7.41 (s, 1H, H_i), 7.30 – 7.22 (m, 12H, $H_{b'}$, H_b, H_n), 7.16 – 7.05 (m, 12H, H_c, H_m, H_p), 7.02 – 6.94 (m, 8H, H_l, $H_{e'}$, H_d), 6.80 (d, J = 8.9 Hz, 2H, H_q), 6.73 (d, J = 8.9 Hz, 2H, H_k), 6.55 – 6.52 (m, 6H, $H_{f'}$, $H_{k'}$), 6.47 – 6.42 (m, 3H, H_e, $H_{j'}$), 4.84 (s, 2H, H_j), 4.60 (s, 2H, H_u), 4.57 (s, 2H, $H_{m'}$), 4.47 (s, 2H, $H_{l'}$), 4.45 (s, 4H, $H_{d'}$), 4.23 (s, 4H, $H_{c'}$), 4.10 (t, J = 6.2 Hz, 2H, H_r), 4.07 – 4.00 (m, 4H, $H_{i'}$), 3.94 (t, J = 5.8 Hz, 4H, $H_{g'}$), 3.79 (t, J = 7.1 Hz, 2H, H_h), 3.69 (t, J = 6.1 Hz, 2H, H_t), 3.30 (t, J = 5.9 Hz, 2H, H_f), 2.12 – 2.07 (m, 6H, $H_{h'}$, H_s), 1.63 – 1.56 (m, 2H, H_g), 1.27 (s, 27H, H_a), 1.25 (s, 18H, H_o); ^{13}C NMR (125

MHz, acetone-d_6) δ 161.13, 159.45, 158.76, 157.93, 157.28, 157.27, 157.04, 157.01, 156.70, 156.68, 150.66, 150.60, 150.16, 150.16, 149.02, 149.00, 145.44, 145.41, 143.98, 141.81, 141.26, 141.05, 140.50, 140.33, 140.18, 138.26, 138.24, 137.86, (137.85 x 2), 137.79, 132.78, 132.66, 132.55, 131.44, 131.41, 130.59, 130.47, 130.46, 129.18, 129.04, 127.83, 127.80, 125.07, 125.03, 125.01, 124.99, 124.45, 121.82, 121.80, 120.56, 119.16, 115.01, 114.29, 114.11, 106.28, 101.61, 72.83, 72.80, 72.62, 72.18, 71.76, 67.44, 65.40, 65.03, 64.91, 64.73, 63.92, 63.65, 62.11, 47.16, 34.86, 34.83, 31.69, 31.68, 30.54, 30.40, 29.93.; HR-ESMS: *m/z* = 1182.1223 [**5b**+2H]$^{2+}$ (calc. for $C_{157}H_{162}N_{10}O_{11}$, 1182.1142) ; Anal. calc. for $C_{157}H_{160}N_{10}O_{11}$•0.3($CHCl_3$): C, 79.10; H, 6.76; N, 5.87; Found: C, 79.14; H, 6.97; N, 5.55.

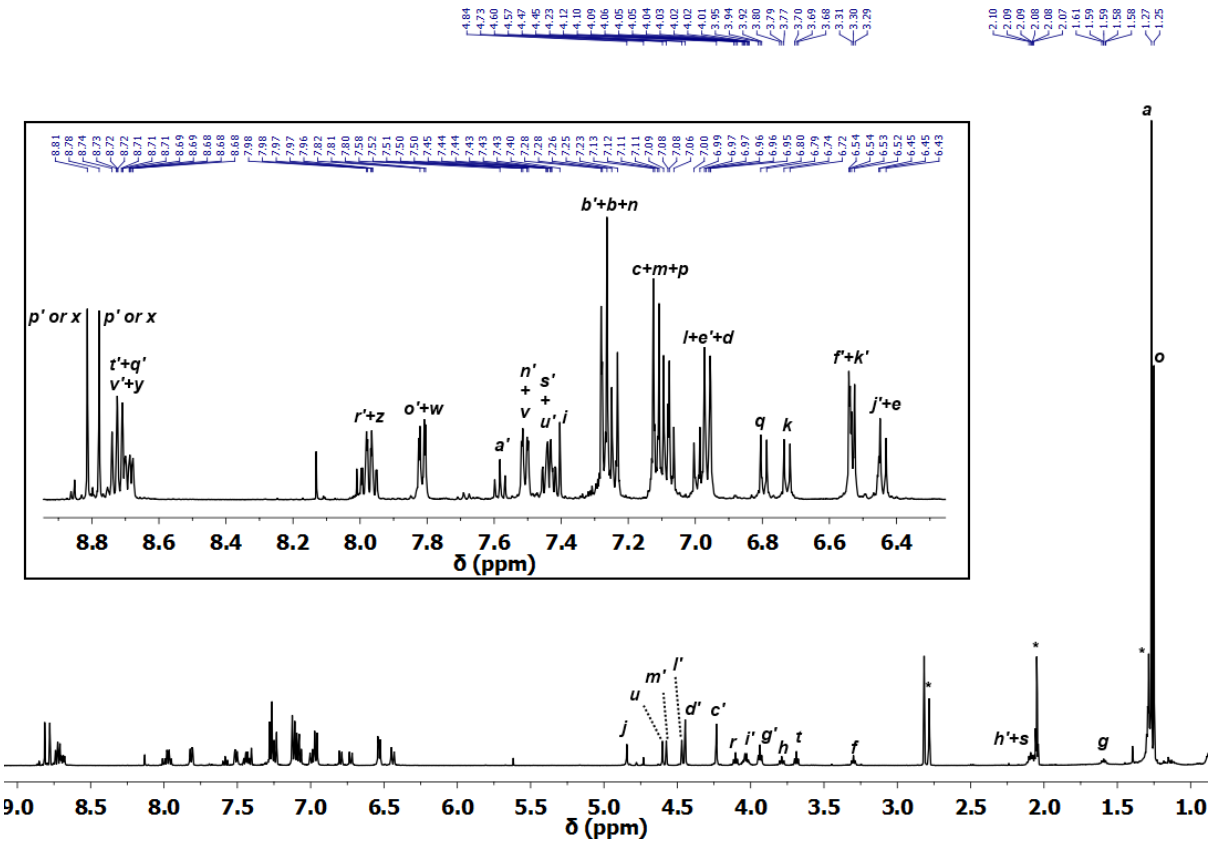

Figure S 46 ^{1}H NMR spectrum (500 MHz, acetone-d_6, 298K) of **5b** (* peaks due to H_2O, ethyl acetate and acetone)

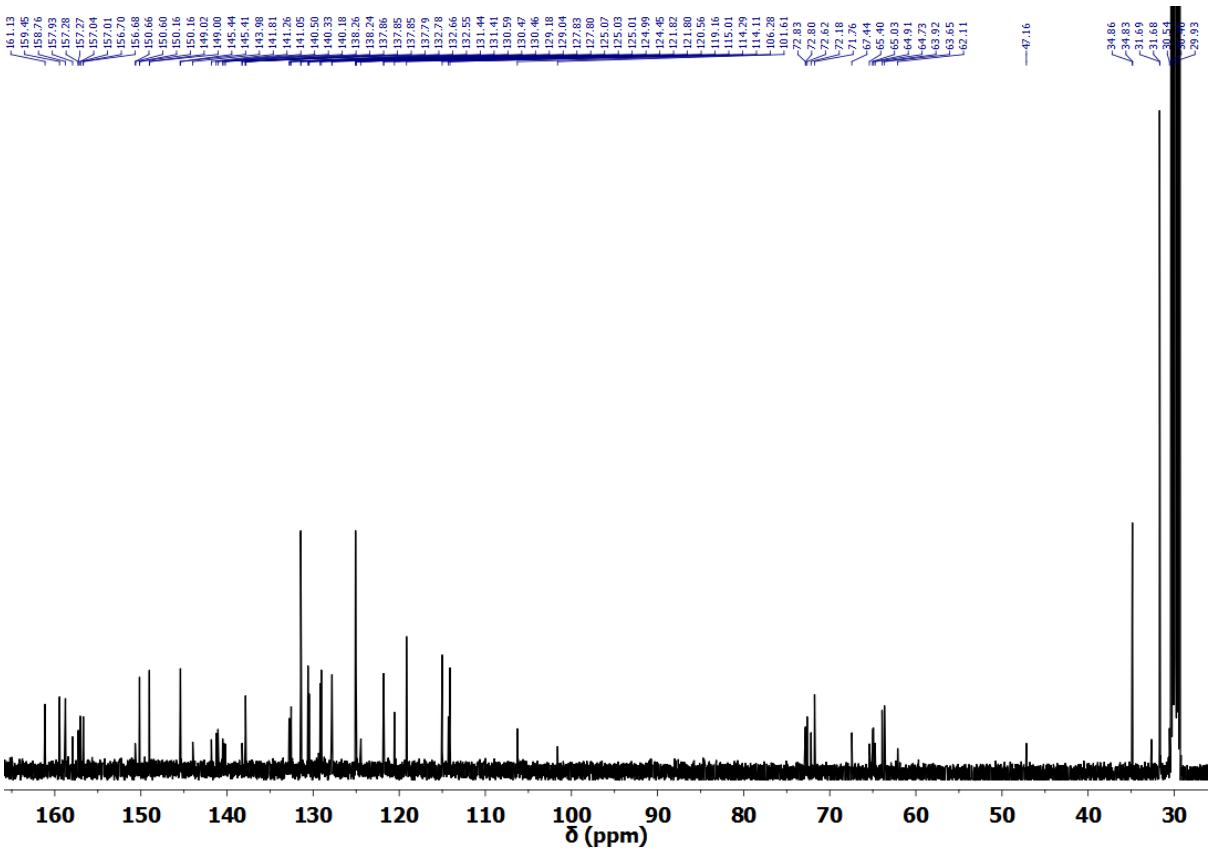

Figure S 47 ^{13}C NMR spectrum (125 MHz, acetone-d_6, 298K) of **5b**

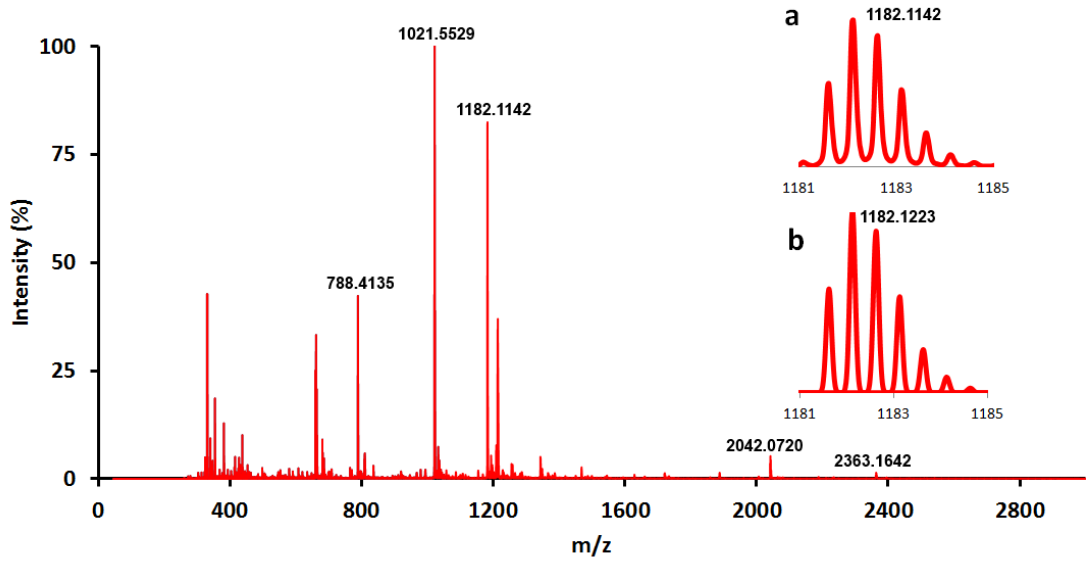

Figure S 48 HR-ESMS spectrum of **5b**, inset a) observed and b) calculated isotopic patterns for [**5b**+2H]$^{2+}$ at *m/z* = 1182.1142, also showing peaks due to [**5b**+H]$^{+}$ (*m/z* = 2363.1642), [**5b**+3H]$^{3+}$ (*m/z* = 788.4135), [**5b**-terpy+H]$^{+}$ (*m/z* = 2042.0720), [**5b**-terpy+2H]$^{2+}$ (*m/z* = 1021.5529) (other peaks due to unknown fragments).

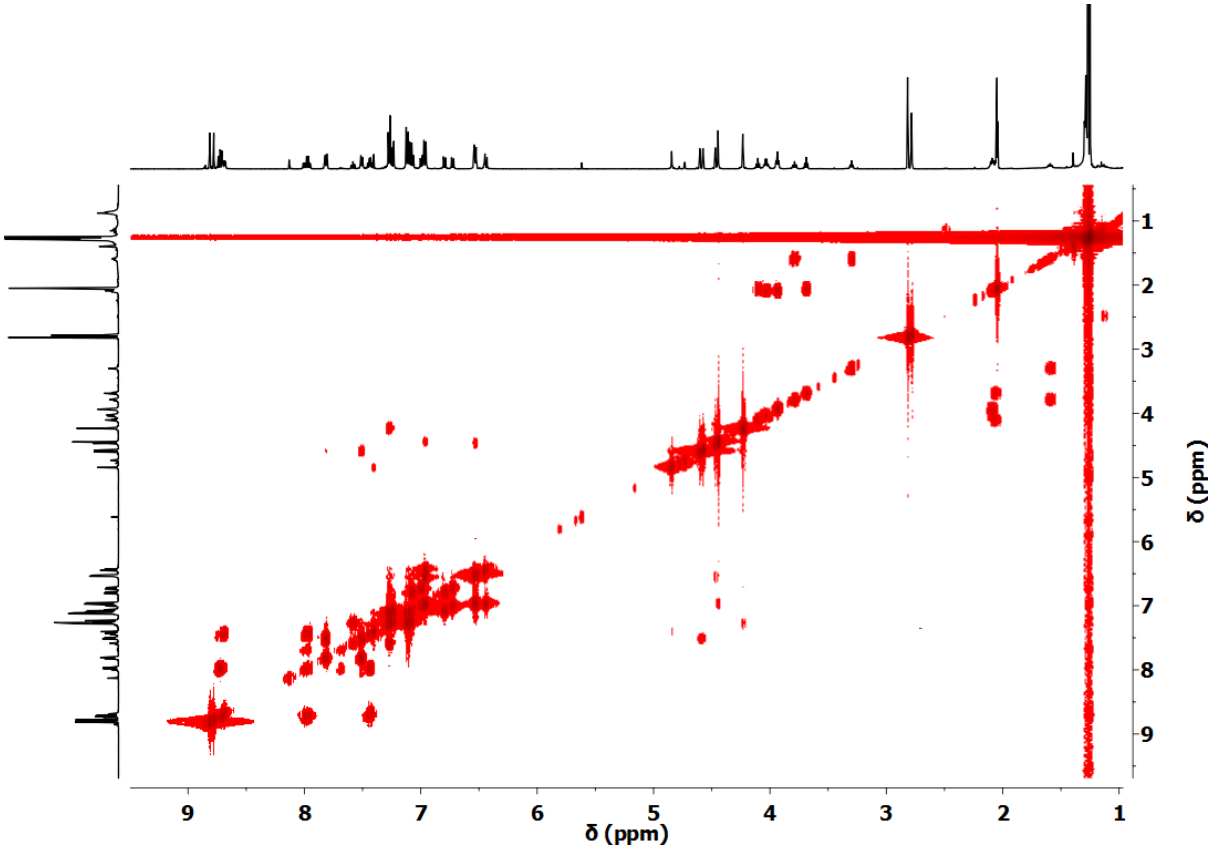

Figure S 49 ^{1}H COSY NMR spectrum (500 MHz, acetone-d_6, 298K) of **5b**

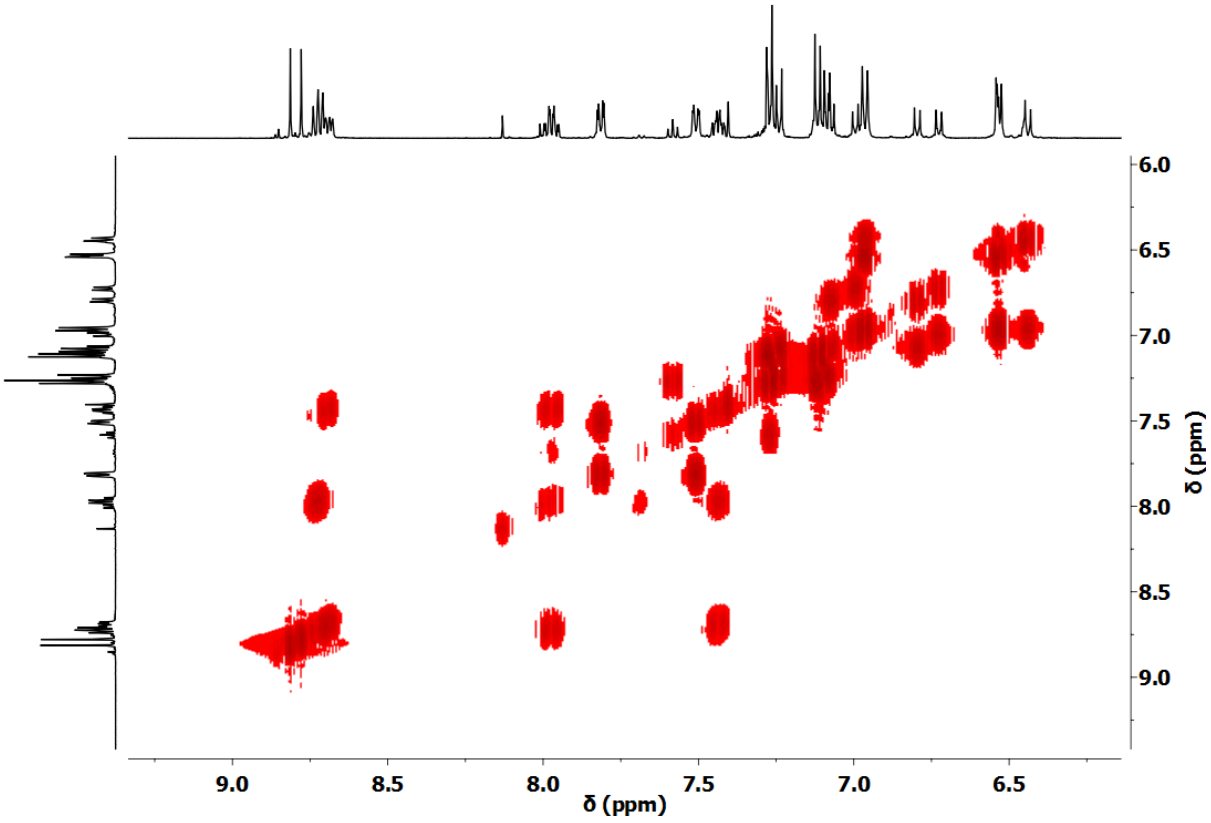

Figure S 50 Partial ^{1}H COSY NMR spectrum (500 MHz, acetone-d_6, 298K) for aromatic region of **5b**

5 Fe(II) Complexes of [2]Rotaxane Ligands

5.1 [Fe(S14)$_2$](BF$_4$)$_2$

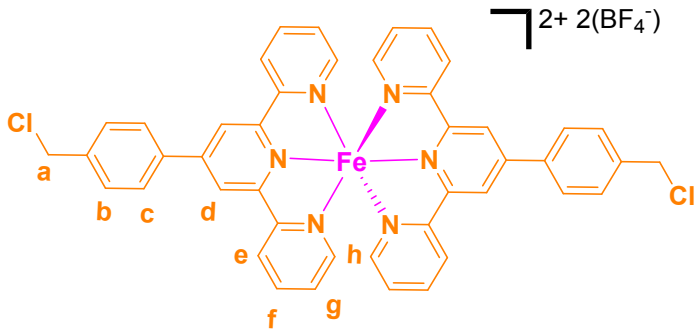

A solution of terpy ligand **S14** (25 mg, 0.07 mmol) and [Fe(H$_2$O)$_6$](BF$_4$)$_2$. (12 mg, 0.035 mmol) in acetonitrile (2 mL) was stirred at RT for 30 min. Vapour diffusion of diethyl ether to the solution gave X-ray quality crystals of [Fe(**S14**)$_2$](BF$_4$)$_2$ (38 mg, 71%). ^{1}H NMR (400 MHz, DMSO-d_6) δ 9.68 (s, 4H, H$_d$), 9.05 (d, J = 8.0 Hz, 4H, H$_e$), 8.56 (d, J = 7.9 Hz, 4H, H$_h$), 8.03 (t, J = 7.7 Hz, 4H, H$_g$), 7.88 (d, J = 7.8 Hz, 4H, H$_b$), 7.26 (d, J = 5.5 Hz, 4H,

H_c), 7.18 (t, J = 6.4 Hz, 4H, H_f), 4.99 (s, 4H, H_a); ^{13}C NMR (100 MHz, DMSO-d_6) δ 160.37, 158.27, 153.25, 148.86, 140.69, 139.23, 136.28, 130.34, 128.56, 128.06, 124.55, 121.53, 46.04; HR-ESMS: m/z = 385.0703 $[Fe(\mathbf{S14})_2]^{2+}$ (calc. for $C_{44}H_{32}FeN_6Cl_2$, 385.0726). UV-Vis (CH_2Cl_2): λ_{max} nm (ε L. mol^{-1} cm^{-1}) = 569 (5284), 320 (13024), 285 (15248).

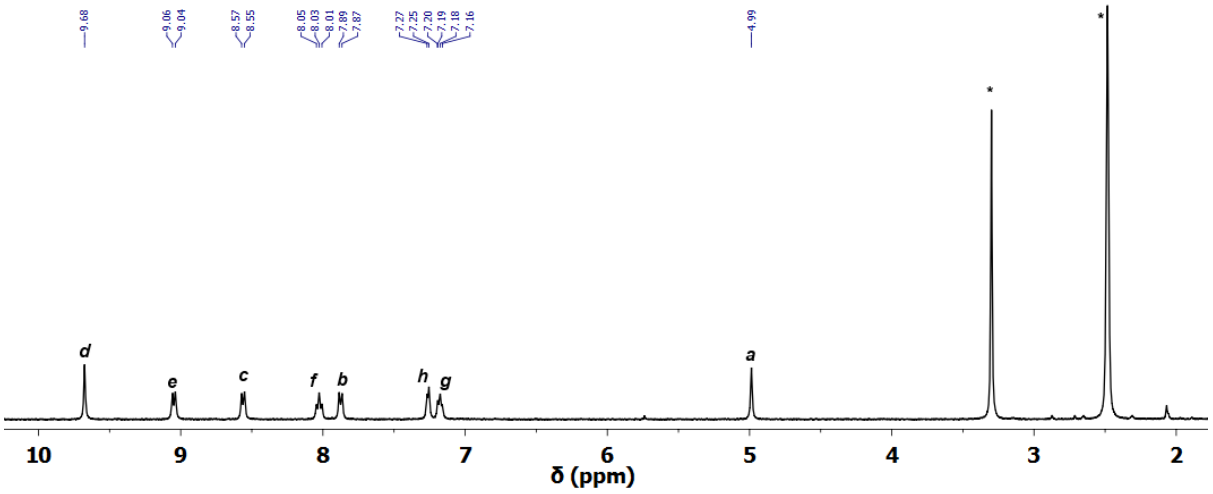

Figure S 51 ^{1}H NMR spectrum (400 MHz, DMSO-d_6, 298K) of $[Fe(\mathbf{S14})_2](BF_4)_2$ (* peaks due to H_2O and DMSO)

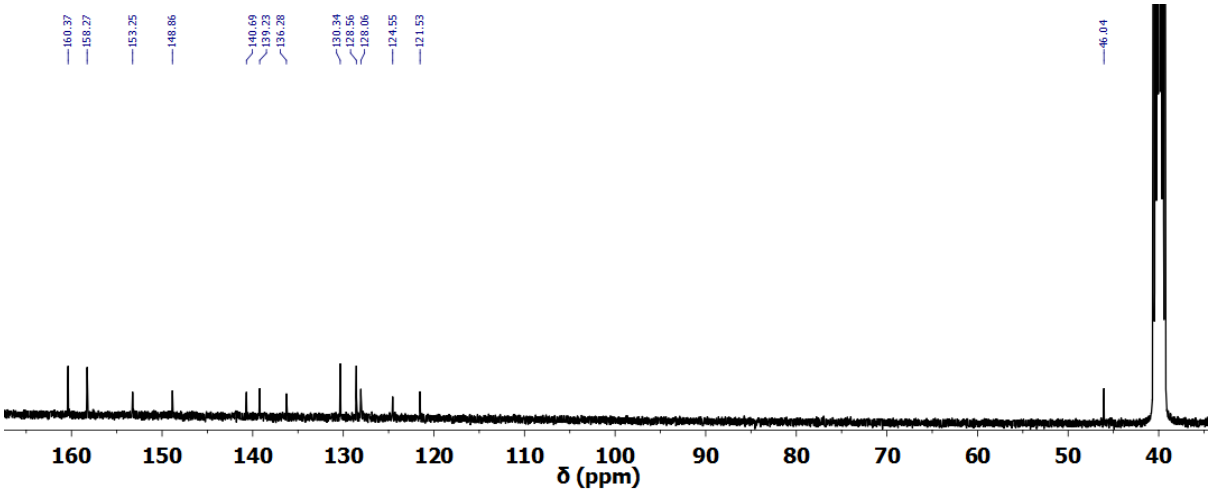

Figure S 52 ^{13}C NMR spectrum (100 MHz, DMSO-d_6, 298K) of $[Fe(\mathbf{S14})_2](BF_4)_2$

5.2 [Fe(S15)$_2$](BF$_4$)$_2$

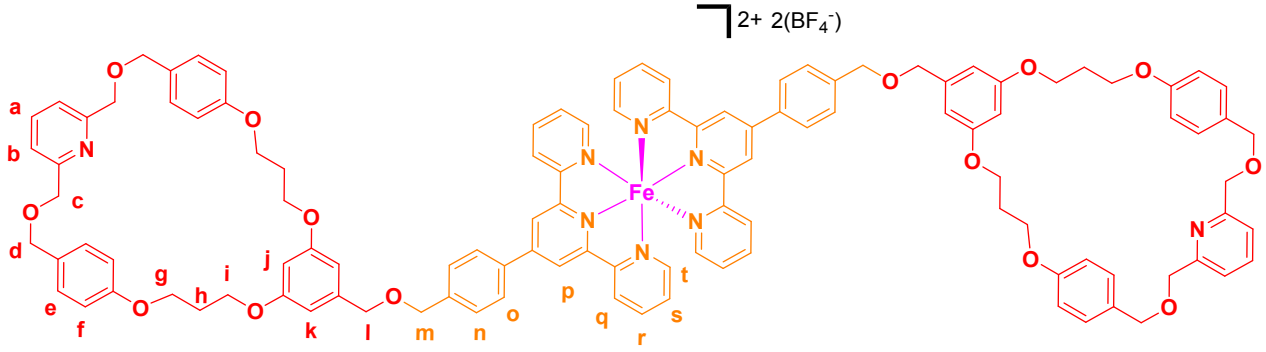

An acetonitrile solution (5 mL) of macrocycle **S15** (50 mg, 0.056 mmol) and $[Fe(H_2O)_6](BF_4)_2$ (10 mg, 0.028 mmol) was stirred at RT for 30 min. The solvent was removed under reduced pressure and the residue was subjected to column chromatography with CH_2Cl_2/methanol (19:1) to give iron(II) complex [Fe(**S15**)$_2$](BF$_4$)$_2$ (48 mg, 85%) as purple solid. ^{1}H NMR (400 MHz, acetone-d_6) δ 9.65 (s, 4H, H, H$_p$), 9.04 (d, J = 7.9 Hz, 4H, H$_q$), 8.47 (d, J = 8.1 Hz, 4H, H$_o$), 8.11 – 8.03 (m, 4H, H$_r$), 7.82 (d, J = 8.4 Hz, 4H, H$_n$), 7.77 (t, J = 7.7 Hz, 2H, H$_a$), 7.60 – 7.56 (m, 4H, H$_t$), 7.37 (d, J = 7.7, 0.6 Hz, 4H, H$_b$), 7.28 – 7.23 (m, 12H, H$_e$, H$_s$), 6.89 (d, J = 8.1 Hz, 8H, H, H$_f$), 6.65 (d, J = 1.7 Hz, 4H, H$_k$), 6.58 (t, J = 2.3 Hz, 2H, H$_j$), 4.79 (s, 4H, H$_m$), 4.65 (s, 4H, H$_l$), 4.58 (s, 8H, H$_d$), 4.35 (s, 8H, H$_c$), 4.25 – 4.07 (m, 16H, H$_g$, H$_i$), 2.31 – 2.18 (m, 8H, H$_h$). ^{13}C NMR (100 MHz, acetone-d_6) δ 160.70, 160.41, 158.78, 158.45, 153.37, 150.28, 142.04, 140.97, 139.90, 139.00, 135.51, 130.03, 129.80, 128.79, 128.57, 127.92, 127.68, 124.22, 121.44, 120.27, 114.22, 105.99, 100.14, 72.11, 72.09, 71.56, 71.18, 64.39, 64.14, 29.04.; HR-ESMS: m/z = 920.8422 [Fe(**S15**)$_2$]$^{2+}$ (calc. for $C_{112}H_{105}FeN_8O_{14}$, 920.8542); UV-Vis ($CH_2Cl_2$): λ_{max}/nm (ε/L mol^{-1} cm^{-1}) = 569 (3440), 285 (12940).

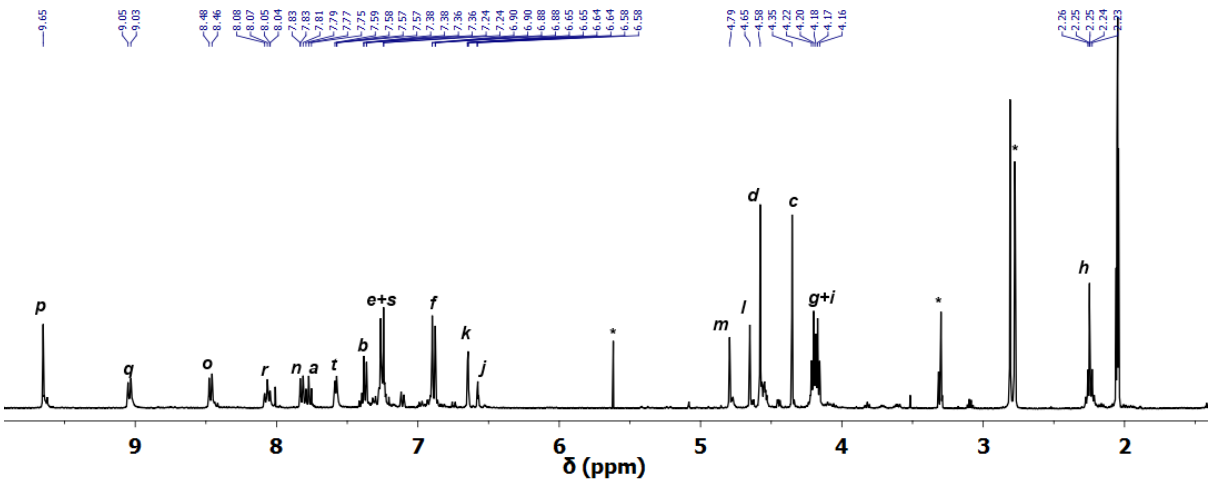

Figure S 53 ^{1}H NMR spectrum (400 MHz, acetone-d_6, 298K) of [Fe(**S15**)$_2$](BF$_4$)$_2$ (* peaks due to H_2O and CH_2Cl_2)

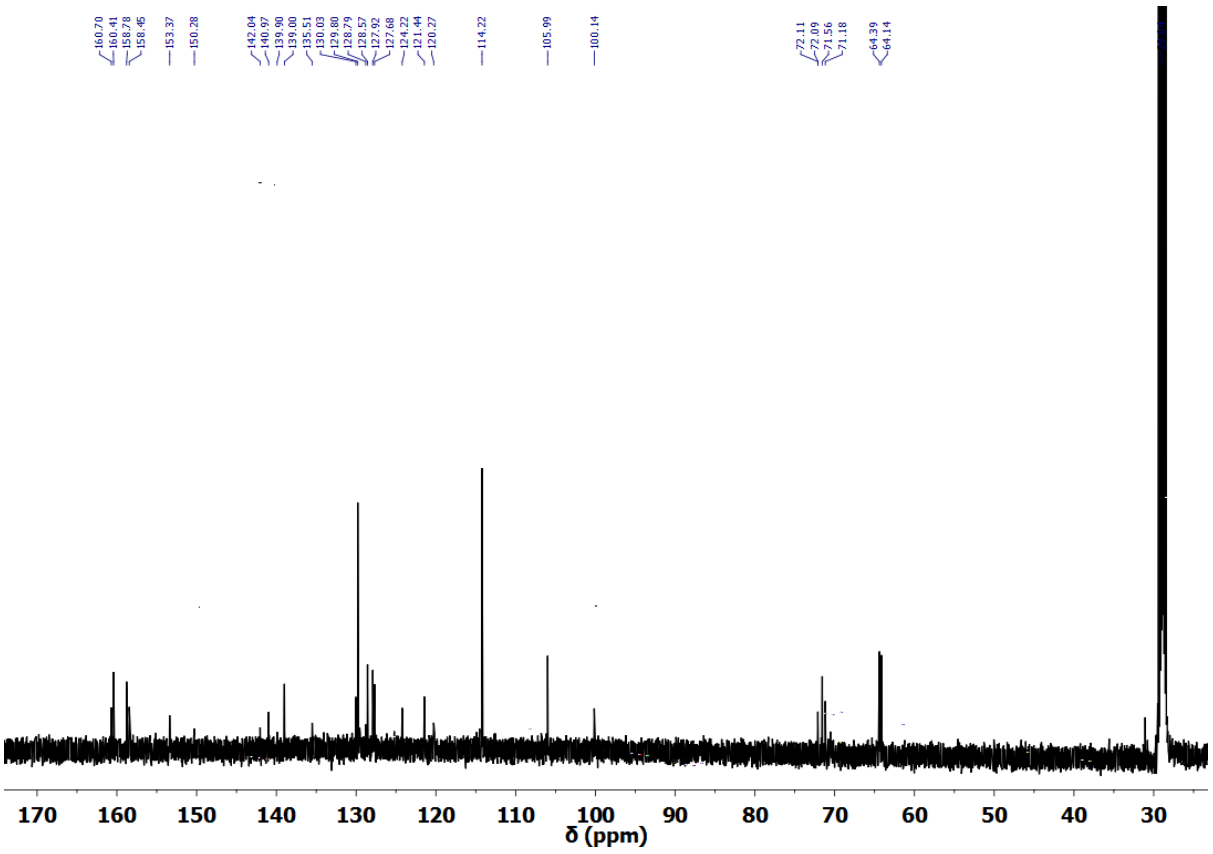

Figure S 54 ^{13}C NMR spectrum (100 MHz, acetone-d_6, 298K) of [Fe(**S15**)$_2$](BF$_4$)$_2$

5.3 [Fe(5a)$_2$](BF$_4$)$_2$

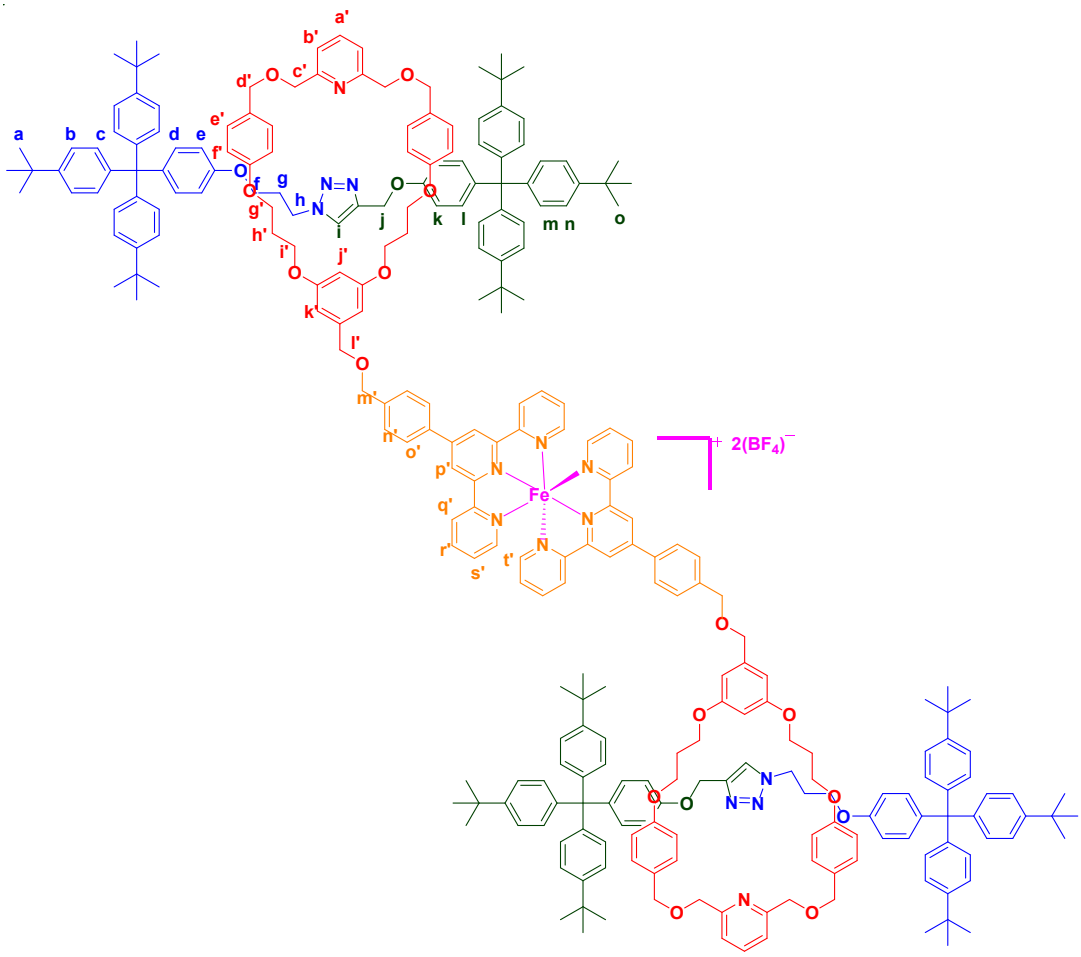

An acetonitrile solution (5 mL) of rotaxane **5a** (50 mg, 0.025 mmol) and [Fe(H$_2$O)$_6$](BF$_4$)$_2$ (4 mg, 0.013 mmol) was stirred at RT for 30 min. The solvent was removed under reduced pressure and the residue was subjected to column chromatography (silica gel, CH$_2$Cl$_2$/methanol, 19:1) to give pure iron complex [Fe(**5a**)$_2$](BF$_4$)$_2$ (43 mg, 82%). ^{1}H NMR (500 MHz, acetone-d_6) δ 9.62 (s, 4H, H$_{p'}$), 9.00 (d, J = 8.1 Hz, 4H, H$_{q'}$), 8.45 (d, J = 8.3 Hz, 4H, H$_{o'}$), 8.03 (td, J = 7.8, 1.5 Hz, 4H, H$_{r'}$), 7.78 (d, J = 8.1 Hz, 4H, H$_{n'}$), 7.61 (t, J = 7.7 Hz, 2H, H$_{a'}$), 7.55 (ddd, J = 5.7, 1.5, 0.7 Hz, 4H, H$_{t'}$), 7.49 (s, 2H, H$_i$), 7.34 – 7.26 (m, 28H, H$_{b'}$, H$_b$, H$_n$), 7.21 (ddd, J = 7.6, 5.7, 1.3 Hz, 4H, H$_{s'}$), 7.18 – 7.09 (m, 24H, H$_c$, H$_m$), 7.05 – 6.97 (m, 16H, H$_l$, H$_{e'}$, H$_d$), 6.77 (d, J = 8.9 Hz, 4H, H$_k$), 6.62 (d, J = 2.2 Hz, 4H, H$_{k'}$), 6.59 – 6.54 (m, 10H, H$_{f'}$, H$_{j'}$), 6.49 (d, J = 8.9 Hz, 4H, H$_e$), 4.89 (s, 4H, H$_j$), 4.74 (s, 4H, H$_{m'}$), 4.60 (s, 4H, H$_{l'}$), 4.48 (s, 8H, H$_{d'}$), 4.26 (s, 8H, H$_{c'}$), 4.16 – 4.07 (m, 8H, H$_{g'}$), 4.00 (t, J = 5.8 Hz, 8H, H$_{i'}$), 3.87 (t, J = 7.1 Hz, 4H, H$_h$), 3.38 (t, J = 6.0 Hz, 4H, H$_f$), 2.20 – 2.10 (m, 8H, H$_{h'}$), 1.68 (p, J = 6.5 Hz, 4H, H$_g$), 1.30 (s, 54H, H$_a$ or H$_o$), 1.29 (s, 54H, H$_a$ or H$_o$); ^{13}C NMR (125 MHz, acetone-d_6) δ 161.55, 161.26, 159.43, 159.27, 158.76, (157.32 x 2), 154.10, 151.18,

149.13, 149.10, 145.41, 145.30, 143.97, 142.92, 141.72, 140.37, 140.20, 137.86, 137.85, 136.36, 132.73, 132.59, (131.45 x 2), 130.65, 130.55, 129.43, 128.75, 128.54, 128.52, 128.51, 125.11, 125.08, 122.23, 120.62, 115.02, 114.29, 114.16, 106.52, 101.47, 73.07, 72.64, 72.11, 71.80, 65.22, 64.94, 64.92, 64.81, 63.95, 63.92, 47.25, 34.89, 34.87, 31.70, 31.68, 30.09, 29.94.; HR-ESMS: *m/z* = 2051.5980 $[Fe(\mathbf{5a})_2]^{2+}$ (calc. for $C_{272}H_{294}FeN_{14}O_{18}$, 2051.5921); UV-Vis ($CH_2Cl_2$): λ_{max} nm (ε L. $mol^{-1}cm^{-1}$) = 569 (3704), 321 (10768), 283 (15204).

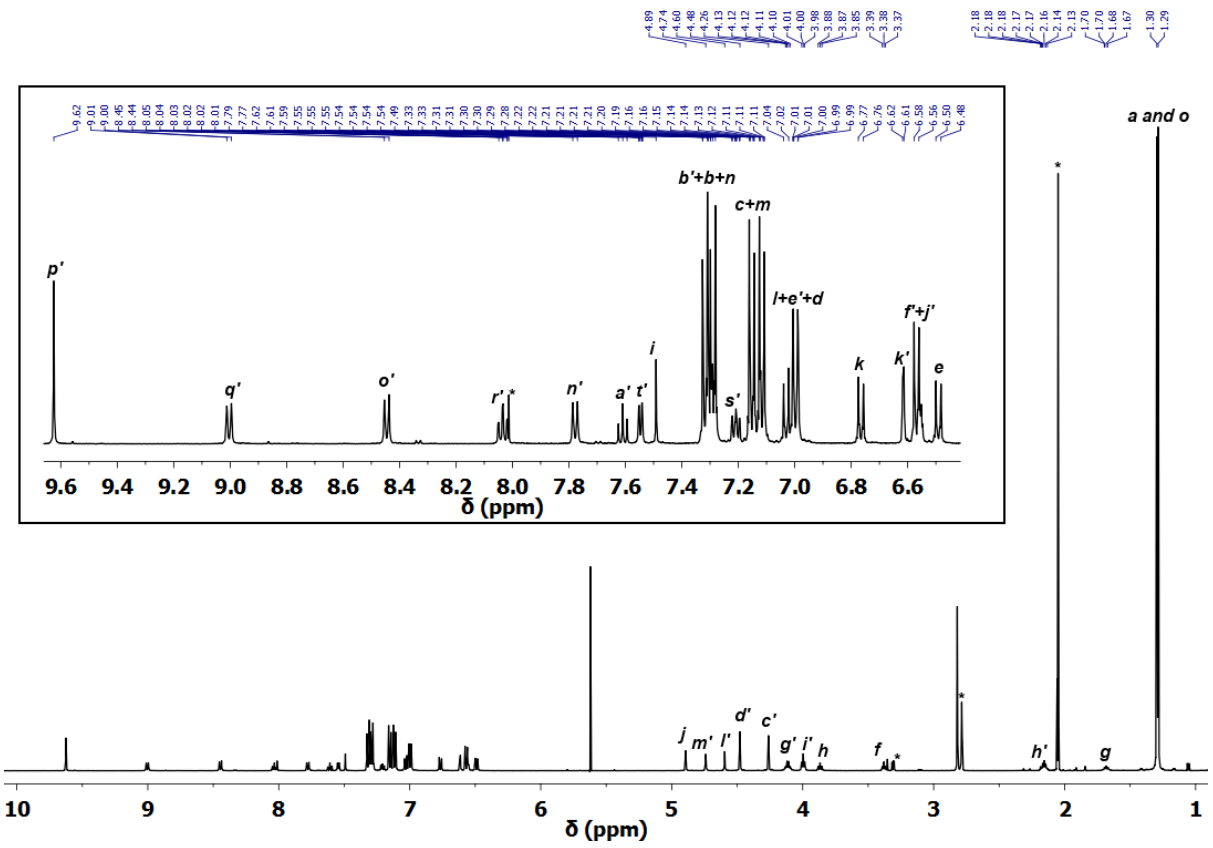

Figure S 55 ^{1}H NMR spectrum (500 MHz, acetone-d_6, 298K) of $[Fe(\mathbf{5a})_2](BF_4)_2$ (* peaks due to H_2O, acetonitrile and CH_2Cl_2)

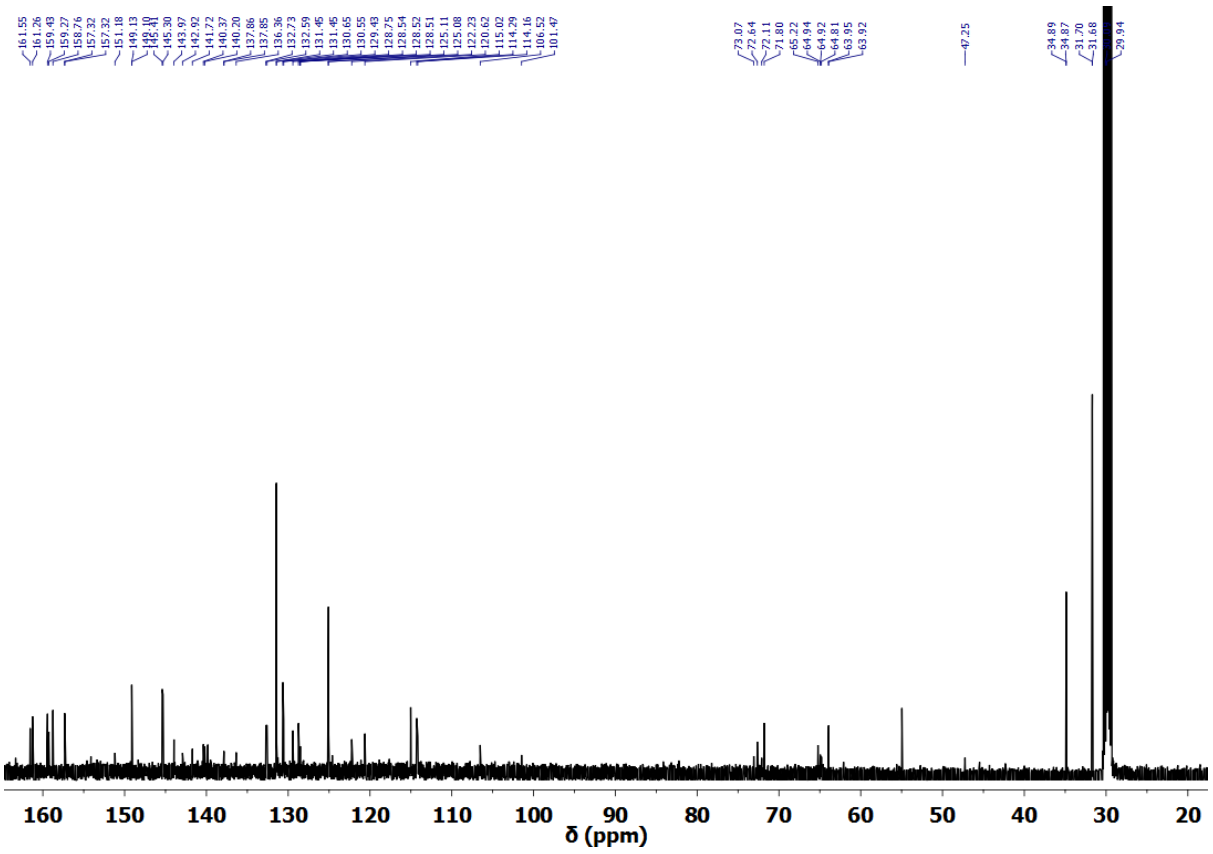

Figure S 56 ^{13}C NMR spectrum (125 MHz, acetone-d_6, 298K) of [Fe(**5a**)$_2$](BF$_4$)$_2$

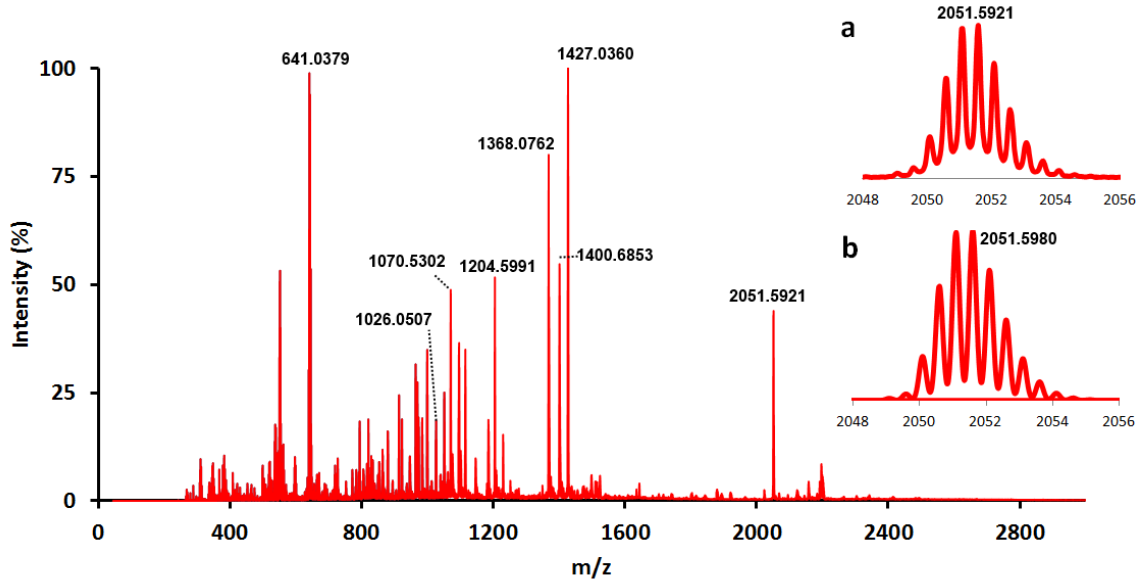

Figure S 57 HR-ESMS spectrum of [Fe(**5a**)$_2$](BF$_4$)$_2$, inset a) observed and b) calculated isotopic patterns for [Fe(**5a**)$_2$]$^{2+}$ at *m/z* = 2051.5921, also showing peaks due to [Fe(**5a**)$_2$]$^{3+}$ (*m/z* = 1368.0762), [Fe(**5a**)$_2$]$^{4+}$ (*m/z* = 1026.0507) (other peaks due to unknown fragments).

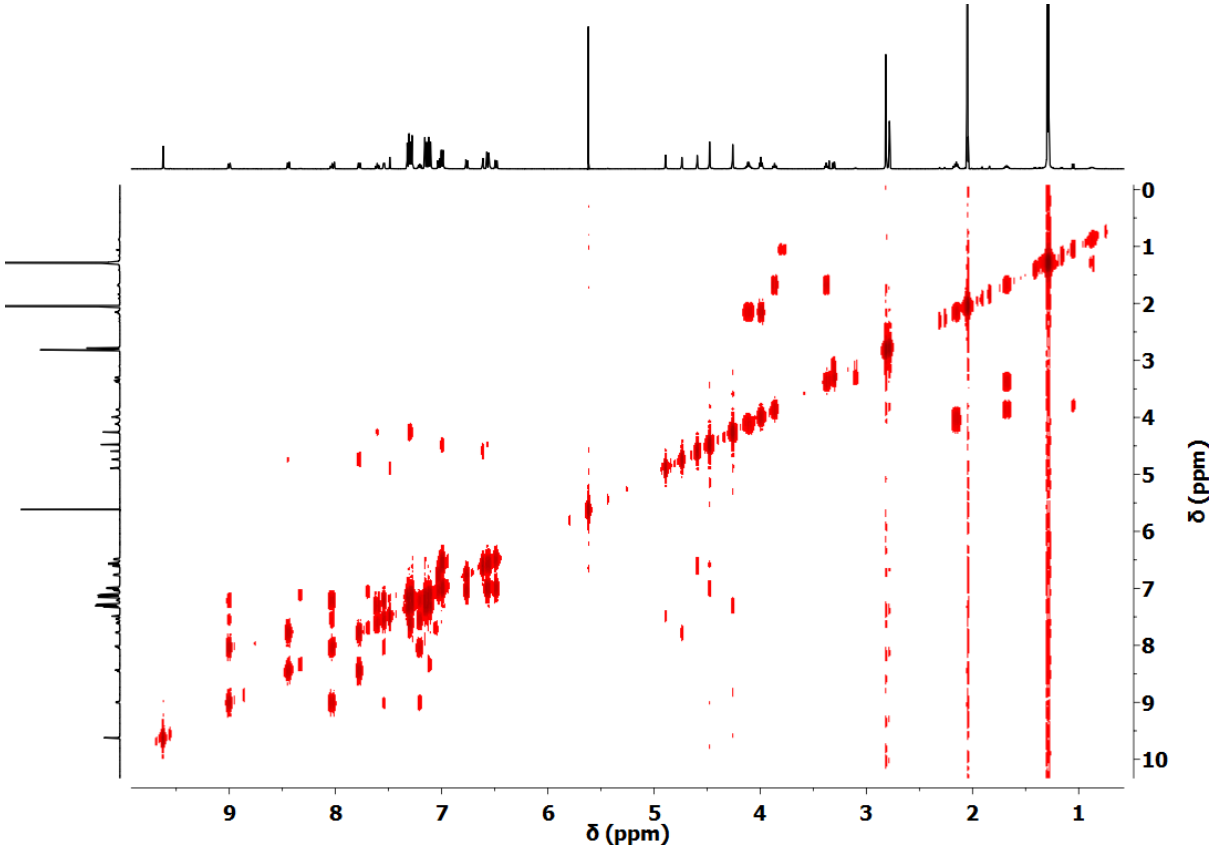

Figure S 58 ^{1}H COSY NMR spectrum (500 MHz, acetone-d_6, 298K) of [Fe(**5a**)$_2$](BF$_4$)$_2$.

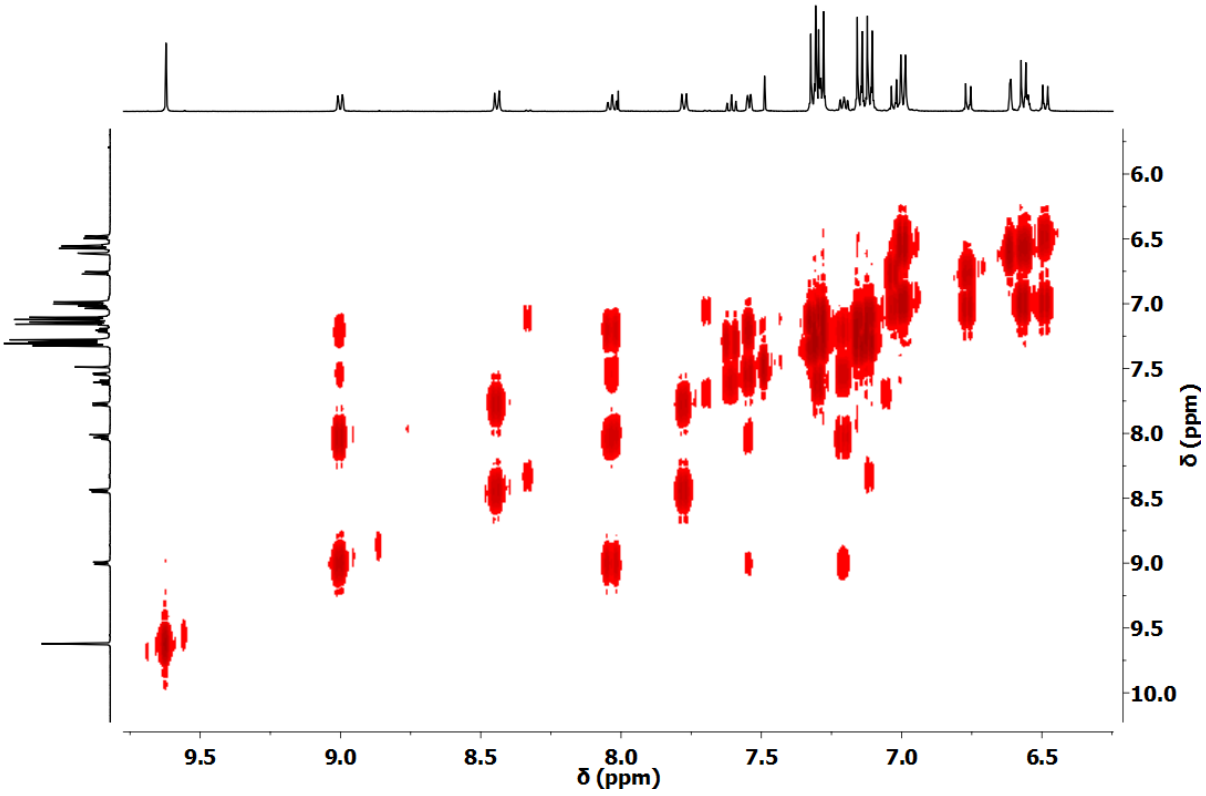

Figure S 59 Partial ^{1}H COSY NMR spectrum (500 MHz, acetone-d_6, 298K) for aromatic region of [Fe(**5a**)$_2$](BF$_4$)$_2$.

5.4 [Fe(5b)](BF$_4$)$_2$

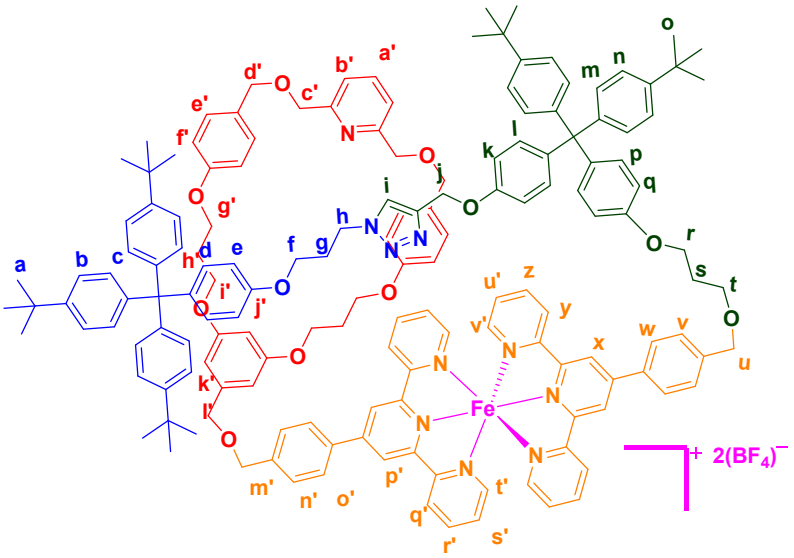

An acetonitrile (100 mL) solution of rotaxane **5b** (30 mg, 0.013 mmol) and [Fe(H$_2$O)$_6$](BF$_4$)$_2$ (4 mg, 0.013 mmol) was stirred at RT over 24 hours. The solvent was removed under reduced pressure and the residue was subjected to column chromatography (silica gel, CH$_2$Cl$_2$/methanol, 9:1) to give pure iron complex [Fe(**5b**)](BF$_4$)$_2$ (25 mg, 76%); ^{1}H NMR (500 MHz, acetone-d_6) δ 9.53 (s, 2H, H$_{p'}$ or H$_x$), 9.48 (s, 2H, H$_{p'}$ or H$_x$), 8.91 (d, J = 8.1 Hz, 2H, H$_{q'}$ or H$_y$), 8.75 (d, J = 8.0 Hz, 2H, H$_{q'}$ or H$_y$), 8.43 (d, J = 8.2 Hz, 2H, H$_{o'}$ or H$_w$), 8.24 (d, J = 8.2 Hz, 2H, H$_{o'}$ or H$_w$), 7.95 (td, J = 7.8, 1.4 Hz, 2H, H$_{r'}$ or H$_z$), 7.86 (td, J = 7.8, 1.4 Hz, 2H, H$_{r'}$ or H$_z$), 7.78 (d, J = 8.1 Hz, 2H, H$_{n'}$ or H$_v$), 7.70 (d, J = 8.1 Hz, 2H, H$_{n'}$ or H$_v$), 7.57 (s, 1H, H$_i$), 7.50 (ddd, J = 5.7, 1.4, 0.7 Hz, 2H, H$_{t'}$ or H$_{v'}$), 7.46 – 7.41 (m, 3H, H$_{a'}$, H$_{t'}$ or H$_{v'}$), 7.36 – 7.29 (m, 10H, H$_b$, H$_n$), 7.20 (d, J = 8.8 Hz, 2H, H$_p$), 7.17 – 7.12 (m, 14H, H$_{b'}$, H$_{c'}$, H$_m$, H$_{u'}$ or H$_{s'}$), 7.01 – 6.97 (m, 4H, H$_l$, H$_{u'}$ or H$_{s'}$), 6.93 – 6.87 (m, 6H, H$_m$, H$_q$, H$_{e'}$), 6.84 (d, J = 8.9 Hz, 2H, H$_d$), 6.57 (d, J = 2.3 Hz, 2H, H$_{k'}$), 6.44 (d, J = 8.5 Hz, 4H, H$_{f'}$), 6.21 – 6.17 (m, 3H, H$_k$, H$_{j'}$), 6.03 (d, J = 8.8 Hz, 2H, H$_e$), 4.90 (s, 2H, H$_u$ or H$_{m'}$), 4.78 (s, 2H, H$_u$ or H$_{m'}$), 4.61 (s, 2H, H$_{l'}$), 4.42 and 4.38 (ABq, J = 12.1, 4H, H$_{d'}$), 4.17 – 4.12 (m, 8H, H$_r$, H$_j$, H$_{c'}$), 4.04 (t, J = 5.8 Hz, 4H, H$_{i'}$), 3.93 (t, J = 5.8 Hz, 4H, H$_{g'}$), 3.82 (t, J = 7.2 Hz, 2H, H$_h$), 3.68 (t, J = 5.7 Hz, 2H, H$_t$), 3.01 (t, J = 6.0 Hz, 2H, H$_f$), 2.17 – 2.12 (m, 4H, H$_{h'}$), 2.09 – 2.06 (m, 2H, H$_s$), 1.56 (p, J = 6.5 Hz, 2H, H$_g$), 1.31 (s, 27H, H$_a$), 1.23 (s, 18H, H$_o$).; ^{13}C NMR (125 MHz, acetone-d_6) δ 161.60, 161.45, 160.86, 159.38, 159.30, 158.91, 158.65, 158.14, 156.94, 156.92, 154.29, 153.75, 151.39, 151.06, 149.24, 149.03, 145.88, 145.52, 143.17, 142.99, 142.93, 142.40, 140.52, 139.92, 139.83, 139.71, 137.69, 136.68, 136.48, 132.66, 132.46, 132.35, 132.30, 131.50, 131.44, 131.19, 130.58, 130.55, 130.14, 129.73,

128.83, 128.75, 128.53, 128.36, 125.37, 125.24, 125.10, 125.07, 124.79, 122.47, 122.11, 120.36, 116.00, 115.92, 115.04, 114.95, 114.42, 114.00, 113.82, 105.69, 102.21, 72.84, 72.63, 72.57, 72.17, 71.78, 65.69, 64.79, 64.70, 64.40, 63.94, 63.80, 61.31, 60.87, 54.96, 47.45, 34.91, 34.86, 31.72, 31.62, 30.09, 29.93; HR-ESMS: *m/z* = 1209.0821 $[Fe(\mathbf{5b})]^{2+}$ (calc. for $C_{157}H_{160}FeN_{10}O_{11}$, 1209.0889); UV-Vis ($CH_2Cl_2$): λ_{max} nm (ε L. $mol^{-1}cm^{-1}$) = 570 (5252), 321 (14436), 285 (18524).

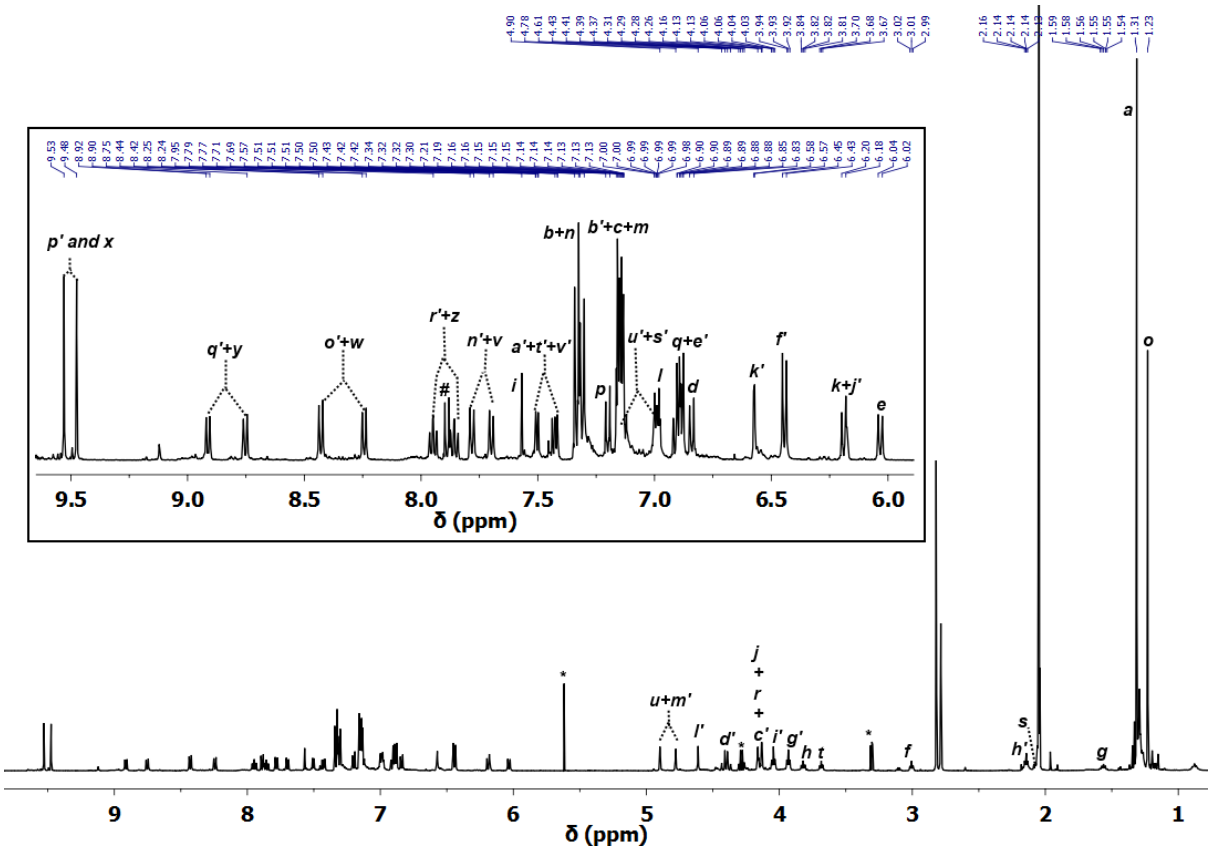

Figure S 60 ^{1}H NMR spectrum (500 MHz, acetone-d_6, 298K) of $[Fe(\mathbf{5b})_2](BF_4)_2$ (* peaks due to H_2O, acetonitrile and CH_2Cl_2, # unassigned peak).

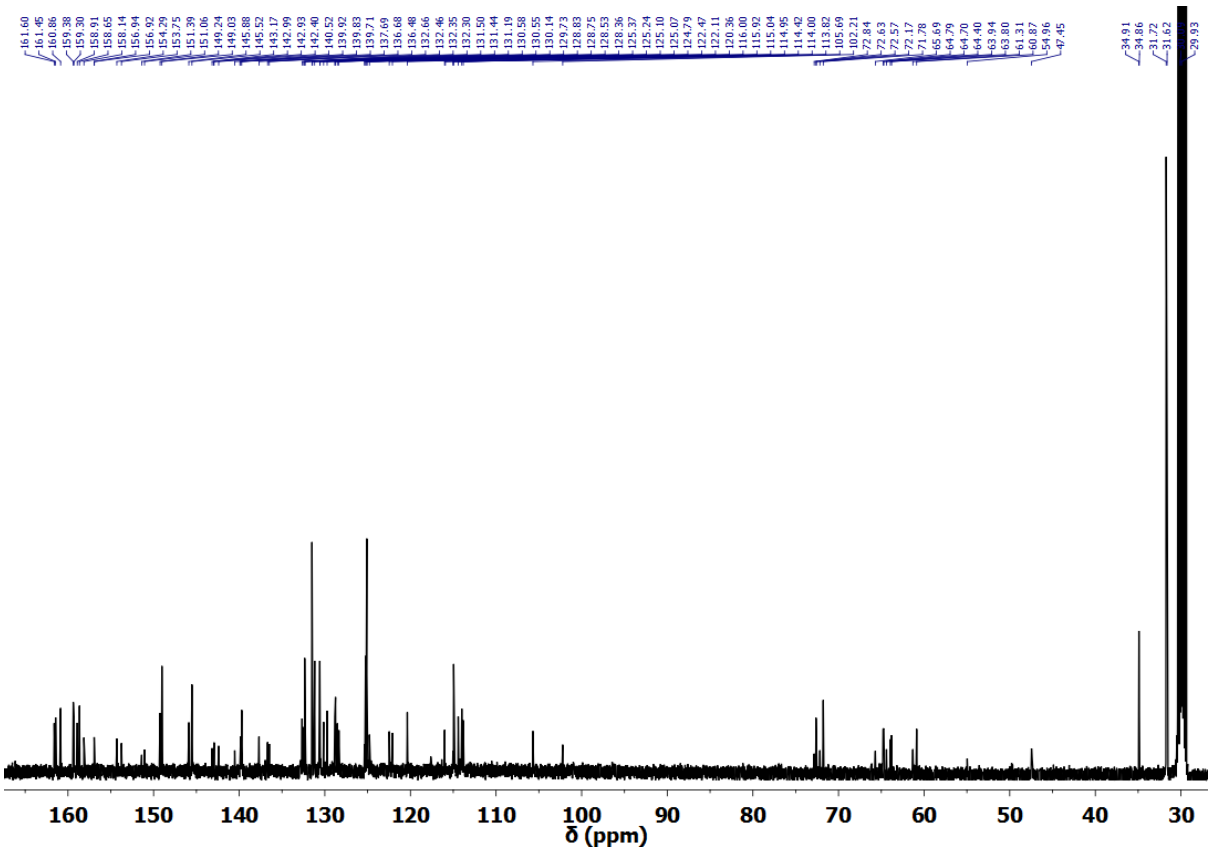

Figure S 61 ^{13}C NMR spectrum (125 MHz, acetone-d_6, 298K) of [Fe(**5b**)$_2$](BF$_4$)$_2$.

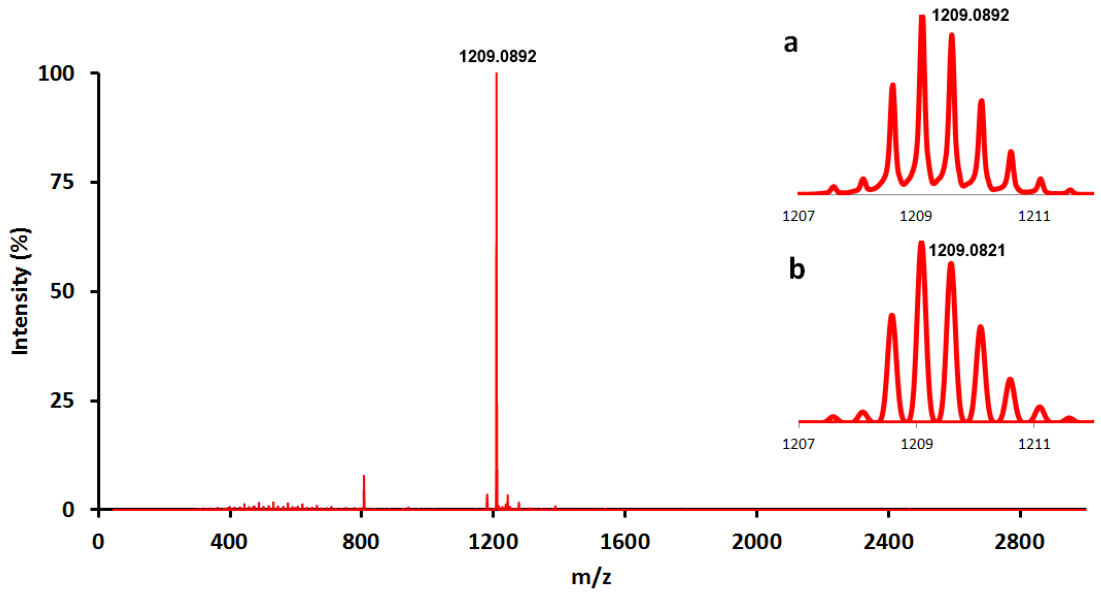

Figure S 62 63 HR-ESMS spectrum of [Fe(**5b**)$_2$](BF$_4$)$_2$, inset a) observed and b) calculated isotopic patterns for [Fe(**5b**)]$^{2+}$ at *m/z* = 1209.0621.

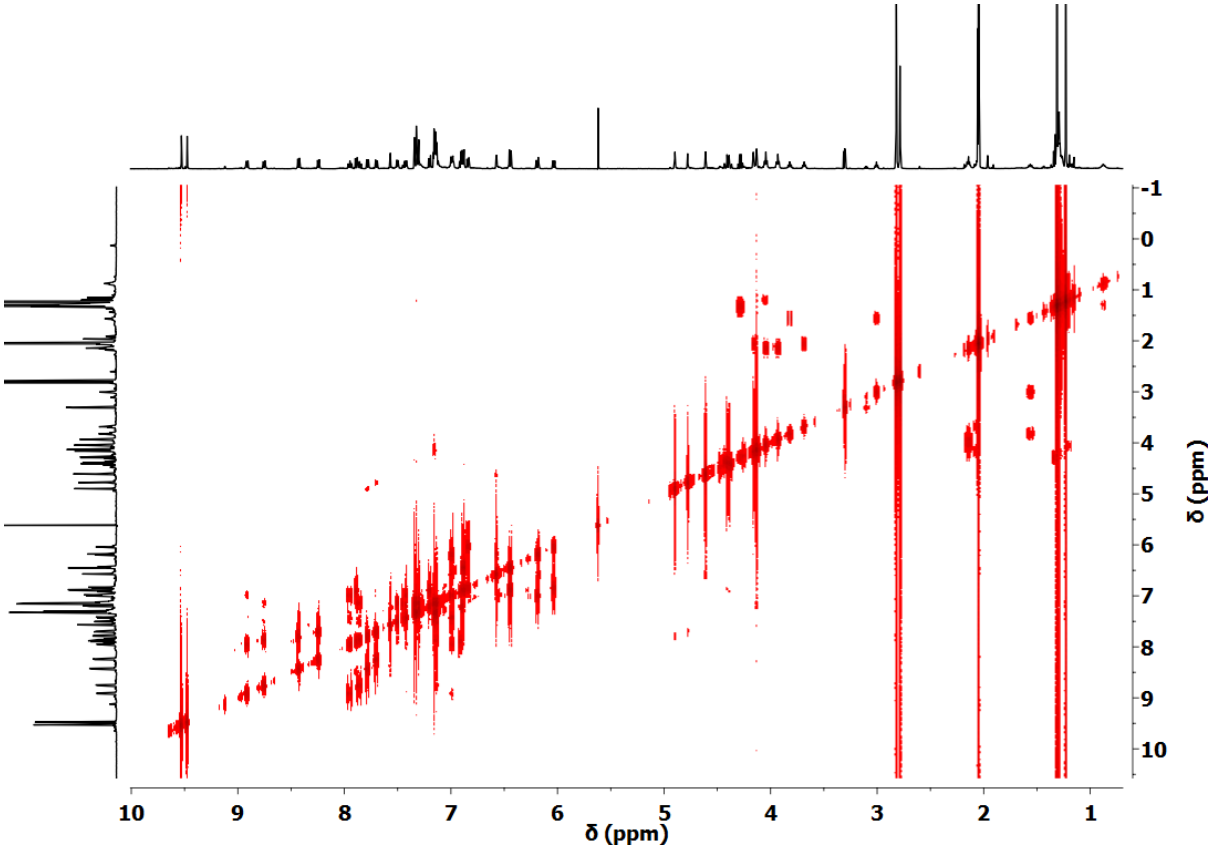

Figure S 64 ^{1}H COSY NMR spectrum (500 MHz, acetone-d_6, 298K) of [Fe(**5b**)$_2$](BF$_4$)$_2$.

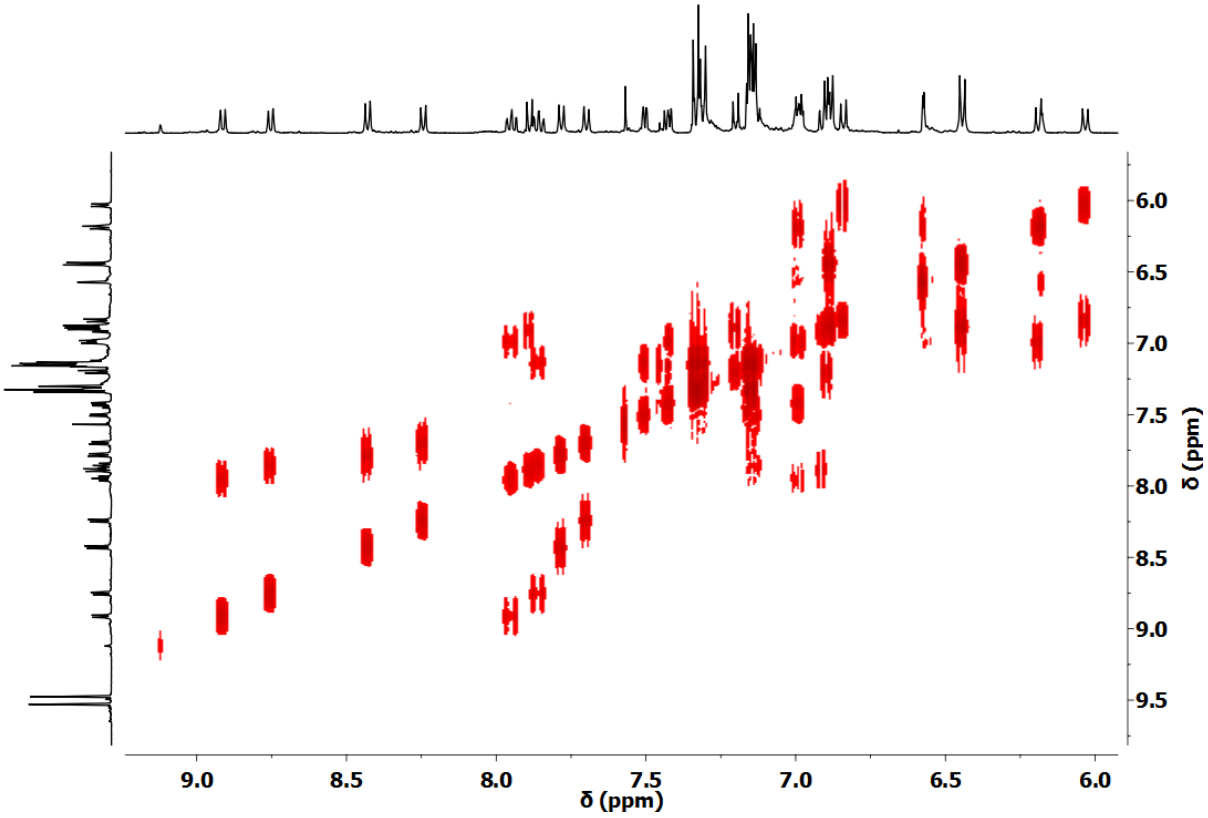

Figure S 65 Partial ^{1}H COSY NMR spectrum (500 MHz, acetone-d_6, 298K) for aromatic region of [Fe(**5a**)$_2$](BF$_4$)$_2$.

5.5 [Fe(5b)]$_n$(PF$_6$)$_{2n}$

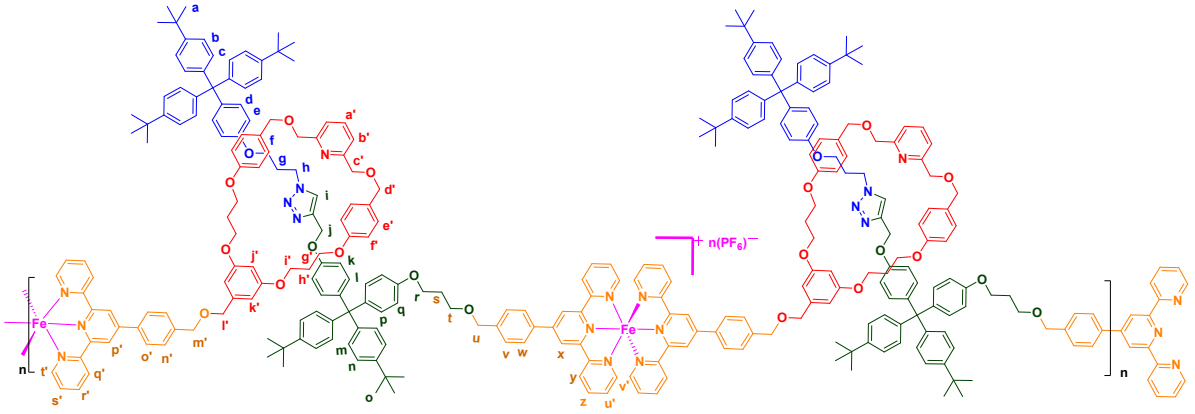

To a chloroform (0.5 mL) solution of rotaxane **5b** (75 mg, 0.032 mmol) was added a solution of $FeCl_2$ (4 mg, 0.013 mmol) in methanol (0.5 mL) under a nitrogen atmosphere. The mixture was stirred for 20 h at RT. NH_4PF_6 (207 mg, 1.270 mmol) in methanol (5 mL) was added and the resulting mixture was stirred for a further 30 min then diethyl ether (20 mL) was added to the solution to precipitate the product, which was filtered, washed with methanol and dried to give [Fe(**5b**)]$_n$(PF$_6$)$_{2n}$ as purple powder (60 mg, 76%). ^{1}H NMR (500 MHz, acetone-d_6) δ 9.65 – 9.48 (m, 4H, H$_{p'}$, H$_x$), 9.11 – 8.81 (m, 4H, H$_{q'}$, H$_y$), 8.52 – 8.34 (m, 4H, H$_{o'}$, H$_w$), 8.08 – 7.94 (m, 4H, H$_{r'}$, H$_z$), 7.83 – 7.72 (m, 4H, H$_{n'}$, H$_v$), 7.60 – 7.45 (m, 6H, H$_i$, H$_{a'}$, H$_{t'}$, H$_{v'}$), 7.41 – 6.92 (m, 38H, H$_{aromatic}$), 6.92 – 6.84 (m, 2H, H$_{aromatic}$), 6.83 – 6.71 (m, 2H, H$_{aromatic}$), 6.67 – 6.41 (m, 11H, H$_{aromatic}$), 4.89 (s, 2H, H$_{aliphatic}$), 4.79 – 4.70 (m, 2H, H$_{aliphatic}$), 4.59 (s, 2H, H$_{aliphatic}$), 4.53 – 4.44 (m, 4H, H$_{aliphatic}$), 4.37 – 4.22 (m, 4H, H$_{aliphatic}$), 4.22 – 4.16 (m, 2H, H$_{aliphatic}$), 4.15 – 4.06 (m, 2H, H$_{aliphatic}$), 4.03 – 3.95 (m, 4H, H$_{aliphatic}$), 3.91 – 3.85 (m, 2H, H$_{aliphatic}$), 3.85 – 3.78 (m, 2H, H$_{aliphatic}$), 3.44 – 3.33 (m, 2H, H$_{aliphatic}$), 2.22 – 2.11 (m, 6H, H$_{aliphatic}$), 1.74 – 1.63 (m, 2H, H$_{aliphatic}$), 1.33 – 1.19 (m, 45H, H$_{tertiarybutyl}$).; UV-Vis (CH_2Cl_2): λ_{max} nm (ε L. mol^{-1} cm^{-1}) = 568 (26208), 320 (65660), 286 (74816); GPC (5×10^{-3} M NH_4PF_6 in DMF, UV-detector): $\bar{M}_w$ = 31410, PDI = 1.26; ^{1}H DOSY (500 MHz, acetone-d_6, 298 K) D = 1.94 (10^{-10} m^2/s), $\bar{M}_w$ (DOSY) = 29007.

6 Molecular Modelling of the Interlocked Assemblies

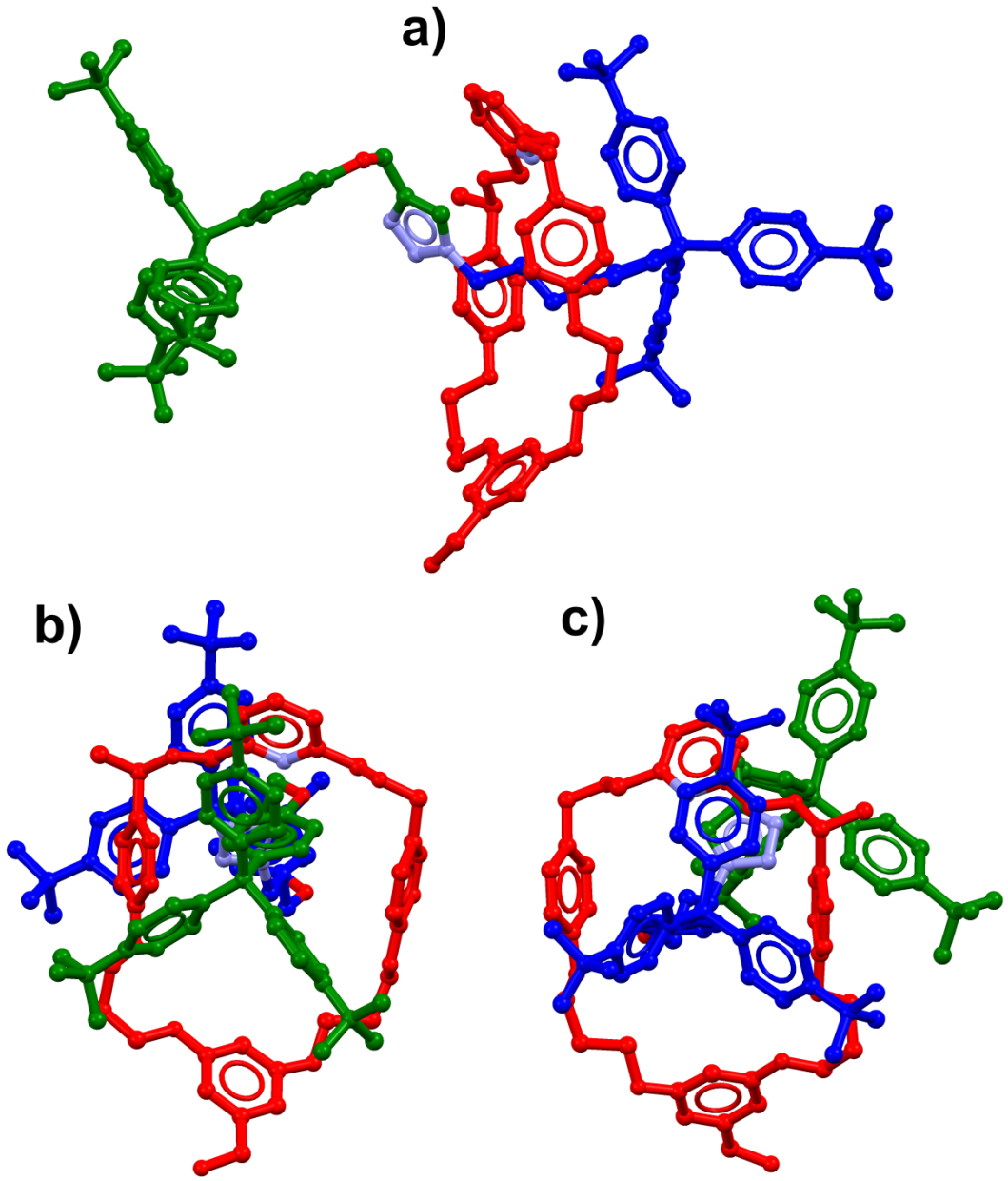

Figure S 66 Ball-and-stick molecular model of **4a** showing one of the low energy conformations of the interlocked molecule (MMFF, SPARTAN '06). Hydrogen atoms are omitted for clarity, colouring correspond to the structure shown in compound **4a** in experimental section.

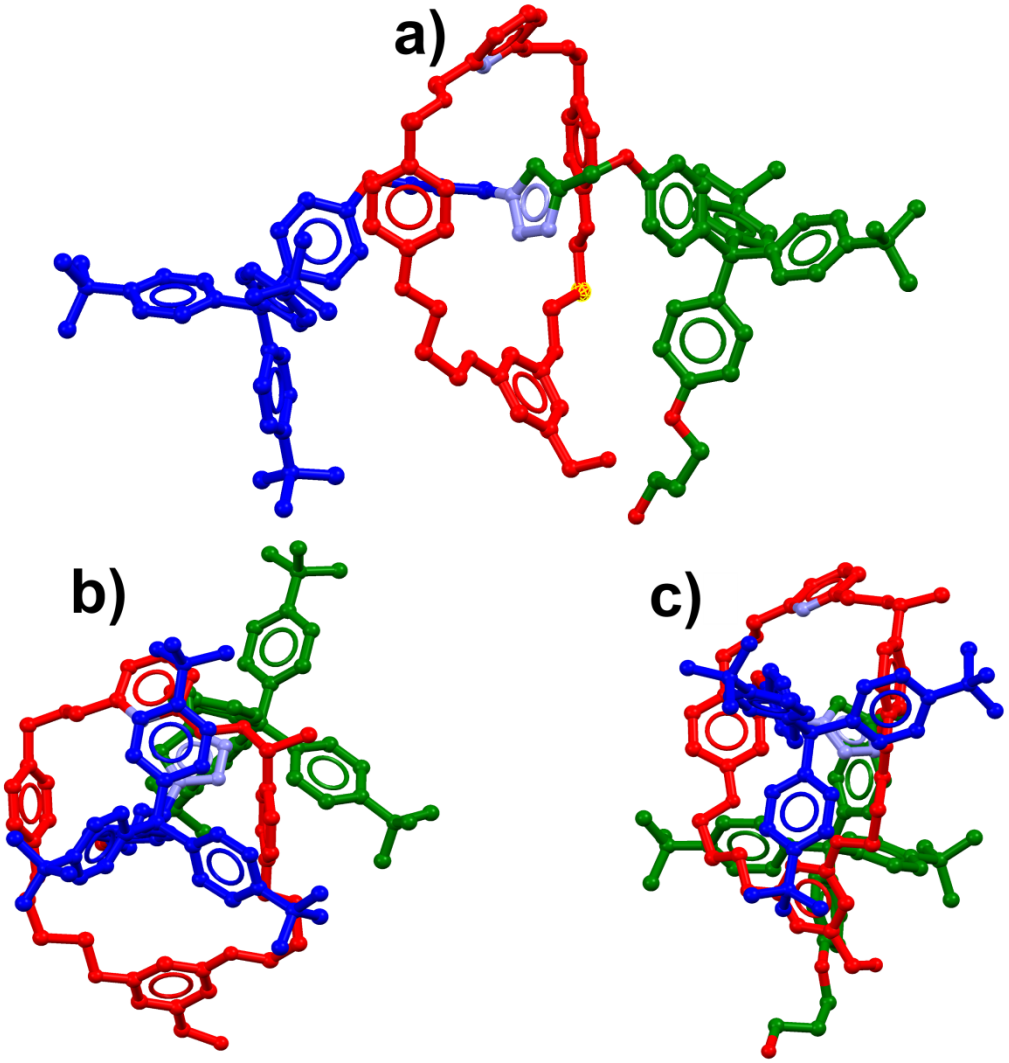

Figure S 67 Ball-and-stick molecular model of **4b** showing low energy conformations of the interlocked molecule (MMFF, SPARTAN '06). Hydrogen atoms are omitted for clarity, colouring correspond to the structure shown in compound **4b** in experimental section.

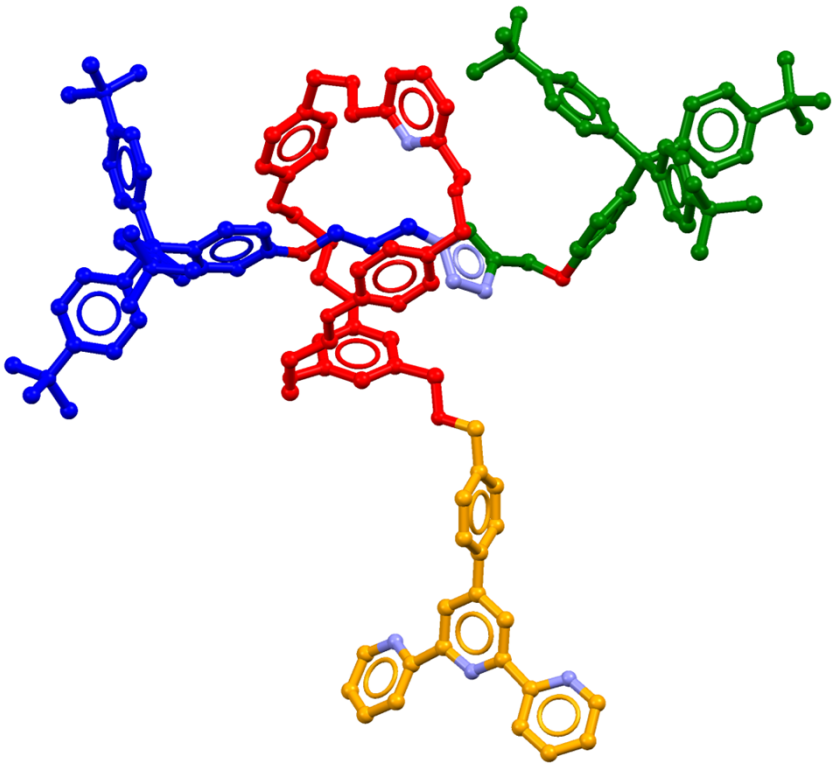

Figure S 68 Ball-and-stick molecular model of **5a** showing low energy conformations of the interlocked molecule (MMFF, SPARTAN '06). Hydrogen atoms are omitted for clarity, colouring correspond to the structure shown in compound **5a** in experimental section.

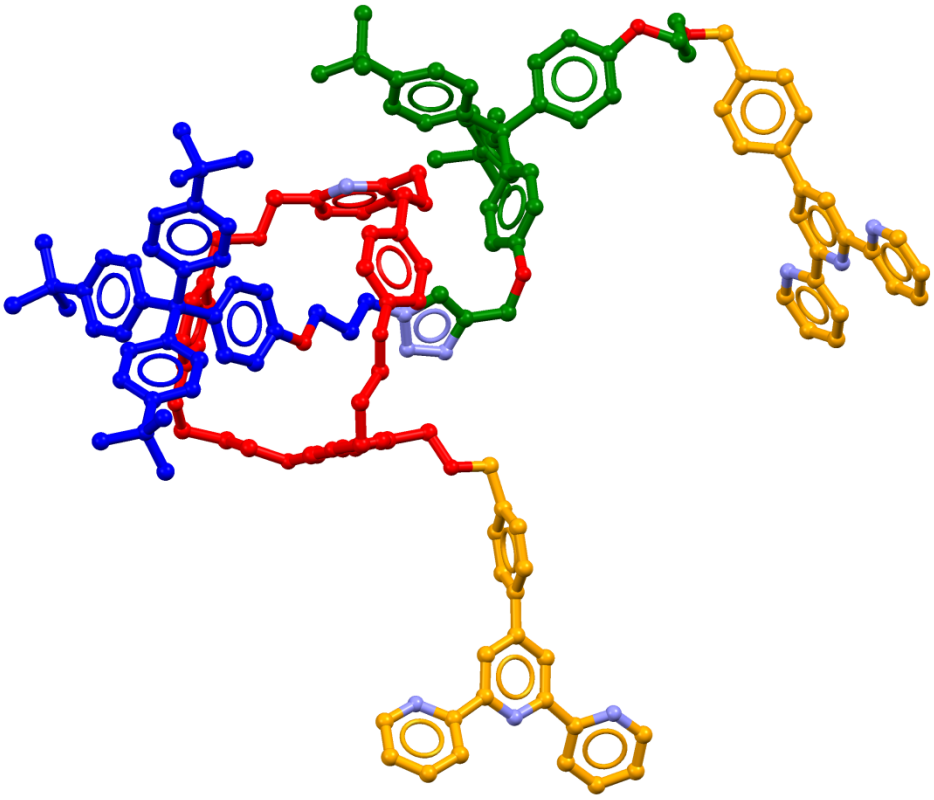

Figure S 69 Ball-and-Stick molecular model of **5b** showing low energy conformations of the interlocked molecule (MMFF, SPARTAN '06). Hydrogen atoms are omitted for clarity, colouring correspond to the structure shown in compound **5b** in experimental section.

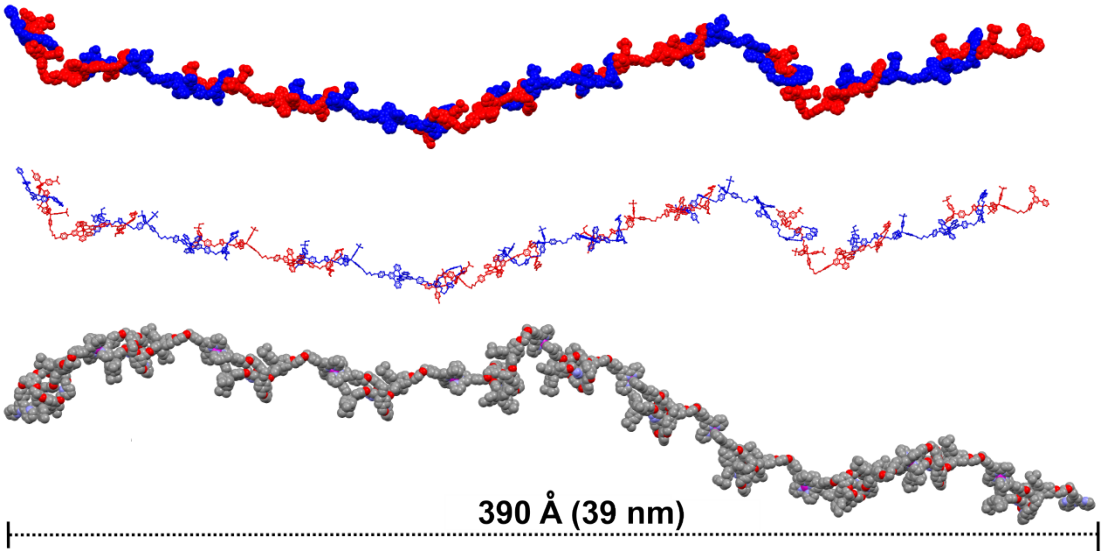

Figure S 70 Different representations of molecular model (MMFF, SPARTAN '06) of $[Fe(\mathbf{5b})]_n(PF_6)_{2n}$ showing one low energy conformation of the interlocked coordinated linear chain molecule consisting of 11 units. Hydrogen atoms are omitted for clarity.

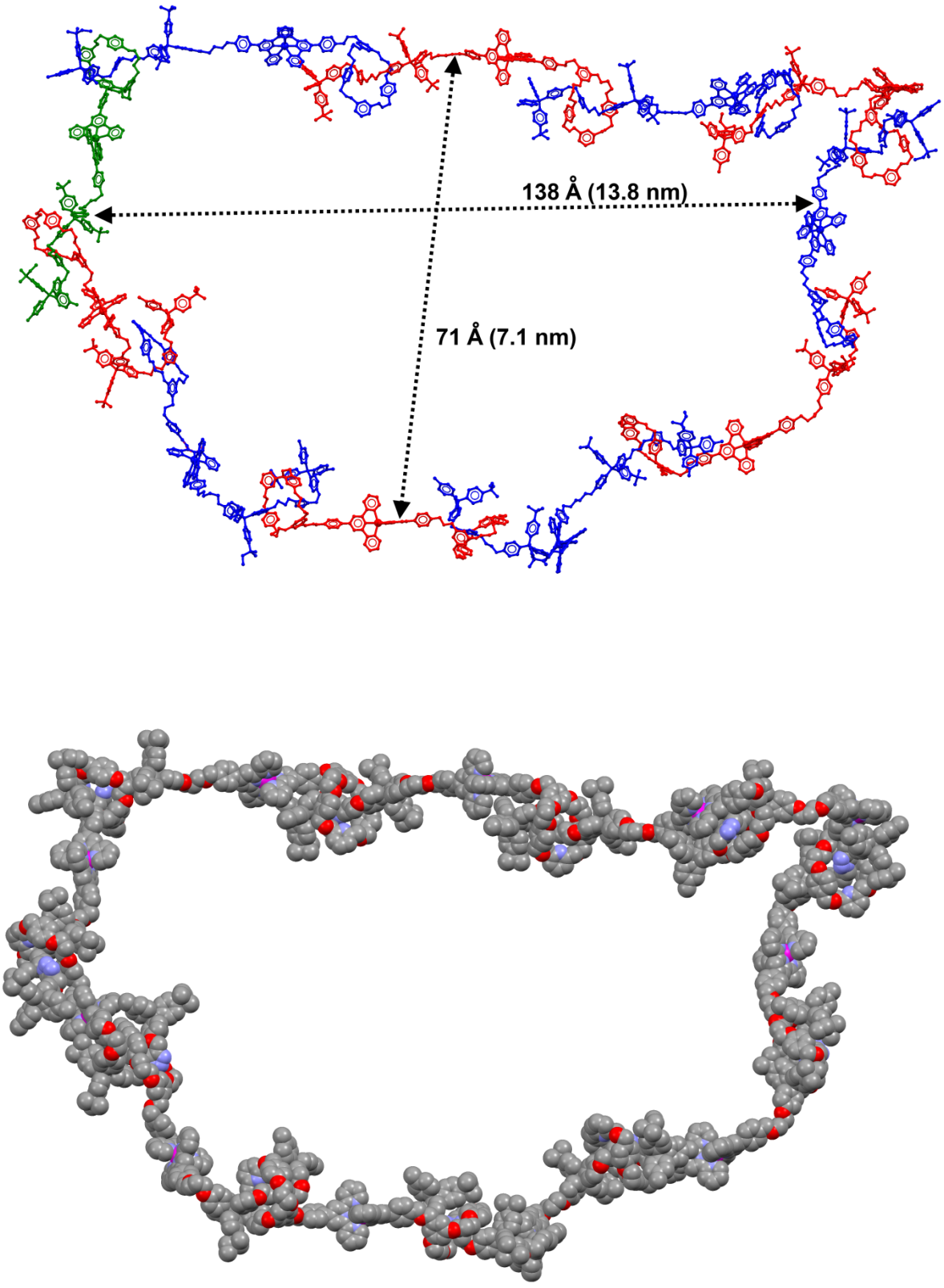

Figure S 71 Different representations of molecular model (MMFF, SPARTAN '06) of $[Fe(\mathbf{5b})]_n(PF_6)_{2n}$ showing one low energy conformation of the interlocked coordinated polycyclic molecule consisting of 11 units. Hydrogen atoms are omitted for clarity.

7 GPC and UV/Vis Analyses

GPC analyses were performed on Polymer Laboratories PL-GPC 50-*Plus* with two PL-Gel 20 µm Mixed-A columns in series with a pre-column installed. A solution of 5×10^{-3} M NH_4PF_6 in DMF was used as the eluent at a flow rate of 0.5 mL/min at 50 °C. Molecular weights were calculated using a standard polystyrene calibration curve. The samples were prepared at a concentration of 2 mg/mL in DMF. The traces were detected using a UV-visible detector at a wavelength of 560 nm.

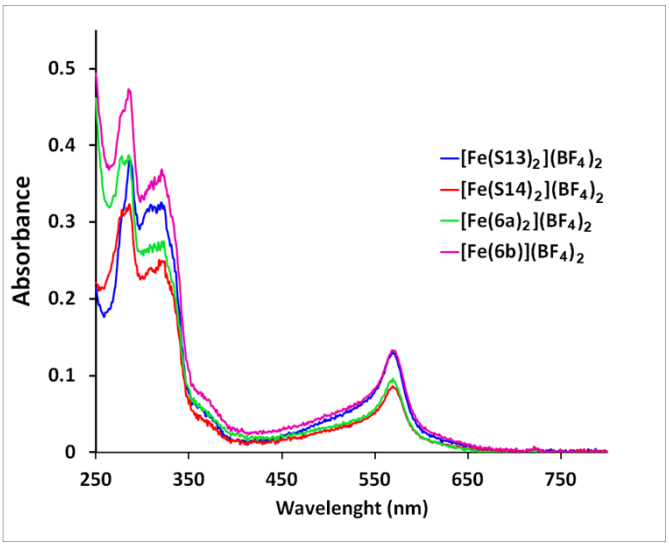

Figure S 72 UV-Vis spectra of [Fe(II)]$(BF_4)_2$ complexes (25 µM in CH_2Cl_2) showing MLCT bands at 570 nm.

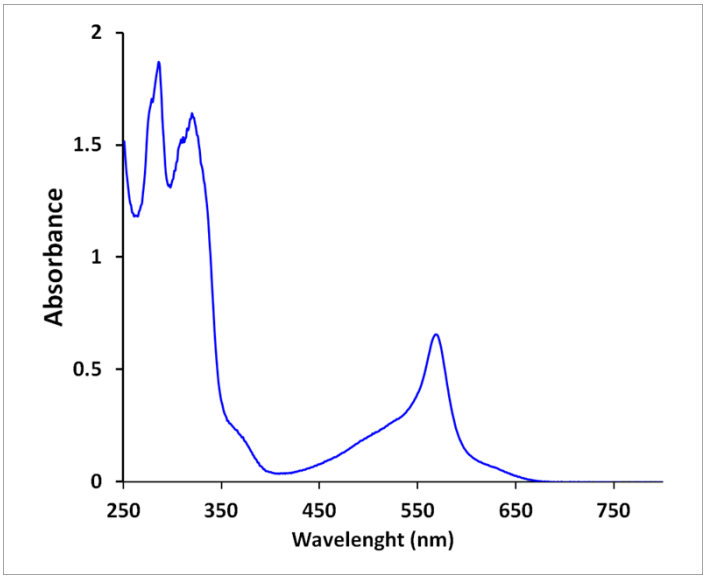

Figure S 73 UV-Vis spectrum of [Fe(**5b**)]$_n(PF_6)_{2n}$ (25 µM in CH_2Cl_2) showing MLCT bands at 570 nm.

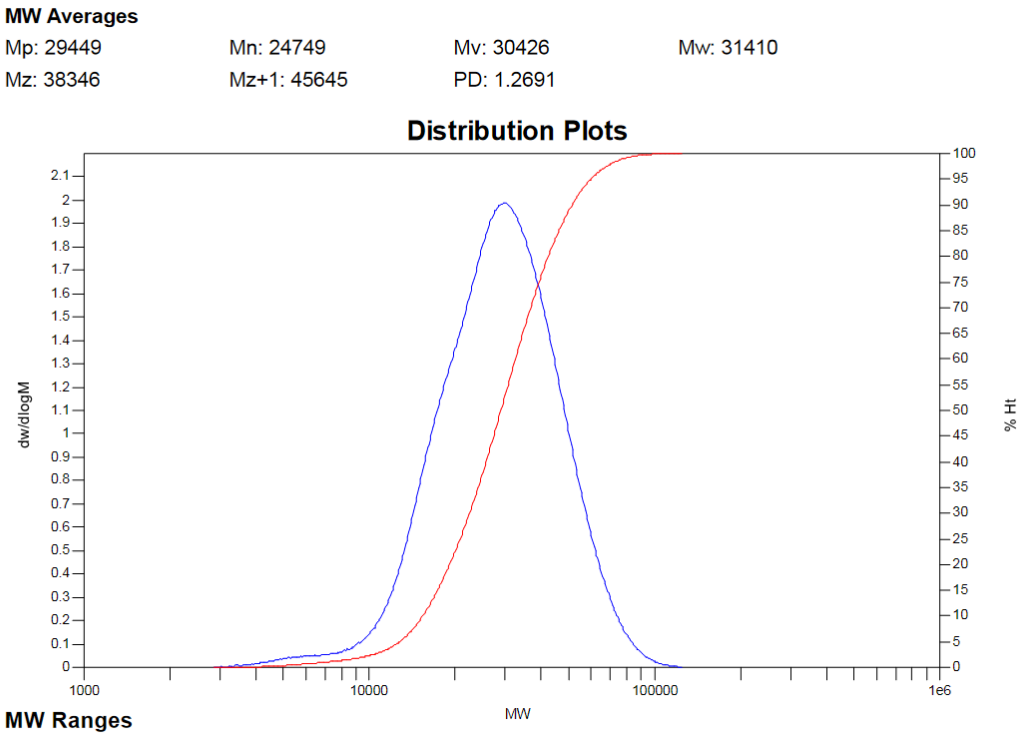

Figure S 74 Molecular weight distribution plots for metallo-polyrotaxane [Fe(**5b**)]$_n$(PF$_6$)$_{2n}$

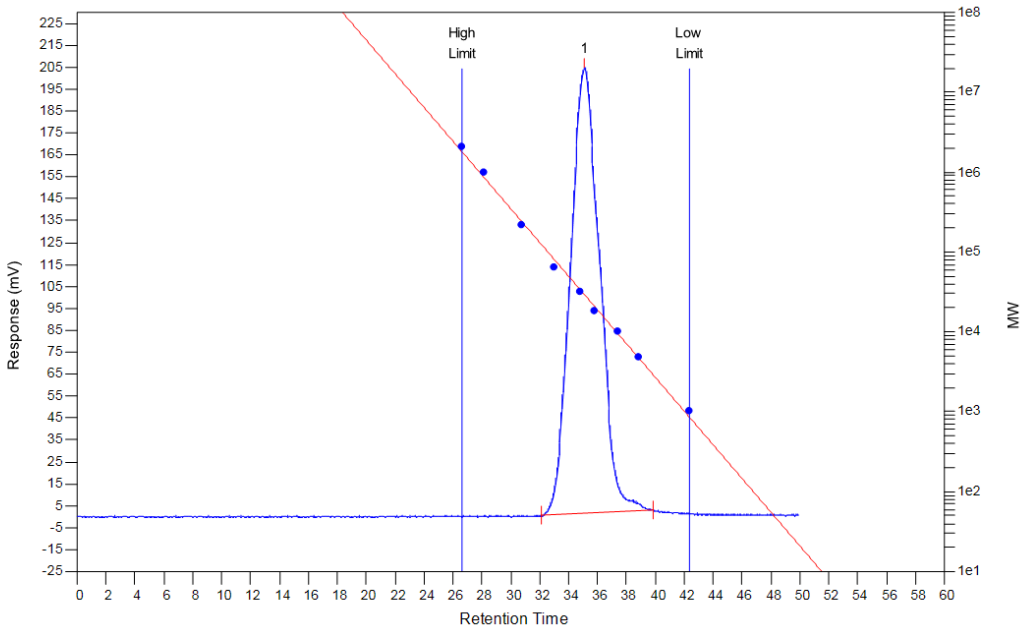

Figure S 75 GPC curves (5×10^{-3} M NH_4PF_6 in DMF) for metallo-polyrotaxane [Fe(**5b**)]$_n$(PF$_6$)$_{2n}$ (UV-detector at 560nm)

8 ^{1}H DOSY NMR Experiments

All DOSY experiments were carried out on a Varian 500 MHz AR spectrometer. All samples were prepared at a concentration of 2 mg/mL in acetone-d_6 for the narrow disperse polystyrene (PS) standards and prepared supramolecular complexes. All samples were analysed at 25 °C with gradient stimulated echo with spin, lock and convection compensation experiments using 16 gradient steps. The spectrums were processed by VnmrJ 3.2 software and the calibration curve was drawn using the following relationship.[5]

$$Log\ D = -\frac{1}{3}\log M + \frac{1}{3}\log \rho - log\ \eta - \frac{1}{3}log\frac{162\pi^2}{k^3T^3N_A}$$

Table S 1 Calculated diffusion coefficients for the standard polystyrene calibration curve.

Standard samples	Molecular weight ($\bar{M_w}$)[a] (g/mol)	Diffusion Coefficient (D) (10^{-10} m^2 s^{-1})	Log $\bar{M_w}$	Log D
Polystyrene	1000	8.81	3.00	0.94
Polystyrene	2330	6.12	3.37	0.79
Polystyrene	10000	3.01	4.00	0.48
Polystyrene	18000	2.38	4.26	0.38
Polystyrene	30000	1.97	4.48	0.29

[a] Molecular weights as according to commercial standard samples

Table S 2 Measurement of $\bar{M_w}$ for[2]rotaxanes and their Fe(II) complexes (calculated from the fitted calibration curve).

Complexes	Actual Molecular Weight (M)[a] (g/mol)	Average Diffusion Coefficient (D) (10^{-10} m^2/s)	Calculated Molecular Weight ($\bar{M_w}$) (g/mol)
4a	1702	7.04	1640±160
4b	1720	6.75	1800±180
5a	2022	6.10	2260±220
5b	2363	5.82	2510±250
[Fe(**5a**)$_2$](BF$_4$)$_2$	4276	4.50	4450±440
[Fe(**5b**)](BF4)2	2592	5.81	2520±250
[Fe(**5b**)]$_n$(PF6)$_n$	27080 (n = 10) 29788 (n = 11) 32496 (n = 12)	1.94	29000±290

[a] Molecular weights including counter ions

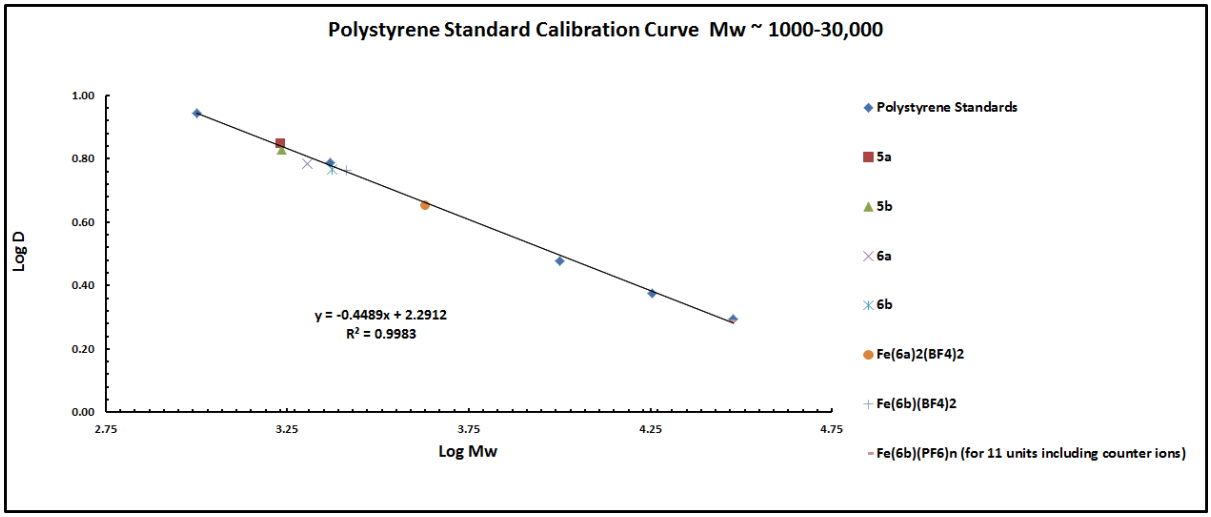

Figure S 76 Polystyrene standard calibration curve (500 MHz, acetone-d_6, 298 K).

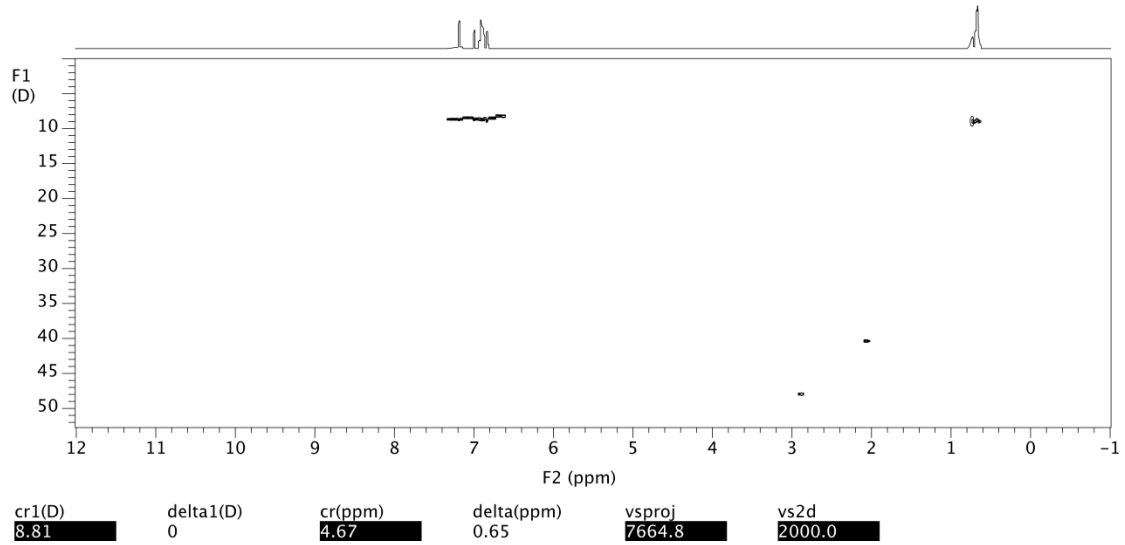

Figure S 77 ^{1}H DOSY NMR spectrum (500 MHz, acetone-d_6, 298K) of **PS 1000**

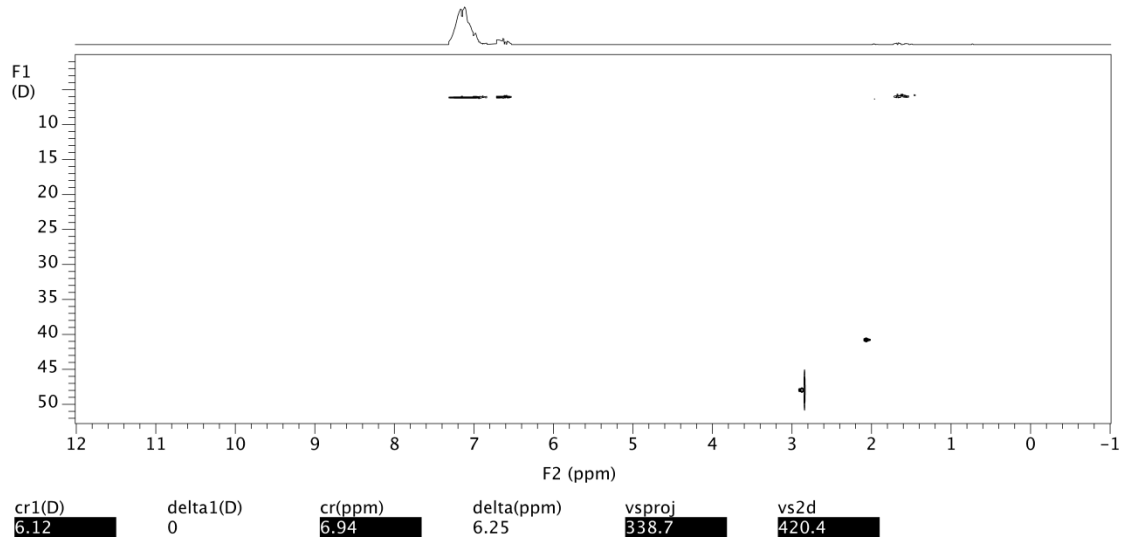

Figure S 78 ^{1}H DOSY NMR spectrum (500 MHz, acetone-d_6, 298K) of **PS 2330**

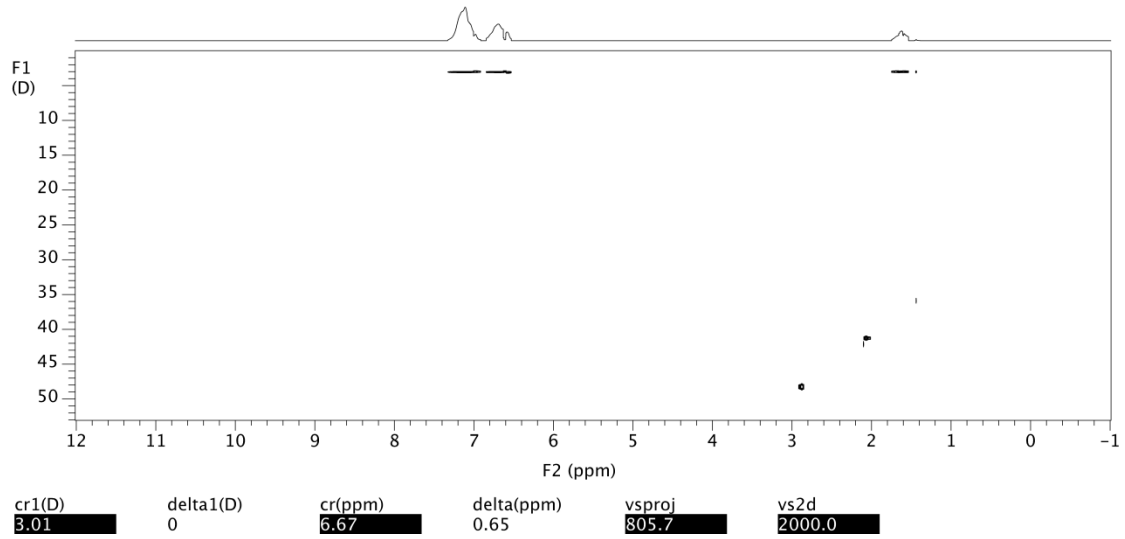

Figure S 79 ^{1}H DOSY NMR spectrum (500 MHz, acetone-d_6, 298K) of **PS 10000**

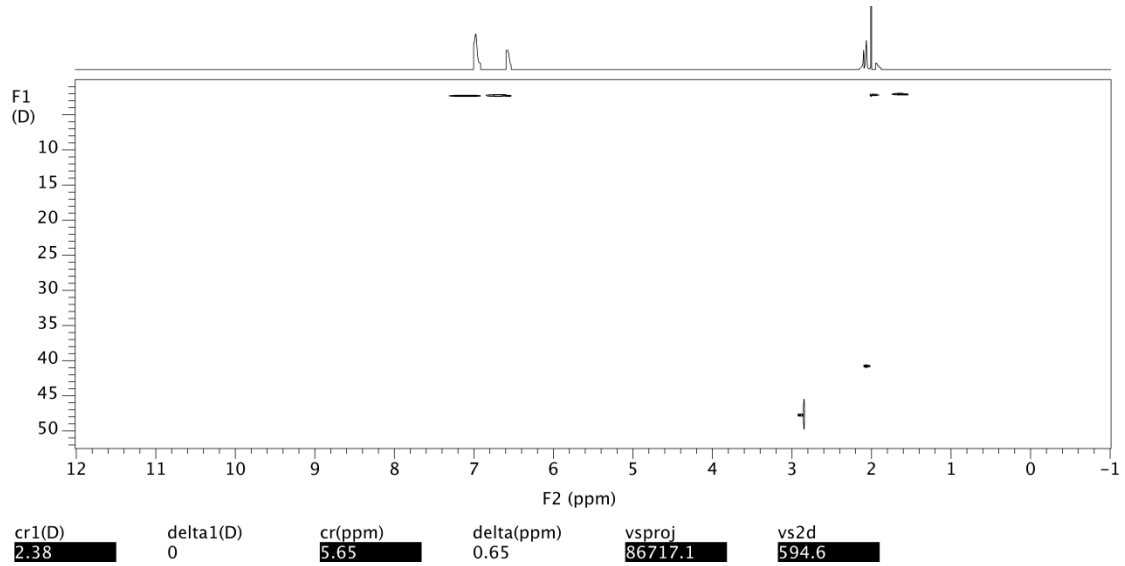

Figure S 80 ^{1}H DOSY NMR spectrum (500 MHz, acetone-d_6, 298K) of **PS 18000**

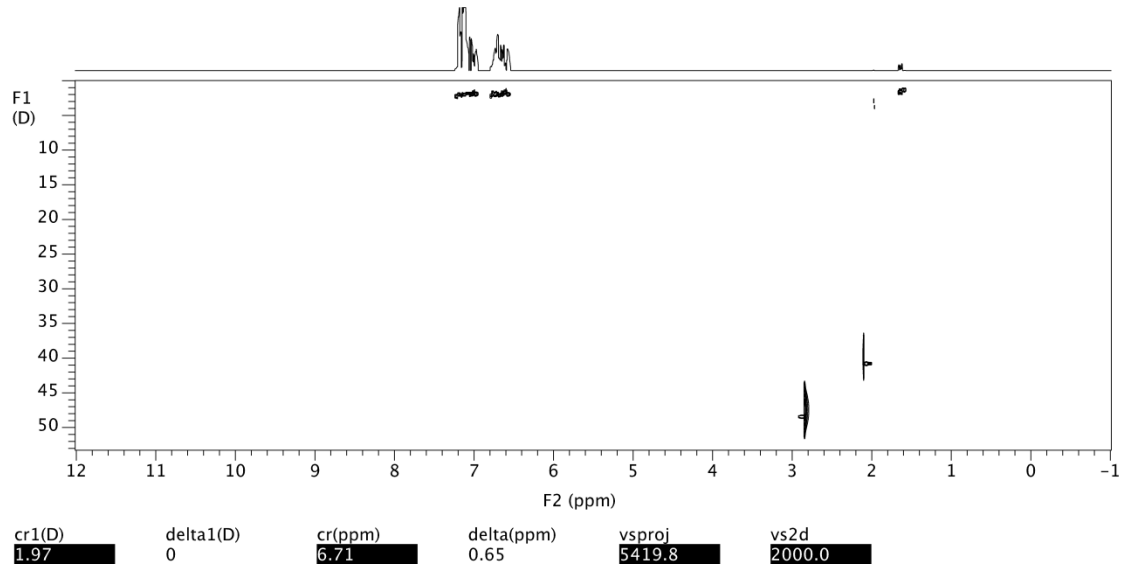

Figure S 81 ^{1}H DOSY NMR spectrum (500 MHz, acetone-d_6, 298K) of **PS 30000**

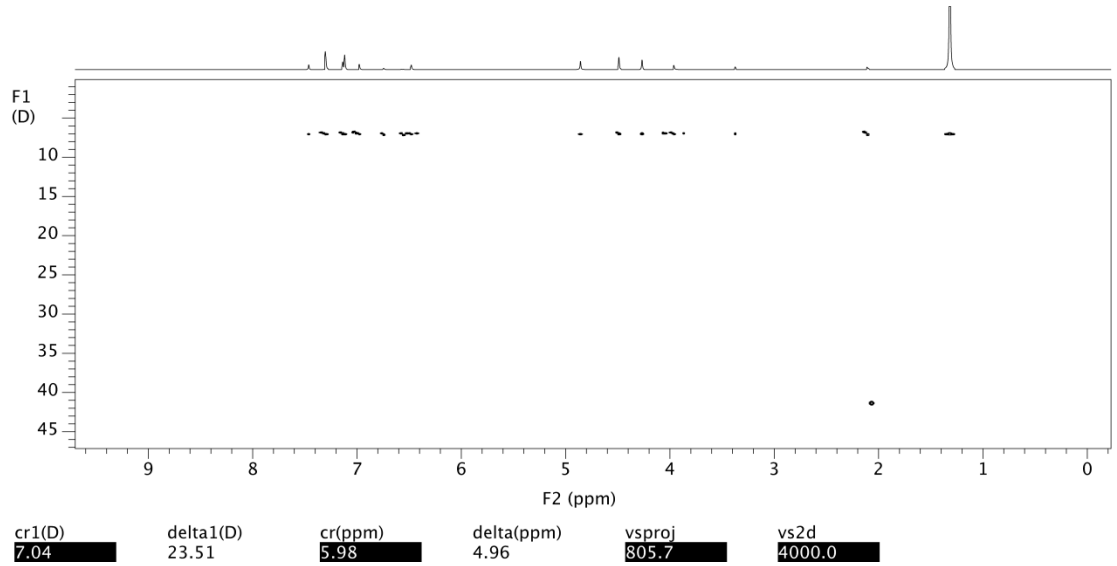

Figure S 82 ^{1}H DOSY NMR spectrum (500 MHz, acetone-d_6, 298K) of **4a**

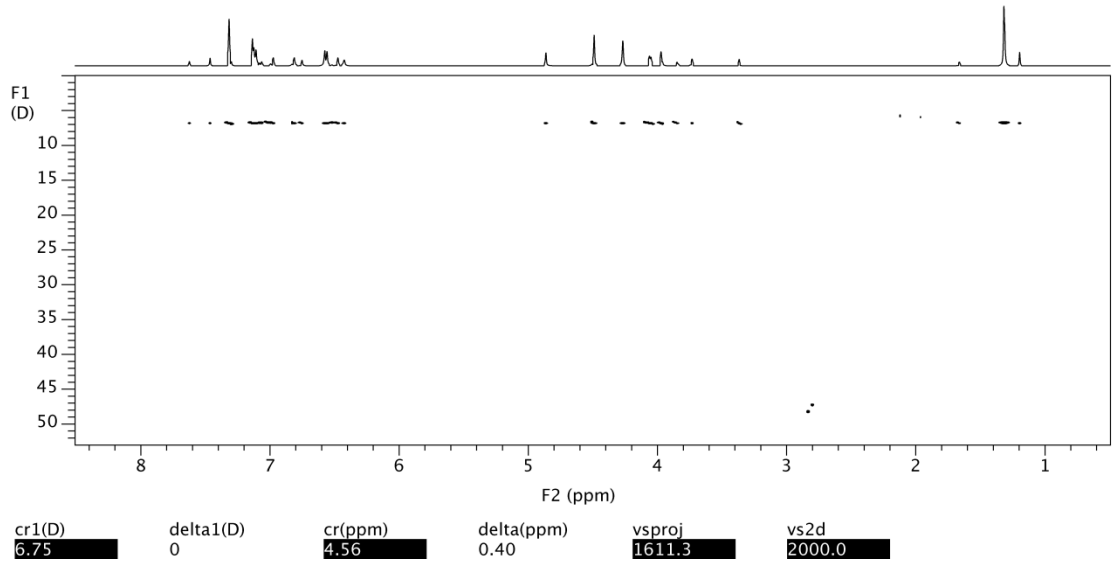

Figure S 83 ^{1}H DOSY NMR spectrum (500 MHz, acetone-d_6, 298K) of **4b**

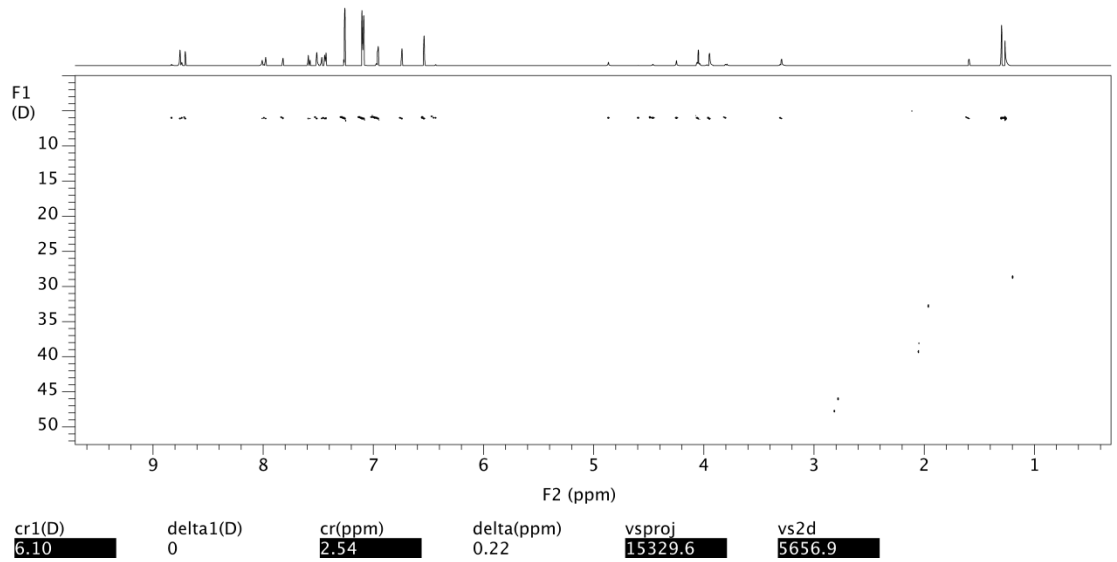

Figure S 84 ^{1}H DOSY NMR spectrum (500 MHz, acetone-d_6, 298K) of **5a**

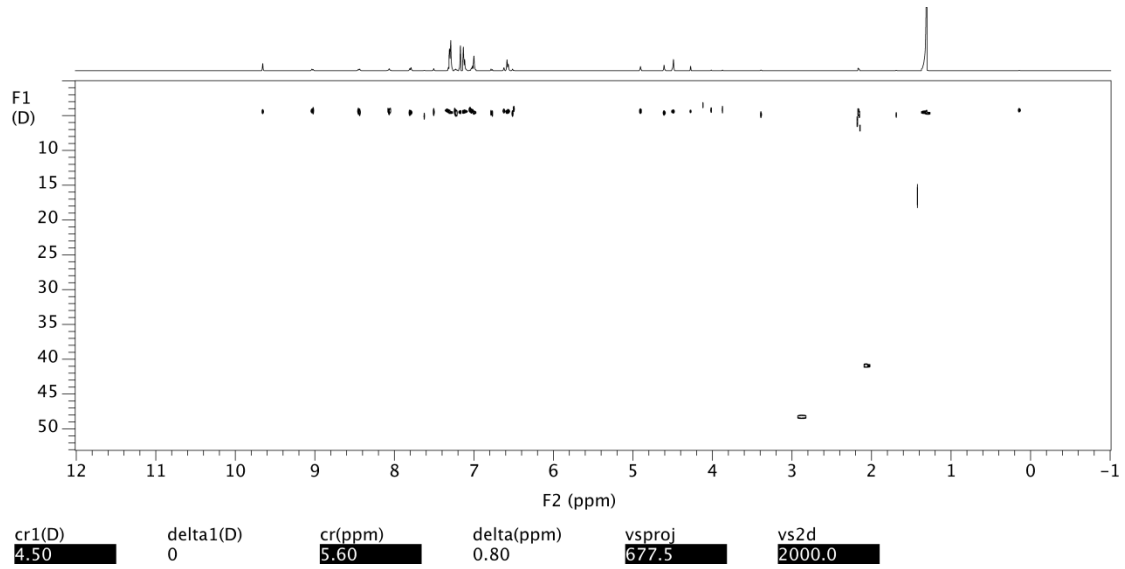

Figure S 85 ^{1}H DOSY NMR spectrum (500 MHz, acetone-d_6, 298K) of [Fe(**5a**)$_2$](BF$_4$)$_2$

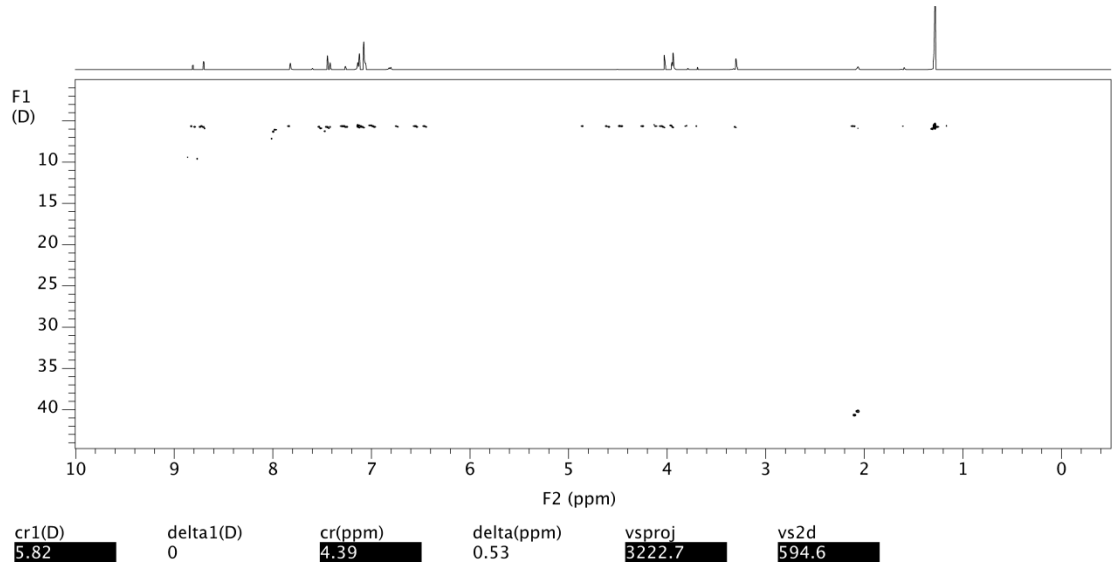

Figure S 86 ^{1}H DOSY NMR spectrum (500 MHz, acetone-d_6, 298K) of **5b**

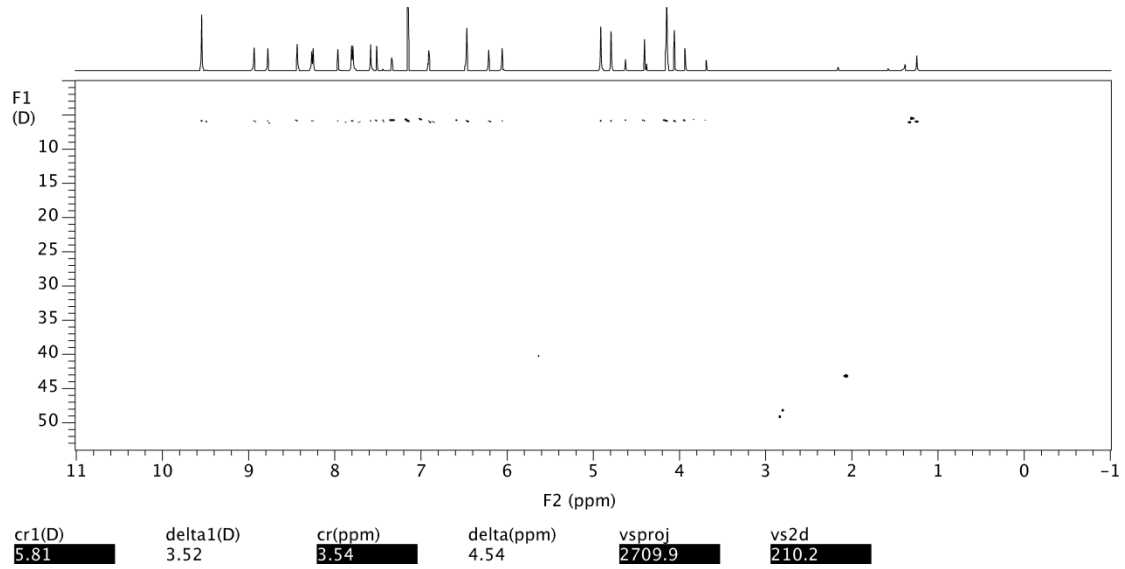

Figure S 87 ^{1}H DOSY NMR spectrum (500 MHz, acetone-d_6, 298K) of [Fe(**5b**)$_2$](BF$_4$)$_2$

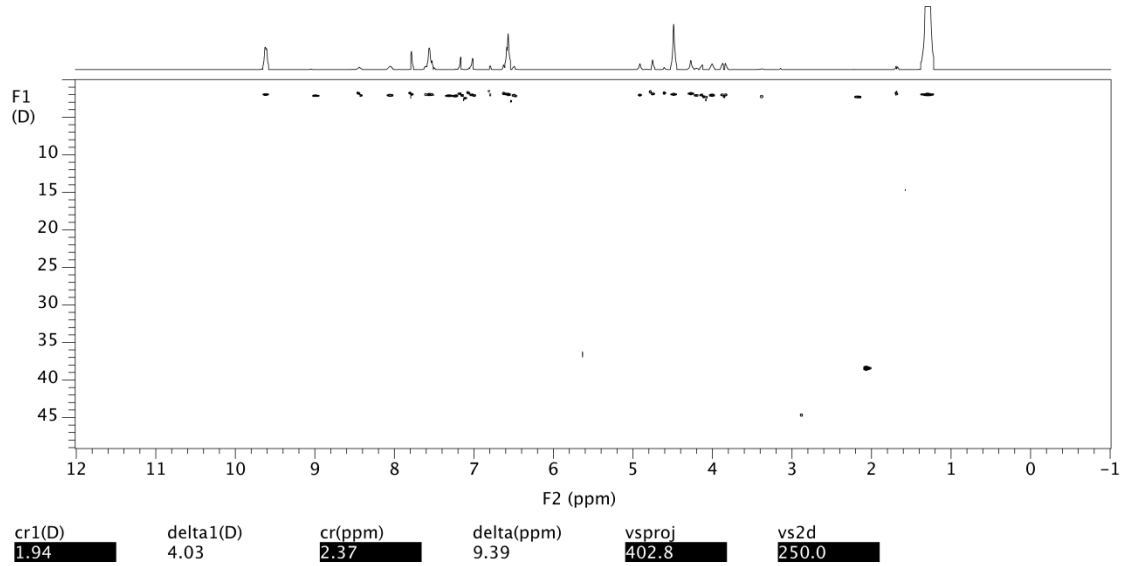

Figure S 88 ^{1}H DOSY NMR spectrum (500 MHz, acetone-d_6, 298K) of [Fe(**5a**)]$_n$(PF$_6$)$_n$

9 X-Ray Data Collection and Structure Refinement

9.1 Macrocycle 1

X-ray data for macrocycle **1** was collected at 100 K on a CrysAlisPro[6], Agilent Technologies diffractometer using SuperNova Cu Kα radiation. The structure was solved by direct methods and refined against F^2 using anisotropic thermal displacement parameters for all non-hydrogen atoms using the xSeed[7] and SHELXS-97[8] program. Hydrogen atoms were placed in calculated positions and refined using a riding model. The structure was solved in the primitive triclinic space group $P\bar{1}$ and refined to a R_1 value of 6.9%.

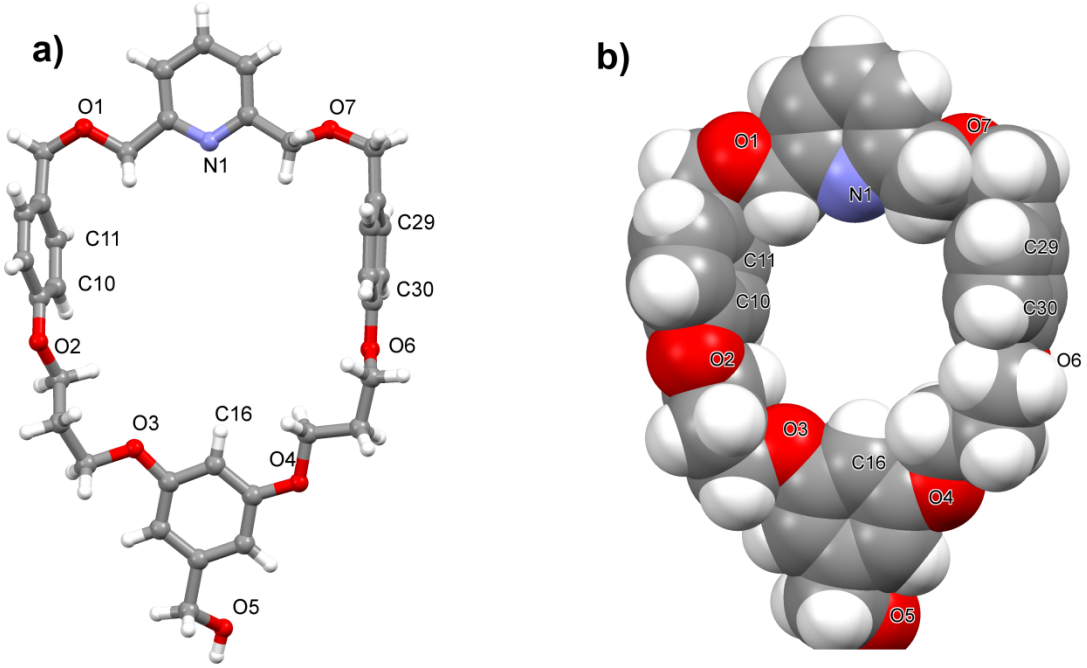

Figure S 89 X-ray crystal structures of **1**, a) ball-and-stick model, b) space filling model, $CHCl_3$ solvent molecule is omitted for clarity. Selected distances (Å) and angles (°):1 N1-C16 9.130(3), C11-C29 9.270(4), C10-C30 9.130(4)

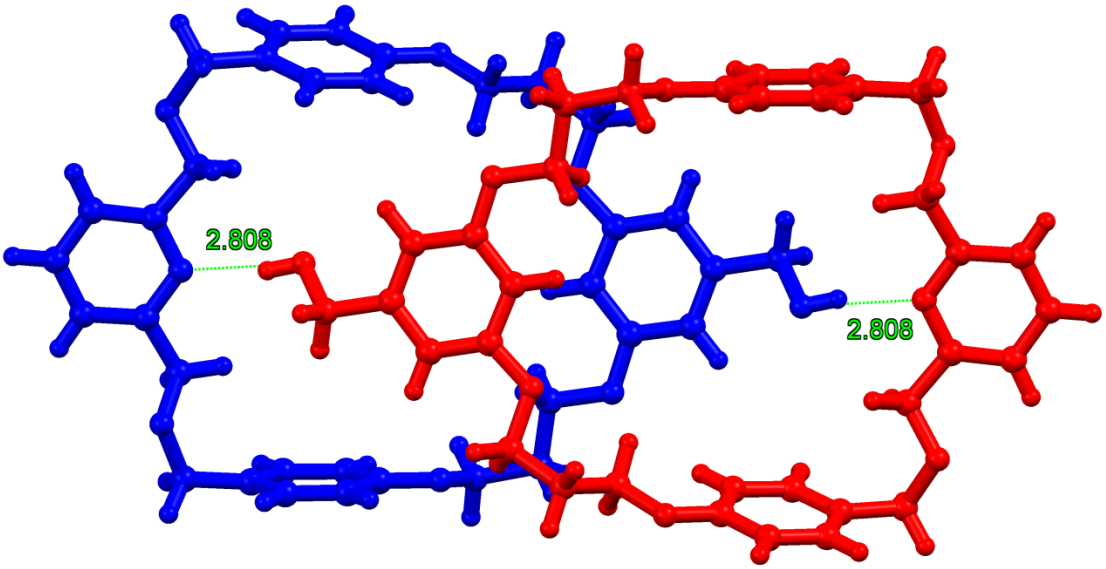

Figure S 90 91 Extended X-ray crystal structures of **1**, showing hydrogen bonding ineration between pyridyl nitrogen atom and the alcohol oxygen atom, N1—O5 2.808(2) (Å).

9.2 Ag(I) complex of macrocycle 1-Ag

X-ray data for silver complex of macrocycle **1-Ag** was collected at 89 K on a Bruker Kappa Apex II area detector diffractometer using monochromated Mo Kα radiation. The structure was solved by direct methods and refined against F^2 using anisotropic thermal displacement parameters for all non-hydrogen atoms using APEX II software. Hydrogen atoms attached to carbons were placed in calculated positions and refined using a riding model. Alcohol hydrogens of coordinated methanol and coordinated macrocycle *exo*-alcohol functionality were found (Q peaks) and refined freely as isotopic atoms. The structure was solved in the primitive triclinic space group $P\bar{1}$ and refined to a R_1 value of 4.2%.

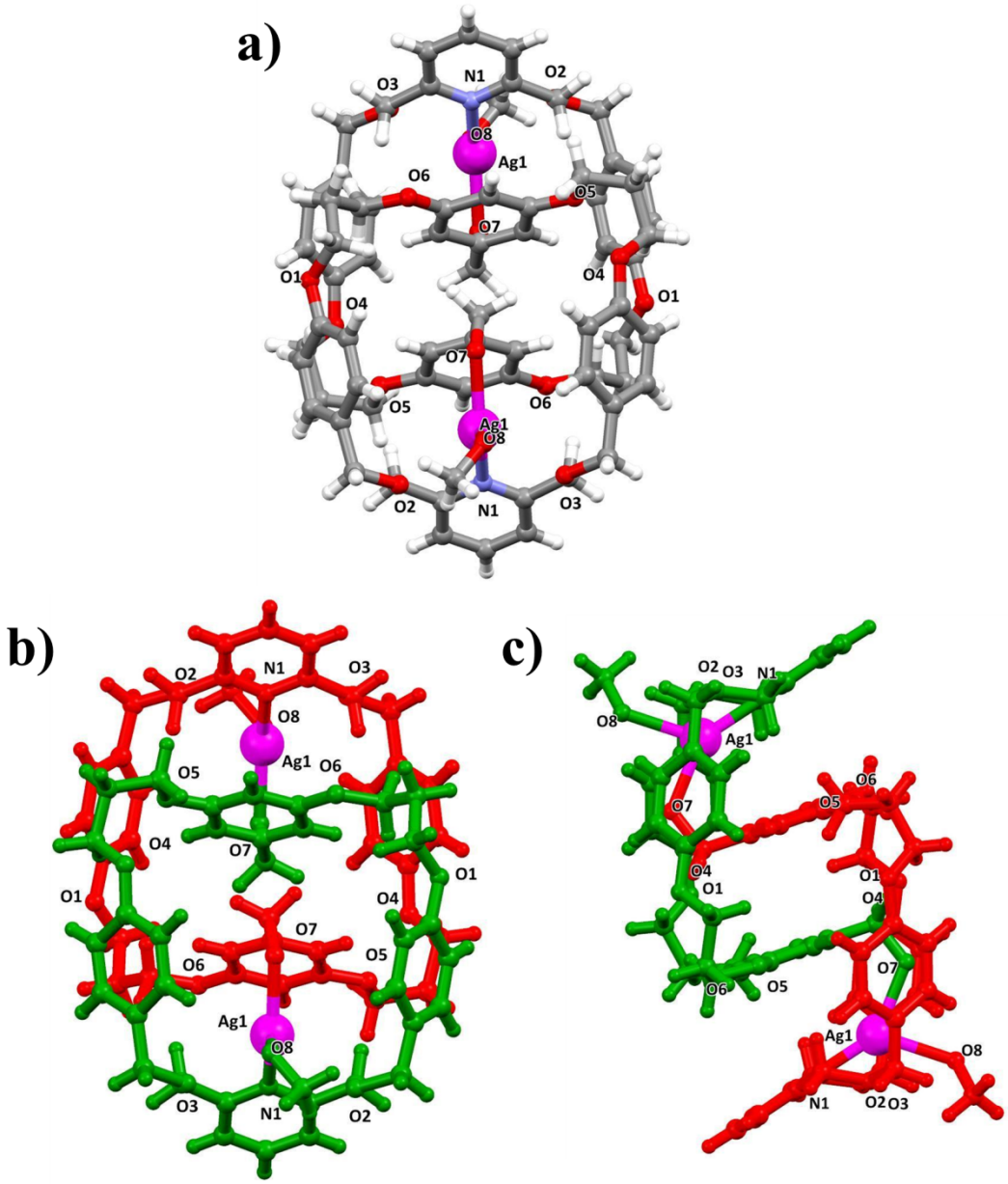

Figure S 92 Labelled mercury diagrams for the X-ray crystal structures of silver complex of macrocycle **1**-Ag a) ball-and-stick model, b) front view and c) side view as coloured by symmetry equivalence (counterions have been omitted for clarity). Selected distances (Å) and angles (°): Ag1-N1 2.218(3), Ag1-O8 2.433(2), N1-Ag1-O8 128.6(1)

9.3 [Fe(S14)$_2$](BF$_4$)$_2$

X-ray data for macrocycle Fe(**S14**)$_2$](BF$_4$)$_2$ was collected at 100 K on a CrysAlisPro[6], Agilent Technologies diffractometer using SuperNova Cu Kα radiation. The structure was solved by direct methods and refined against F^2 using anisotropic thermal displacement parameters for all non-hydrogen atoms using the xSeed[7] and SHELXS-97[8] program. Hydrogen atoms were placed in calculated positions and refined using a riding model. The structure was solved in monoclinic space group $P2_1/c$ and refined to a R_1 value of 5.3%.

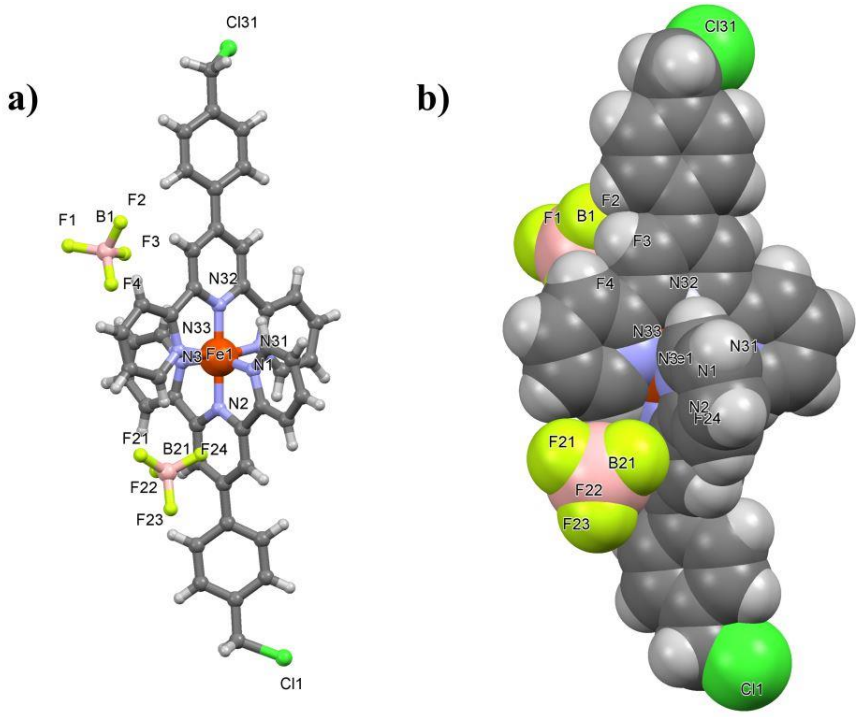

Figure S 93 X-ray crystal structure of Fe(II) complex of the ligand [Fe(**S14**)$_2$](BF$_4$)$_2$ a) ball & stick model, b) spacefilling model. Selected distances (Å) and angles (°); Fe1-N32 1.886(2), Fe1-N2 1.888(2), Fe1-N33 1.973(2), Fe1-N1 1.980(2), Fe1-N3 1.982(2), Fe1-N31 1.988(2), N32-Fe1-N2 177.30(10), N32-Fe1-N33 0.91(9), N2-Fe1-N33101.13(9), N32-Fe1-N1 101.17(9), N2-Fe1-N1 80.63(9), N33-Fe1-N1 90.93(9), N32-Fe1-N3 97.55(9), N2-Fe1-N3 80.76(9), N33-Fe1-N3 89.40(9), N1-Fe1-N3 161.09(9), N32-Fe1-N31 80.61(9), N2-Fe1-N31 97.35(9), N33-Fe1-N31 161.51(9), N1-Fe1-N31 91.94(9), N3-Fe1-N31 93.71(9)

Table S 3 Crystal data and structure refinement for **1**

CCDC	**1002573**
Empirical formula	$C_{35}H_{38}C_{l3}NO_7$
Formula weight	691.01
Temperature	100.0(1) K
Wavelength	1.5418 Å
Crystal system	Triclinic
Space group	$P\bar{1}$
Unit cell dimensions	a = 10.4484(2) Å
a= 105.509(2)°.	
	b = 12.9132(2) Å
b= 110.788(2)°.	
	c = 14.4521(3) Å
g = 101.371(2)°.	
Volume	1661.71(5) $Å^3$
Z	2
Density (calculated)	1.381 Mg/m^3
Absorption coefficient	2.912 mm^{-1}
F(000)	724
Crystal size	0.43 x 0.26 x 0.15 mm^3
Theta range for data collection	3.52 to 76.67°.
Index ranges	-13<=h<=12, -12<=k<=16, -18<=l<=18
Reflections collected	18060
Independent reflections	6656 [R(int) = 0.0212]
Completeness to theta = 76.67°	95.2 %
Absorption correction	Semi-empirical from equivalents
Max. and min. transmission	0.6692 and 0.3674
Refinement method	Full-matrix least-squares on F^2
Data / restraints / parameters	6656 / 0 / 416
Goodness-of-fit on F^2	2.637
Final R indices [I>2sigma(I)]	R1 = 0.0699, wR2 = 0.2765
R indices (all data)	R1 = 0.0709, wR2 = 0.2795
Largest diff. peak and hole	1.232 and -1.324 $e.Å^{-3}$

Table S 4 Crystal data and structure refinement for **1-Ag**

CCDC	**1002574**
Empirical formula	$C_{72}H_{82}Ag_2F_6N_2O_{22}S_2$
Formula weight	1721.26
Temperature	89(2) K
Wavelength	0.71073 Å
Crystal system	Triclinic
Space group	$P\bar{1}$
Unit cell dimensions	a = 11.0298(7) Å
a= 87.500(4)°.	
	b = 12.4731(10) Å
b= 72.011(4)°.	
	c = 15.6946(12) Å
g = 67.114(4)°.	
Volume	1884.8(2) $Å^3$
Z	1
Density (calculated)	1.516 Mg/m^3
Absorption coefficient	0.665 mm^{-1}
F(000)	884
Crystal size	0.20 x 0.16 x 0.09 mm^3
Theta range for data collection	1.37 to 26.43°.
Index ranges	-13<=h<=13, -15<=k<=15, -19<=l<=19
Reflections collected	34942
Independent reflections	7687 [R(int) = 0.0676]
Completeness to theta = 26.43°	99.0 %
Absorption correction	Semi-empirical from equivalents
Max. and min. transmission	0.9426 and 0.8786
Refinement method	Full-matrix least-squares on F^2
Data / restraints / parameters	7687 / 0 / 487
Goodness-of-fit on F^2	1.050
Final R indices [I>2sigma(I)]	R1 = 0.0420, wR2 = 0.0919
R indices (all data)	R1 = 0.0661, wR2 = 0.1109
Largest diff. peak and hole	0.606 and -0.469 $e.Å^{-3}$

Table S 5 Crystal data and structure refinement for complex $[Fe(\mathbf{S14})_2](BF_4)_2$

CCDC	**1002575**
Empirical formula	$C_{44}H_{32}B_2Cl_2F_8FeN_6$
Formula weight	945.13
Temperature	100(2) K
Wavelength	0.71069 Å
Crystal system	Monoclinic
Space group	$P2_1/c$
Unit cell dimensions	a = 17.892(5) Å
a= 90.000(5)°.	
	b = 14.886(5) Å
b= 110.371(5)°.	
	c = 15.952(5) Å
g = 90.000(5)°.	
Volume	3983(2) $Å^3$
Z	4
Density (calculated)	1.576 Mg/m^3
Absorption coefficient	0.594 mm^{-1}
F(000)	1920
Crystal size	0.41 x 0.34 x 0.23 mm^3
Theta range for data collection	1.83 to 26.64°.
Index ranges	-20<=h<=22, -18<=k<=18, -19<=l<=13
Reflections collected	24933
Independent reflections	8281 [R(int) = 0.0302]
Completeness to theta = 26.64°	98.7 %
Max. and min. transmission	0.8755 and 0.7928
Refinement method	Full-matrix least-squares on F^2
Data / restraints / parameters	8281 / 0 / 568
Goodness-of-fit on F^2	1.152
Final R indices [I>2sigma(I)]	R1 = 0.0529, wR2 = 0.1298
R indices (all data)	R1 = 0.0569, wR2 = 0.1320
Largest diff. peak and hole	1.014 and -0.882 $e.Å^{-3}$

10 Selected Stacked ^{1}H NMR Spectra

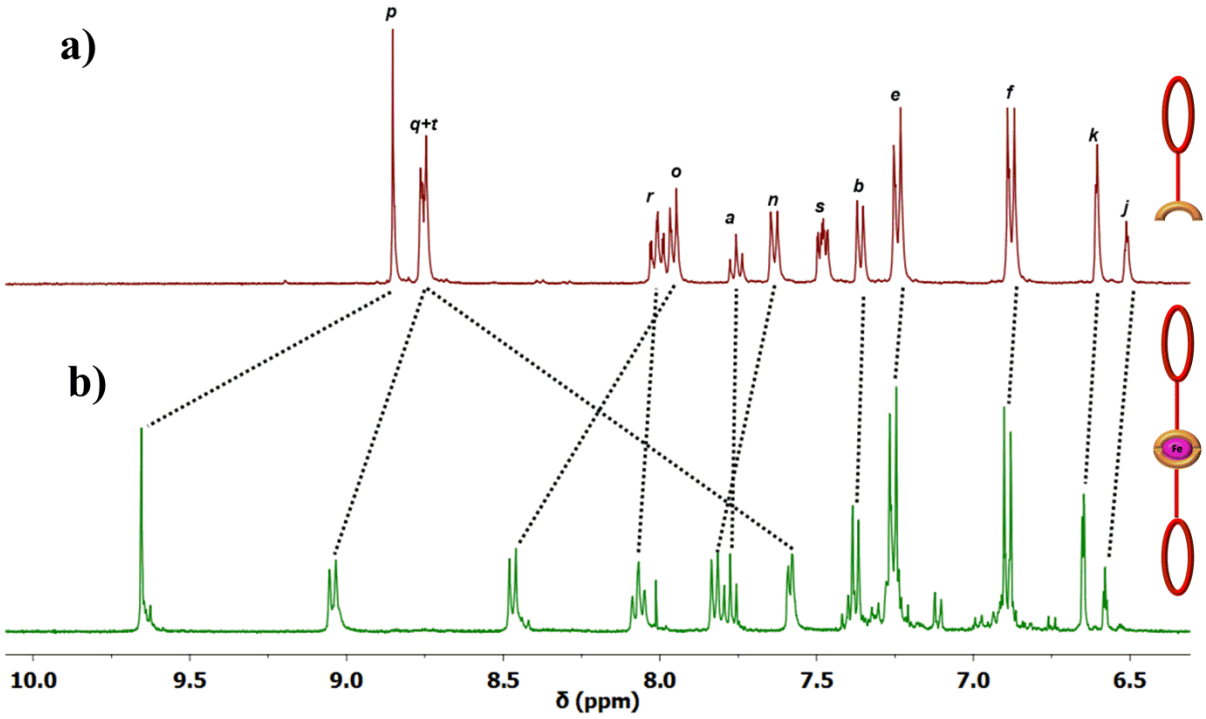

Figure S 94 Partial stacked ^{1}H NMR spectra (500 MHz, acetone-d_6, 298K) of a) **S15** and b) [Fe(**S15**)](BF$_4$)$_2$

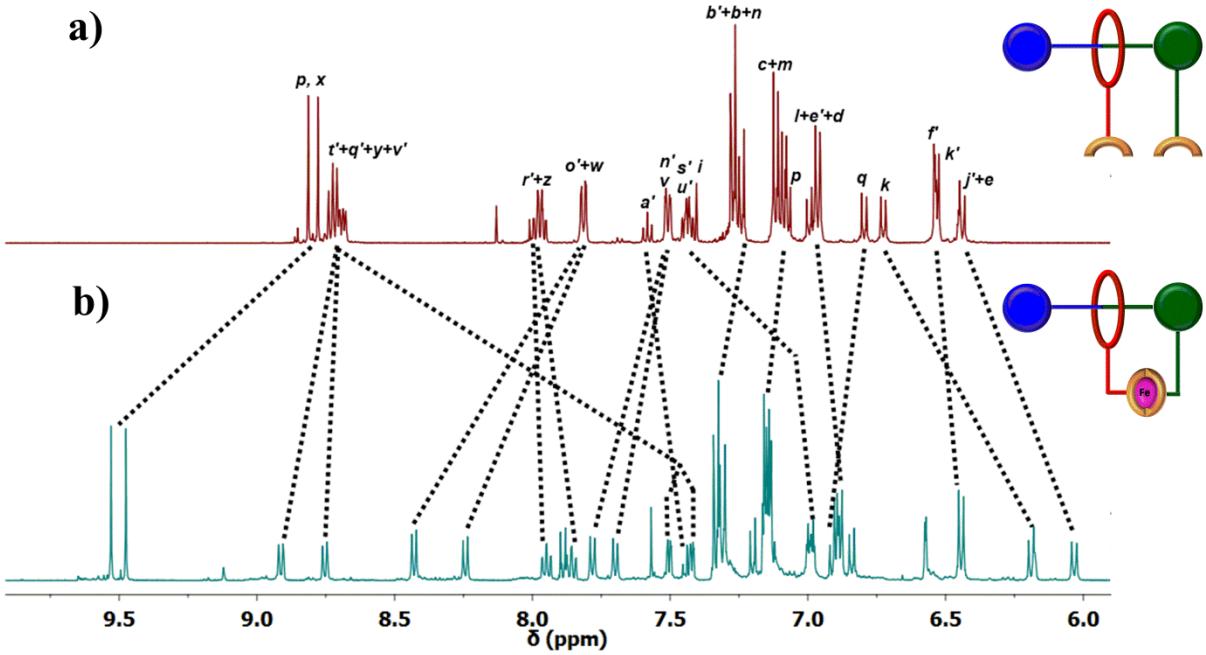

Figure S 95 Partial stacked ^{1}H NMR spectra (500 MHz, acetone-d_6, 298K) of a) **5b** and b) [Fe(**5b**)](BF$_4$)$_2$

11 References:

1. S. Braese, C. Gil, K. Knepper and V. Zimmermann, *Angew. Chem., Int. Ed.*, 2005, **44**, 5188-5240.
2. V. Aucagne, J. Berná, J. D. Crowley, S. M. Goldup, K. D. Hänni, D. A. Leigh, P. J. Lusby, V. E. Ronaldson, A. M. Z. Slawin, A. Viterisi and D. B. Walker, *J. Am. Chem. Soc.*, 2007, **129**, 11950-11963.
3. X. Li, T. G. Upton, C. L. D. Gibb and B. C. Gibb, *J. Am. Chem. Soc.*, 2002, **125**, 650-651.
4. A. Winter, A. M. J. van den Berg, R. Hoogenboom, G. Kickelbick and U. S. Schubert, *Synthesis*, 2006, **2006**, 2873-2878.
5. W. Li, H. Chung, C. Daeffler, J. A. Johnson and R. H. Grubbs, *Macromolecules*, 2012, **45**, 9595-9603.
6. CrysAlisPro, *Agilent Technologies: Yarnton, Oxfordshire, England, 2012*.
7. L. J. Barbour, *J. Supramol. Chem.*, 2001, **1**, 189-191.
8. G. Sheldrick, *Acta Cryst.*, 2008, **A64**, 112-122.